Bactericidal efficacy of wound gauze treated with chitosan nanomaterial hybrids of zinc, silver and copper on common wound bacteria.

By

BLESSING TATENDA SHEKEDE

NDANCH, BTech (Cape Peninsula University of Technology)

Thesis submitted in fulfilment of the requirements for the degree

Master of Applied Sciences: Chemistry

In the Faculty of Applied Sciences

At the Cape Peninsula University of Technology

Supervisor: Prof. M. C. Matoetoe

Cape Town

August 2018

DECLARATION

I, **Blessing Tatenda Shekede**, declare that the contents of this dissertation/thesis represent my own unaided work, and that the dissertation/thesis has not previously been submitted for academic examination towards any qualification. Furthermore, it represents my own opinions and not necessarily those of the Cape Peninsula University of Technology.

Signed _____ Date _____

ABSTRACT

Maintenance of optimum wound chemistry is important to ensure timely healing of a wound. Bacterial infections impair the process of wound healing by producing toxins that alter the chemical environment in and around the wound. The imbalance in the wound chemistry prolongs healing and opens doors to opportunistic infections. Bacteria have developed resistance to conventional bactericides hence, there is need for search of new bactericides that can control bacteria in and around the wound. Therefore, new chemical or biochemical bactericides, which are not resisted by the bacteria, can be explored to control bacterial life around the wound in a bid to maintain optimum wound healing chemistry. Materials such as chitosan, zinc oxide, copper oxide and silver have showed remarkable potential as both bactericidal and wound healing agents.

In this work silver, zinc oxide, and copper oxide nanoparticles (NPs) and their chitosan composites (CH-NPs) were synthesized using the chemical reduction method and simple chelation respectively to produce nanoparticles of Ag, ZnO, and CuO as well as composites of CH-ZnO, CH-Ag, CH-CuO, and CH-ZnO-Ag-CuO.

Formation of the NPs was confirmed by the exhibition of characteristic peaks in UV-Visible and Fourier Transform Infrared Resonance (FTIR) spectroscopy as well as X-ray diffraction. The nanoparticles (NPs) had optical and electronic band gaps in the range 1 to 5eV indicating their semi-conductive nature. X-ray diffraction (XRD) investigations depicted the crystalline structures of the NPs to be base-centred, face-centred, and hexagonal for Ag, CuO, and ZnO respectively. Transmission electron microscopy (TEM) studies exhibited spherical, hexagonal, and rod-shaped shapes for silver, copper oxide, zinc oxide NPs respectively. Electrochemical investigations of the pure NPs indicated the existence of both the adsorption and the diffusion controlled electron transfer processes at electrode surfaces as well as fast electron transfer rate as depicted by the charge transfer coefficient and standard rate constant parameter values.

FTIR spectra of CH-NPs composites depicted new excitation bands absent in spectra of both chitosan and the NPs. The spectra also indicated the deformation and absence of the amine ($-NH_2$) and hydroxyl bands (-OH) within the CH-NPs composites. UV-Visible spectroscopy investigations of the CH-NPs composites exhibited blue-shifts of the λ_{max} with respect to the NPs. The FTIR and UV-Visible spectra confirmed the existence of bonding between the chitosan and the NPs. The optical band gap energies of all the CH-NPs composites fell within the range of 2.0 to 4.5 eV indicating that the CH-NPs fell in the category of the semi-conducting materials after chelating with the chitosan. XRD studies of the CH-NPs showed

that the chitosan did not have influence in the crystalline structure of the NPs within the composite. Electrochemical studies of the CH-NPs composites indicated the Dannon effect and irreversibility of reactions taking place at the electrode. The charge transfer coefficient and standard rate constant parameters are typically for slow electron transfer kinetics. The adsorption controlled electron transfer process are dominant at the electrode surface for all composites.

The gauzes were modified via drip-dry-cure method. Scanning electron microscopy (SEM) images depicted an increase in surface area and aeration pores along the surface of the modified gauze, which was confirmed by a significant increase in water retention abilities of the gauze. All CH-NPs composites showed a degree of efficacy in bacterial growth inhibition of *Staphylococcus aureus* and *Escherichia coli* with the highest activity being of the prototype (CH-Ag-CuO-ZnO) and CH-Ag. The prototype modified gauze, achieved bactericidal vigour of 96% and 99% against *Staphylococcus aureus* and *Escherichia coli* respectively. The results indicated that the proposed composites carry much potential to be used as alternative bactericidal and wound healing agents.

ACKNOWLEDGEMENTS

First I would like to thank God Almighty for His grace throughout these studies; I would have not made it without Him.

To my supervisor and academic mentor Professor M.C Matoetoe, thank you for your instruction and counsel in this research. It was indeed an honour to learn from you and work with you in this research. This research would not have materialised if it were not for your continuous guidance, evaluation, and supervision. Thank you so much for patience as I grew in knowledge of research and your continuous encouragement throughout the period.

To Professor Ntwampe, thank you for the technical support.

To Cape Peninsula University of Technology and University of Western Cape your support towards this research is acknowledged.

To my partner Tlaleng Lesemela,thank you for the all-round support. You made this academic journey lighter.

Finally, to my parents and life mentors, Dr and Mrs Dida, thank you for believing in my potential and sacrificially investing in it. Thank you for the financial support, the faith, and the sacrifice.

Dr and Mrs Dida, this is for you.

TABLE OF CONTENTS

LIST OF FIGURES

LIST OF TABLES

GLOSSARY

Terms/Acronyms/Abbreviations	Definition/Explanation
AATCC	American Association of Textile Chemists and Colourists
AFM	Atomic Force Microscopy
CH-Ag	Chitosan-Silver Composite
CH-CuO	Chitosan-Copper Oxide Composite
CH-NPS	Chitosan-Nanoparticle Composite
CH-ZnO	Chitosan-Zinc Oxide Composite
CV	Cyclic Voltammetry
DNA	Deoxyribonucleic Acid
E_{bg}	Band Gap Energy
FTIR	Fourier Transform Infrared
HOMO	Highest Occupied Molecular Orbital
LUMO	Lowest Unoccupied Orbital
MBC	Minimum Bactericidal Concentration
MIC	Minimum Inhibitory Concentration
NPs	Nanoparticles
SD	Standard Deviation
SEM	Scanning Electron Microscopy
SPR	Surface Plasmon Resonance
TEM	Transmission Electron Microscopy
UV	Ultraviolet Radiation
UV-Visible	Ultra Violet –Visible Spectroscopy
λ_{max}	Maximum Wavelength

CHAPTER ONE
INTRODUCTION

1.1. Background

The chemistry that controls the rate of wound healing involves maintenance of optimum healing environment and the control of microbial life around the wound. Chemistry regulation and microbial control on the wound can be achieved by employing a wound dressing to maintain the environment and by introducing localised or delocalised bactericidal agents to deal with microbial activity. This creates a suitable chemical environment for the effective healing of the wound. Bacterial activity has the ability to influence and affect the chemistry around the wound if not controlled thereby delaying wound healing. Bacterial infections produce toxins which hinder wound healing and has imperative negative influences on wound healing time (Paladini *et al.*, 2016). Bacteria also compete for nutrients and oxygen with the cells of the tissue around the wound area. An ability to control infection and moisture environment in the wound ensures timely recovery and patching up of the wound.

A basic effective wound dressing should be able to act against microorganisms, maintain moisture, promote wound healing, be generally non-toxic and be non-adherent (Sun and Li, 2011). In the past wound dressings were only designed to maintain moisture and keep pathogenic bacteria out with the bactericidal agent being applied as topical ointment or taken orally. However, it has been discovered that the conventional wound dressing absorbs moisture and consequently creates a conducive environment for microbial growth(Davis and McLister, 2016). It has been also discovered that pathogenic wound bacteria have been developing drug resistance against the conventional bactericidal drugs. This challenge can be solved by the use chemo-active cotton wound dressings. These are cotton dressings that have active chemical components incorporated in them to provide anti-microbial action as well as curative properties maintaining the chemistry on the wound. This has created a need of wound gauzes that have bactericidal components that are not resisted by pathogenic wound bacteria.

Metallic and polymeric nanoparticles such as chitosan have shown remarkable potential in their use as bactericidal agents in the production and modification of wound dressings. Chitosan has been used in various medical applications and studies have shown that it exhibits remarkable antimicrobial and hydrating effects (Sudheesh Kumar *et al.*, 2012). This is due to its biocompatibility and relative non-toxicity characteristics. In the treatment of wounds, chitosan has been used as a curative and bactericidal agent as well as structural material for membrane dressing. Studies have been done in modifying cotton wound gauzes

with chitosan and assessing their bactericidal efficacy with remarkable results being achieved (Hajipour *et al.*, 2012). Previous studies have been done in the development of metallic nanoparticles cotton wound gauze complexes and they have proved to have acceptable degree of efficacy (Franci *et al.*, 2015). Various metallic nanomaterial have been used as bactericides in wound treatment but silver, zinc oxide and copper oxide nanomaterial have been favoured for their straightforward synthetic pathways, economy and relatively low toxicity to efficacy ratio (Rai, Yadav and Gade, 2009; Hajipour *et al.*, 2012). The attributes of bulk silver, copper and zinc has been previously utilized for the formulation and development of topical creams, gauzes and other bactericidal. These three, Zinc, copper, and silver have shown greater anti-bacterial effects as their size decrease into the nano range size and have been used for various purposes in medicine due to their bactericidal nature. The various nanoparticles have proved to be effective against the common wound bacteria with bactericidal efficacies of above 70% (Seil and Webster, 2012). These three nanoparticles have been utilised in the modification of cotton wound gauzes and the results showed that the nanoparticles exhibited remarkable antimicrobial activity. Modification of cotton wound gauze using a combination of metallic nanoparticles and chitosan has been considered in this work with the aim of improving the efficacy of the wound gauze.

A chitosan and zinc oxide/silver nanoparticles hybrid wound gauze was developed and the studies conducted showed that the polysaccharide could be combined with metallic nanoparticles to produce enhanced curative and bactericidal efficacy levels (Azuma *et al.*, 2015) . The research indicated remarkable synergetic effects due to chitosan and metallic nanoparticles combinations.

There is room to research within the area by combining different nanoparticles combinations with the chitosan polymer and evaluating the bactericidal effects it has in wound healing. Therefore, there is a need to conduct evaluation studies of different chitosan wound gauze complexes containing different types of metallic nanoparticles combinations with chitosan. It is also imperative that other factors affecting wound gauze utilization in wound healing such as optical activity, water-holding time and relative water absorption be studied in these newly developed gauzes to ensure that the introduction of chitosan-nanoparticles complex in the wound gauze does not affect the general functionality of the wound gauze. All the nanoparticles of interest have their own advantages and disadvantages so the development of a hybrid wound gauze with various combinations could aide in eliminating some of the disadvantages such as bactericidal spectrum coverage and vigour also enhancing the present advantages. For instance, the inability of zinc to have considerable curative ability could be covered by chitosan and copper. While the bacterium that silver is not well effective

against such as *B. subtilis* could be eliminated by the presence of zinc and copper in the combination hybrid dressing.

In this research the hypothesis being considered is that a hybrid wound dressing containing copper, silver, and zinc and chitosan nanoparticles should exhibit better bactericidal efficacy, wound healing capabilities, and less toxicity to the wound cavity tissue. Toxicity is believed to be reduced due to the presence of less toxic component of copper which can eliminate bacteria at low concentration levels causing less adverse effects on the tissue of the wound cavity. Chitosan which is biodegradable and biocompatible aides in water retention and also by binding the nanoparticles fast to the wound dressing and ensuring a steady timely release of the nanoparticles into the wound cavity.

This research is aimed at developing new modified wound gauze that can be applied in wound healing by using chitosan and silver, copper oxide and zinc oxide nanoparticles to modify it. The modified wound gauze is expected to have enhanced bactericidal efficacy and healing properties thereby making it more efficient than its unmodified counterpart. To address this gap in research, we have synthesised nanoparticles and nanoparticle-chitosan composites for the modification of the wound gauze. We have characterised the nanoparticles, composites and assessed the efficacy of the modified wound gauze for wound healing.

1.2. Problem Statement

Due to an increase in drug resistant bacteria and shortcomings of the cotton wound gauzes there is a need for the development of modified wound gauze that is able to control bacterial infections as well as maintain conducive environment for the healing of the wound. The purpose of this research is to prepare chitosan-nanoparticle treated wound gauze and evaluating its bactericidal efficacies. There is also a need to understand the optical and electrochemical behaviour of the modifying components before and after they are in modification. The research seeks to maintain and enhance the advantages of the cotton wound gauze yet eliminating its ability to facilitate the growth of bacterial infection in and around the wound cavity.

1.3. Research aim and objectives

The aim of this research was to develop a wound gauze, by chemical modification of existing cotton gauze, and assessing the bactericidal efficacy and utilities of the wound gauze.

The specific objectives being:

1) To synthesize and characterise zinc oxide, copper oxide and silver nanoparticles.
2) To prepare and characterize chitosan-nanoparticles composites.
3) To modify cotton wound gauze using the nanoparticles-chitosan composites.
4) Conduct utility tests of the prepared dressings.
5) Evaluate the bactericidal efficacy of the modified wound gauzes.

1.4. Delineation of research

The following will not be focused on in this research:

1) Effect of variable nanoparticles size and morphology on bactericidal efficacies.
2) Operational mechanisms of nanoparticles and chitosan as bactericidal.
3) Effect of variable wound gauze surface morphology on the efficacy of the nanoparticles as antimicrobials.

1.5. Assumptions

1) Selected bacterial strains to be used for this study are a true representative of common strains found on wounds, thus their behaviour to the different nanoparticles will be used as indicative of wound infections.
2) *In vitro* bactericidal efficacy studies can sufficiently represent *in situ* environment.

1.6. Thesis overview

This thesis focuses on the nanoparticles/biopolymer modification of a cotton wound gauze that can be used for wound treatment both as wounding healing agent and bactericidal agent. The main objective of the research is to study the chemistry behind the modification in order to ascertain the viability of the gauze. This research is outlined as follows:

Chapter one looks into the background of the research work and expresses the problem or gap that gave rise to the need of this research.

Chapter two reviews the use of nanoparticles and chitosan in wound healing. The chapter also explores the different advantages and disadvantages of silver, copper oxide and zinc oxide nanomaterial as wound healing and bactericidal agents. Previous work involving composites of the nanomaterial and the polymer chitosan is also discussed.

Chapter three describes the synthesis and characterisation of nanoparticles Ag, ZnO, and CuO. It elaborates on how the nanoparticles were synthesised using the chemical reduction

method and their characterisation using UV-Visible spectroscopy, transmission electron microscopy(TEM), Fourier transform infrared(FTIR) and cyclic voltammetry(CV).

Chapter four describes the fabrication of the composites of chitosan with Ag, ZnO, and CuO that will be used to modify the wound gauzes. X-ray diffraction, UV-Visible, FTIR and Cyclic voltammetry was used to confirm and investigate the interaction between the nanoparticles and the chitosan.

Chapter five describes the modification of the cotton wound gauze using the chitosan-nanoparticle composites and investigating its surface morphology, water retention capabilities. The chapter also assess the bactericidal efficacy of the modified wound gauze using the AATCC 100 and AATCC 137 tests.

1.7. References

Abbasipour, M. *et al.* (2014) 'Coated Cotton Gauze with Ag/ZnO/chitosan Nanocomposite as a Modern Wound Dressing', *Journal of Engineered Fibers and Fabrics*, 9(1), pp. 124–130.

AbdElhady, M. M. (2012) 'Preparation and Characterization of Chitosan/Zinc Oxide Nanoparticles for Imparting Antimicrobial and UV Protection to Cotton Fabric', *International Journal of Carbohydrate Chemistry*, 2012, pp. 1–6. doi: 10.1155/2012/840591.

Abiraman, T. *et al.* (2016) 'Antifouling behavior of chitosan adorned zinc oxide nanorods', *RSC Adv.* Royal Society of Chemistry, 6(73), pp. 69206–69217. doi: 10.1039/C6RA13321E.

Ahmed, S. and Ikram, S. (2016) 'Chitosan Based Scaffolds and Their Applications in Wound Healing', *Achievements in the Life Sciences*. Far Eastern Federal University, 10(1), pp. 27–37. doi: 10.1016/j.als.2016.04.001.

Alagumuthu, G. and Kumar, T. A. (2013) 'Synthesis and Characterization of Chitosan / TiO 2 Nanocomposites Using Liquid Phase Deposition Technique', 4(1), pp. 105–111.

Algawi, S. D. A. L. (no date) 'Copper Oxide Nanostructures ; Syntheses and Characterization', 71, pp. 0–4.

Ali, S. W., Rajendran, S. and Joshi, M. (2011) 'Synthesis and characterization of chitosan and silver loaded chitosan nanoparticles for bioactive polyester', *Carbohydrate Polymers*. Elsevier Ltd., 83(2), pp. 438–446. doi: 10.1016/j.carbpol.2010.08.004.

Alvarez, P. J. J. and Lowry, G. (2009) ‘Nanomaterials with Antimicrobial Properties : Mechanisms , Implications and Applications pp I i’.

Applerot, G. *et al.* (2012) ‘Understanding the antibacterial mechanism of CuO nanoparticles: Revealing the route of induced oxidative stress’, *Small*, 8(21), pp. 3326–3337. doi: 10.1002/smll.201200772.

Arefi, M. R. and Rezaei-Zarchi, S. (2012) ‘Synthesis of zinc oxide nanoparticles and their effect on the compressive strength and setting time of self-compacted concrete paste as cementitious composites’, *International Journal of Molecular Sciences*, 13(4), pp. 4340–4350. doi: 10.3390/ijms13044340.

Atiyeh, B. S. *et al.* (2007) ‘Effect of silver on burn wound infection control and healing: Review of the literature’, *Burns*, 33(2), pp. 139–148. doi: 10.1016/j.burns.2006.06.010.

Azuma, K. *et al.* (2015) *Chitin, Chitosan, and Its Derivatives for Wound Healing: Old and New Materials*, *Journal of Functional Biomaterials*. doi: 10.3390/jfb6010104.

Babu, V. S. (2010) *Solid State Devices and Technology*. 3rd edn, *Solid states devices and technology.* 3rd edn. Mumbai: Pearson.

Bagabas, A. *et al.* (2013) ‘Room-temperature synthesis of zinc oxide nanoparticles in different media and their application in cyanide photodegradation’, *Nanoscale Research Letters*, 8(1), p. 516. doi: 10.1186/1556-276X-8-516.

Balamurugan, B. and Mehta, B. R. (2001) ‘Optical and structural properties of nanocrystalline copper oxide thin films prepared by activated reactive evaporation’, *Thin Solid Films*, 396(1–2), pp. 90–96. doi: 10.1016/S0040-6090(01)01216-0.

Balu, S. S. and Bhakat, C. (2012) ‘SYNTHESIS OF SILVER NANOPARTICLES BY CHEMICAL REDUCTION AND THEIR ANTIMICROBIAL ACTIVITY Materials and Methods ’:, 1(6), pp. 1–5.

Bard, A. J. *et al.* (1944) *ELECTROCHEMICAL METHODS Fundamentals and Applications*, *Electrochemistry. I. Faulkner, Larry R*. doi: 10.1016/B978-0-12-381373-2.00056-9.

Benavente, M. (2008) *Adsorption of metallic ions onto chitosan: equilibrium and kinetic studies*. doi: 976–988.

Beyth, N. *et al.* (2015) ‘Alternative Antimicrobial Approach: Nano-Antimicrobial Materials’, *Evidence-Based Complementary and Alternative Medicine*, 2015, pp. 1–16. doi:

10.1155/2015/246012.

Biovation, L. (2010) *Testing for Antimicrobial Activity in Textiles.* Boothbay.

Bonnemann, H. and Richards, R. M. (2001) 'Nanoscopic metal particles - synthetic methods and potential applications', *Eur. J. Inorg. Chem.*, pp. 2455–2480. doi: 10.1002/1099-0682(200109)2001:10<2455::AID-EJIC2455>3.0.CO;2-Z.

Brintha, S. R. and Ajitha, M. (2015) 'Synthesis and characterization of ZnO nanoparticles via aqueous solution, sol-gel and hydrothermal methods', *IOSR Journal of Applied Chemistry*, 8(11), pp. 66–72. doi: 10.9790/5736-081116672.

Brown, J. H. (2015) 'Development and Use of a Cyclic Voltammetry Simulator To Introduce Undergraduate Students to Electrochemical Simulations', *Journal of Chemical Education*. American Chemical Society, 92(9), pp. 1490–1496. doi: 10.1021/acs.jchemed.5b00225.

Brown, K. and Gray, S. B. (2010) 'Cyclic Voltammetric Studies of Electropolymerized Films Based on Ruthenium (II/III) Bis (1, 10phenanthroline)(4-methyl-4'vinyl-2, 2'-bipyridine).', *International Journal of Chemistry*, 2(2), pp. 3–9. Available at: http://search.ebscohost.com/login.aspx?direct=true&profile=ehost&scope=site&authtype=crawler&jrnl=19169698&AN=52739860&h=s7r8gpPlt9tlQXU1DwQKvth6GpoG/uSIl9+y7buDKd4ozaZ6T7n2jMZlVbnZRzIKzPwKahBTG9vQKJVjeYgNcA==&crl=c.

Brownson, D. A. C. and Banks, C. E. (2014) *The Handbook of Graphene Electrochemistry*, *The Handbook of Graphene Electrochemistry*. doi: 10.1007/978-1-4471-6428-9.

Brugnerotto, J. *et al.* (2001) 'An infrared investigation in relation with chitin and chitosan characterization', *Polymer*, 42(8), pp. 3569–3580. doi: 10.1016/S0032-3861(00)00713-8.

Budhiraja, N. *et al.* (2013) 'Synthesis and Optical Characteristics of Silver Nanoparticles on Different Substrates', *International Letters of Chemistry, Physics and Astronomy*, 19, pp. 80–88. doi: 10.18052/www.scipress.com/ILCPA.19.80.

Calvo, E. J. and Wolosiuk, A. (2002) 'Donnan permselectivity in layer-by-layer self-assembled redox polyelectrolye thin films', *Journal of the American Chemical Society*, 124(28), pp. 8490–8497. doi: 10.1021/ja020107h.

Cavassin, E. D. *et al.* (2015) 'Comparison of methods to detect the in vitro activity of silver nanoparticles (AgNP) against multidrug resistant bacteria', *Journal of Nanobiotechnology*. BioMed Central, 13(1). doi: 10.1186/s12951-015-0120-6.

Dai, T. *et al.* (2011) *NIH Public Access*, *Expert Rev Anti Infect Ther*. doi: 10.1586/eri.11.59.Chitosan.

Dash, M. *et al.* (2011) 'Chitosan - A versatile semi-synthetic polymer in biomedical applications', *Progress in Polymer Science (Oxford)*. Elsevier Ltd, 36(8), pp. 981–1014. doi: 10.1016/j.progpolymsci.2011.02.001.

Davis, J. and McLister, A. (2016) 'Chapter Four - Passive and Interactive Dressing Materials', in Davis, J. et al. (eds) *Smart Bandage Technologies*. Academic Press, pp. 93–144. doi: https://doi.org/10.1016/B978-0-12-803762-1.00004-7.

Debanath, M. K. and Karmakar, S. (2013) 'Study of blueshift of optical band gap in zinc oxide (ZnO) nanoparticles prepared by low-temperature wet chemical method', *Materials Letters*. Elsevier, 111, pp. 116–119. doi: 10.1016/j.matlet.2013.08.069.

Dehaghi, S. M. *et al.* (2014) 'Removal of permethrin pesticide from water by chitosan–zinc oxide nanoparticles composite as an adsorbent', *Journal of Saudi Chemical Society*, 18(4), pp. 348–355. doi: https://doi.org/10.1016/j.jscs.2014.01.004.

Devi, H. S. and Singh, T. D. (2014) 'Synthesis of Copper Oxide Nanoparticles by a Novel Method and its Application in the Degradation of Methyl Orange', *Advance in Electronic and Electric Engineering*, 4(1), pp. 83–88.

Douglas Skoog, James Holler, S. C. (2007) 'Principles of instrumental analysis.', in Harris, D. (ed.) *Principles of instrumental analysis.* 6th edn. Belmont: Brooks/Cole, p. 371.

Durga Praveena, V. and Vijaya Kumar, K. (2013) 'Synthesis and Characterization of Chitosan based Silver Nano Composite System for Antibacterial Applications', *Proceedings of the International Conference on Advanced Nanomaterials & Emerging Engineering Technologies*, pp. 76–79.

Faiz, U. *et al.* (2011) 'Efficacy of zinc as an antibacterial agent against enteric bacterial pathogens.', *Journal of Ayub Medical College*, 23(2), pp. 18–21.

Feng, Q. L. *et al.* (2000) 'A mechanistic study of the antibacterial effect of silver ions on <I>Escherichia coli</I> and <I>Staphylococcus aureus</I>', *Journal of Biomedical Materials Research*, pp. 662–668. doi: 10.1002/1097-4636(20001215)52:4<662::aid-jbm10>3.0.co;2-3.

Fielicke, A., Rabin, I. and Meijer, G. (2006) 'Far-infrared spectroscopy of small neutral silver clusters', *Journal of Physical Chemistry A*, 110(26), pp. 8060–8063. doi: 10.1021/jp062095i.

Fievet, P. (2015) ‘Donnan Potential BT - Encyclopedia of Membranes’, in Drioli, E. and Giorno, L. (eds). Berlin, Heidelberg: Springer Berlin Heidelberg, pp. 1–3. doi: 10.1007/978-3-642-40872-4_1716-1.

Franci, G. *et al.* (2015) ‘Silver nanoparticles as potential antibacterial agents’, *Molecules*, 20(5), pp. 8856–8874. doi: 10.3390/molecules20058856.

Gliga, A. R. *et al.* (2014) ‘Size-dependent cytotoxicity of silver nanoparticles in human lung cells: the role of cellular uptake, agglomeration and Ag release’, *Particle and Fibre Toxicology*, 11(1), p. 11. doi: 10.1186/1743-8977-11-11.

Gogoi, S. K. *et al.* (2006) ‘Green fluorescent protein-expressing Escherichia coli as a model system for investigating the antimicrobial activities of silver nanoparticles’, *Langmuir*, 22(22), pp. 9322–9328. doi: 10.1021/la060661v.

Gouda, M. (2012) ‘Nano-zirconium oxide and nano-silver oxide/cotton gauze fabrics for antimicrobial and wound healing acceleration’, *Journal of Industrial Textiles*, 41(3), pp. 222–240. doi: 10.1177/1528083711414960.

Goy, R. C., Britto, D. de and Assis, O. B. G. (2009) ‘A review of the antimicrobial activity of chitosan’, *Polímeros*, 19(3), pp. 241–247. doi: 10.1093/jac/dkg286.

Guidelli, R. *et al.* (2014) ‘Defining the transfer coefficient in electrochemistry: An assessment (IUPAC Technical Report)’, *Pure and Applied Chemistry*, 86(2), pp. 245–258. doi: 10.1515/pac-2014-5026.

Gunalan, S., Sivaraj, R. and Rajendran, V. (2012) ‘Green synthesized ZnO nanoparticles against bacterial and fungal pathogens’, *Progress in Natural Science: Materials International*. Elsevier, 22(6), pp. 693–700. doi: 10.1016/j.pnsc.2012.11.015.

Guo, S. and Dipietro, L. A. (2010) ‘Factors Affecting Wound Healing’, *Obstetrics & Gynecology*, (Mc 859), pp. 219–229. doi: 10.1177/0022034509359125.

Haghighat, S. and Dawlaty, J. M. (2016) ‘pH Dependence of the Electron-Transfer Coefficient: Comparing a Model to Experiment for Hydrogen Evolution Reaction’, *Journal of Physical Chemistry C*, 120(50), pp. 28489–28496. doi: 10.1021/acs.jpcc.6b10602.

Hajipour, M. J. *et al.* (2012) ‘Coated Cotton Gauze with Ag/ZnO/chitosan Nanocomposite as a Modern Wound Dressing’, *Journal of Industrial Textiles*. Elsevier Ltd, 9(6), pp. 143–154. doi: 10.1155/2015/246012.

Hajipour, M. J., Fromm, K. M. and Ashkarran, A. (2012) ‘Antibacterial properties of nanoparticles’, *Trends in Biotechnology*. Elsevier Ltd, 30(10), pp. 499–511. doi: 10.1016/j.tibtech.2012.06.004.

Huh, A. J. and Kwon, Y. J. (2011) ‘“Nanoantibiotics”: A new paradigm for treating infectious diseases using nanomaterials in the antibiotics resistant era’, *Journal of Controlled Release*. Elsevier B.V., 156(2), pp. 128–145. doi: 10.1016/j.jconrel.2011.07.002.

I. Markova-Deneva (2010) ‘Infrared Spectroscopy Investigation of Metallic Nanoparticles Based on Copper, Cobalt, and Nickel Synthesized Through Borohydride Reduction Method’, *Journal of the University of Chemical Technology and Metallurgy*, 45(4), pp. 351–378.

Ijaz, F. *et al.* (2017) ‘Green synthesis of copper oxide nanoparticles using abutilon indicum leaf extract: Antimicrobial, antioxidant and photocatalytic dye degradation activities’, *Tropical Journal of Pharmaceutical Research*, 16(4), pp. 743–753. doi: 10.4314/tjpr.v16i4.2.

ISO (2007) ‘ISO 21348 Definitions of Solar Irradiance Spectral Categories’, *Environment*, (section 5), pp. 6–7.

Jain, K. K. (2007) ‘Applications of nanobiotechnology in clinical diagnostics’, *Clinical Chemistry*, 53(11), pp. 2002–2009. doi: 10.1373/clinchem.2007.090795.

Jemimah, V. H. and Arulpandi, I. (2014) ‘Evaluation of Antimicrobial Property of Biosynthesized Zinc Oxide Nanoparticles (ZnO NPs) and its Application on Baby Diapers’, 6(2), pp. 113–119.

Jin, T. *et al.* (2009) ‘Antimicrobial efficacy of zinc oxide quantum dots against Listeria monocytogenes, Salmonella Enteritidis, and Escherichia coli O157:H7’, *Journal of Food Science*, 74(1). doi: 10.1111/j.1750-3841.2008.01013.x.

John Kotz, Paul Treichel, J. T. (2009) *Chemistry and chemical reactivity .* 2nd edn, *Chemistry and chemical reactivity .* 2nd edn. Edited by Lisa Lockwood. Belmont: Brooks/Cole.

Joseph Wang (2006) *Analytical Electrochemistry*. 3rd edn. New Jersey: John Wiley and Sons.

Jyoti, K., Baunthiyal, M. and Singh, A. (2016) ‘Characterization of silver nanoparticles synthesized using Urtica dioica Linn. leaves and their synergistic effects with antibiotics’, *Journal of Radiation Research and Applied Sciences*. Elsevier Ltd, 9(3), pp. 217–227. doi: 10.1016/j.jrras.2015.10.002.

Kalimuthu, K. *et al.* (2008) ‘Biosynthesis of silver nanocrystals by Bacillus licheniformis’, *Colloids and Surfaces B: Biointerfaces*, 65(1), pp. 150–153. doi: https://doi.org/10.1016/j.colsurfb.2008.02.018.

Kang, X. *et al.* (2009) ‘Glucose Oxidase-graphene-chitosan modified electrode for direct electrochemistry and glucose sensing’, *Biosensors and Bioelectronics*, 25(4), pp. 901–905. doi: 10.1016/j.bios.2009.09.004.

Karim-Nezhad, G. *et al.* (2009) *Kinetic Study of Electrocatalytic Oxidation of Carbohydrates on Cobalt Hydroxide Modified Glassy Carbon Electrode*, *J. Braz. Chem. Soc.* doi: 10.1590/S0103-50532009000100022.

Kayani, Z. N. *et al.* (2012) ‘Synthesis and characterization of CuO nanowires by a simple wet chemical method’, *International Letters of Chemistry, Physics and Astronomy*. Springer Open Ltd, 14(1), pp. 26–36. doi: 10.1186/1556-276X-7-70.

Kayani, Z. N. *et al.* (2015) ‘Characterization of Copper Oxide Nanoparticles Fabricated by the Sol???Gel Method’, *Journal of Electronic Materials*, 44(10), pp. 3704–3709. doi: 10.1007/s11664-015-3867-5.

Khatoon, N. *et al.* (2015) ‘Biosynthesis, Characterization, and Antifungal Activity of the Silver Nanoparticles Against Pathogenic Candida species’, *BioNanoScience*, 5(2), pp. 65–74. doi: 10.1007/s12668-015-0163-z.

Khorsand Zak, A. *et al.* (2011) ‘Synthesis and characterization of a narrow size distribution of zinc oxide nanoparticles’, *International Journal of Nanomedicine*, 6(1), pp. 1399–1403. doi: 10.2147/IJN.S19693.

Kong, M. *et al.* (2010) ‘Antimicrobial properties of chitosan and mode of action: A state of the art review’, *International Journal of Food Microbiology*. Elsevier B.V., 144(1), pp. 51–63. doi: 10.1016/j.ijfoodmicro.2010.09.012.

Krishna Veni (2016) ‘Anti-Bacterial Coating of Chrysanthemum Extract on Bamboo Fabric for Healthcare Applications’, *Journal of Textile Science & Engineering*, 6(4), pp. 6–8. doi: 10.4172/2165-8064.1000267.

Krishnamoorthy, K. and Kim, S. J. (2013) ‘Growth, characterization and electrochemical properties of hierarchical CuO nanostructures for supercapacitor applications’, *Materials Research Bulletin*. Elsevier Ltd, 48(9), pp. 3136–3139. doi: 10.1016/j.materresbull.2013.04.082.

Kumar, H. and Rani, R. (2013) ‘Structural Characterization of Silver Nanoparticles Synthesized by Micro emulsion Route’, *International Journal of Engineering and Innovative Technology*, 3(3), pp. 344–348.

Kurien, S. (2005) ‘Chapter 4: ANALYSIS OF FTIR SPECTRA OF NANOPARTICLES of MgAl2O4, SrAl2O4, and NiAl2O4’, 1595, pp. 64–78. Available at: http://mgutheses.in/page/?q=T 1354&search=siby+kurien&page=1&rad=sc.

Laurent, D. and Schlenoff, J. B. (1997) ‘Multilayer Assemblies of Redox Polyelectrolytes’, *Langmuir*, 13(6), pp. 1552–1557. doi: 10.1021/la960959t.

Laviron, E. (1979) ‘General expression of the linear potential sweep voltammogram in the case of diffusionless electrochemical systems’, *Journal of Electroanalytical Chemistry and Interfacial Electrochemistry*, 101(1), pp. 19–28. doi: https://doi.org/10.1016/S0022-0728(79)80075-3.

Laviron, E. (1979) ‘General expression of the linear potential sweep voltammogram in the case of diffusionless electrochemical systems’, *Journal of Electroanalytical Chemistry*, 101(1), pp. 19–28. doi: 10.1016/S0022-0728(79)80075-3.

Laviron, E. (1995) ‘The use of polarography and cyclic voltammetry for the study of redox systems with adsorption of the reactants. Heterogeneous vs. surface path’, *Journal of Electroanalytical Chemistry*, 382(1–2), pp. 111–127. doi: 10.1016/0022-0728(94)03684-U.

Lionelli, G. T. and Lawrence, W. T. (2003) ‘Wound dressings’, *Surgical Clinics of North America*, pp. 617–638.

Liu, B. *et al.* (2013) ‘Adsorption of heavy metal ions, dyes and proteins by chitosan composites and derivatives --- A review’, *Journal of Ocean University of China*, 12(3), pp. 500–508. doi: 10.1007/s11802-013-2113-0.

Logothetidis, S. (2012) *Nanotechnology : Principles and Applications*. doi: 10.1007/978-3-642-22227-6.

Long, J. *et al.* (2016) ‘A new class of nanocomposites of Zn–Al–Bi layered double oxides: large reversible capacity and better cycle performance for alkaline secondary batteries’, *RSC Adv.* Royal Society of Chemistry, 6(95), pp. 92896–92904. doi: 10.1039/C6RA18164C.

Lović, J. (2017) ‘Glucose Sensing Using Glucose Oxidase-Glutaraldehyde- Cysteine Modified Gold Electrode’, *International Journal of Electrochemical Science*, (July), pp. 5806–

5817. doi: 10.20964/2017.07.65.

Luna, I. Z. *et al.* (2015) ‘Preparation and Characterization of Copper Oxide Nanoparticles Synthesized via Chemical Precipitation Method’, *OALib*, 2(3), pp. 1–8. doi: 10.4236/oalib.1101409.

Ma, A. *et al.* (2011) ‘Evaluation of antibacterial activity of silver nanoparticles against MSSA and MRSA on isolates from skin infections’, *Research Article Biology and Medicine*, 3(2), pp. 141–146.

Malinowska-Pańczyk, E. *et al.* (2009) ‘The combined effect of moderate pressure and chitosan on Escherichia coli and Staphylococcus aureus cells suspended in a buffer and on natural microflora of apple juice and minced pork’, *Food Technology and Biotechnology*, 47(2), pp. 202–209.

Maneerung, T., Tokura, S. and Rujiravanit, R. (2008) ‘Impregnation of silver nanoparticles into bacterial cellulose for antimicrobial wound dressing’, *Carbohydrate Polymers*, 72(1), pp. 43–51. doi: 10.1016/j.carbpol.2007.07.025.

Mansoori, G. A. (2005) ‘Principles of Nanotechnology: Molecular Based Study of Condensed Matter in Small Systems’. doi: 10.1142/5749.

Mazloum-ardakani, M. *et al.* (2010) ‘Voltammetric Determination of Dopamine at the Surface of TiO 2 Nanoparticles Modified Carbon Paste Electrode’, 5, pp. 147–157.

Meftahi, A. *et al.* (2010) *The effects of cotton gauze coating with microbial cellulose*, *Cellulose*. doi: 10.1007/s10570-009-9377-y.

Mehta, B. K., Chhajlani, M. and Shrivastava, D. (2017) ‘Green synthesis of silver nanoparticles and their characterization by XRD’, *Frontiers of Physics and Plasma Science IOP Publishing IOP Conf. Series: Journal of Physics: Conf. Series*, 836. doi: 10.1088/1742-6596/836/1/012050.

Mohammad, F., A. Al-Lohedan, H. and N. Al-Haque, H. (2016) ‘Chitosan-mediated fabrication of metal nanocomposites for enhanced biomedical applicationsf’, *Advanced Materials Letters*, 8(2), pp. 89–100. doi: 10.5185/amlett.2017.6925.

Mohan, A. C. and Renjanadevi, B. (2016) ‘Preparation of Zinc Oxide Nanoparticles and its Characterization Using Scanning Electron Microscopy (SEM) and X-Ray Diffraction(XRD)’, *Procedia Technology*. Elsevier B.V., 24, pp. 761–766. doi: 10.1016/j.protcy.2016.05.078.

Muthukrishnan, A. M. (2015) ‘Green Synthesis of Copper-Chitosan Nanoparticles and Study of its Antibacterial Activity’, *Journal of Nanomedicine & Nanotechnology*, 6(1), pp. 1–6. doi: 10.4172/2157-7439.1000251.

Muzzarelli, R. (1973) *Natural chelating polymers; alginic acid, chitin, and chitosan*. 1st edn. Oxford: Pergamon press.

Muzzarelli, R. A. and Sipos, L. (1971) ‘Chitosan for the collection from seawater of naturally occurring zinc, cadmium, lead and copper’, *Talanta*, 18(9), p. 853—858. doi: 10.1016/0039-9140(71)80141-8.

Nam, H. C. and Schaak, R. E. (2007) ‘Shape-controlled conversion of ??-Sn nanocrystals into intermetallic M-Sn (M = Fe, Co, Ni, Pd) nanocrystals’, *Journal of the American Chemical Society*, 129(23), pp. 7339–7345. doi: 10.1021/ja069032y.

Norfazila, S. M. and Mohd, J. R. (2014) ‘Synthesis and Ultroviolet Visible Spectroscopy Studies of Chitosan Capped Gold Nanoparticles and Theri Reactions with Analytes’, *The Scientific World Journal*, 2014, p. 7. doi: http://dx.doi.org/10.1155/2014/184604.

Okumu, F. and Matoetoe, M. (2016) ‘Electrochemical Characterization of Silver-Platinum Various Ratio Bimetallic Nanoparticles Modified Electrodes’, *Journal of Nano Research*, 44, pp. 114–125. doi: 10.4028/www.scientific.net/JNanoR.44.114.

Olaniyan, O. J. *et al.* (2016) ‘Synthesis and Characterization of Chitosan-Silver Nanocomposite Film’, *Nano Hybrids and Composites*, 11, pp. 22–29. doi: 10.4028/www.scientific.net/NHC.11.22.

Ono, S. *et al.* (2015) ‘Increased wound pH as an indicator of local wound infection in second degree burns’, *Burns*. Elsevier Ltd and International Society of Burns Injuries, 41(4), pp. 820–824. doi: 10.1016/j.burns.2014.10.023.

Padil, V. and Cernik, M. (2013) *Green synthesis of copper oxide nanoparticles using gum karaya as a biotemplate and their antibacterial application*, *International journal of nanomedicine*. doi: 10.2147/IJN.S40599.

Paladini, F. *et al.* (2016) ‘In vitro assessment of the antibacterial potential of silver nano-coatings on cotton gauzes for prevention of wound infections’, *Materials*, 9(6), pp. 1–14. doi: 10.3390/ma9060411.

Panchakarla, L. S., Govindaraj, A. and Rao, C. N. R. (2007) ‘Formation of ZnO nanoparticles

by the reaction of zinc metal with aliphatic alcohols', *Journal of Cluster Science*, 18(3), pp. 660–670. doi: 10.1007/s10876-007-0129-6.

Pankratov, D. V. *et al.* (2014) 'Impact of surface modification with gold nanoparticles on the bioelectrocatalytic parameters of immobilized bilirubin oxidase', *Acta Naturae*, 6(20), pp. 102–106.

Patrulea, V. *et al.* (2015) 'Chitosan as a starting material for wound healing applications', *European Journal of Pharmaceutics and Biopharmaceutics*. Elsevier B.V., 97, pp. 417–426. doi: 10.1016/j.ejpb.2015.08.004.

Paul, H. J. and Leddy, J. (1995) 'Direct Determination of the Transfer Coefficient from Cyclic Voltammetry: Isopoints as Diagnostics', *Analytical Chemistry*, 67(10), pp. 1661–1668. doi: 10.1021/ac00106a003.

de Paz, L. E. C. *et al.* (2011) 'Antimicrobial effect of chitosan nanoparticles on Streptococcus mutans biofilms', *Applied and Environmental Microbiology*, 77(11), pp. 3892–3895. doi: 10.1128/AEM.02941-10.

Pinho, E. *et al.* (2011) 'Antimicrobial activity assessment of textiles: Standard methods comparison', *Annals of Microbiology*, 61(3), pp. 493–498. doi: 10.1007/s13213-010-0163-8.

Prodomis, M. I. *et al.* (2000) 'The Importance of Surface Coverage in the Electrochemical Study of Chemically Modified Electrodes', *Electroanalysis*, 12(18), pp. 1498–1501.

Puchalski, M. *et al.* (2007) 'The study of silver nanoparticles by scanning electron microscopy, energy dispersive X-ray analysis and scanning tunnelling microscopy', *Materials Science-Poland*, 25(2), pp. 473–478.

Raafat, D. and Sahl, H. G. (2009) 'Chitosan and its antimicrobial potential - A critical literature survey', *Microbial Biotechnology*, 2(2 SPEC. ISS.), pp. 186–201. doi: 10.1111/j.1751-7915.2008.00080.x.

Radecka, M. *et al.* (2008) 'Importance of the band gap energy and flat band potential for application of modified TiO2 photoanodes in water photolysis', *Journal of Power Sources*, 181(1), pp. 46–55. doi: https://doi.org/10.1016/j.jpowsour.2007.10.082.

Raghupathi, K. R., Koodali, R. T. and Manna, A. C. (2011) 'Size-dependent bacterial growth inhibition and mechanism of antibacterial activity of zinc oxide nanoparticles.', *Langmuir : the ACS journal of surfaces and colloids*, 27(7), pp. 4020–4028. doi: 10.1021/la104825u.

Rahman, A. *et al.* (2009) 'SYNTHESIS OF COPPER OXIDE NANO PARTICLES BY USING Phormidium cyanobacterium', *Indonesian Journal of Chemistry*, 9(3), pp. 355–360.

Rai, M., Yadav, A. and Gade, A. (2009) 'Silver nanoparticles as a new generation of antimicrobials', *Biotechnology Advances*. Elsevier Inc., 27(1), pp. 76–83. doi: 10.1016/j.biotechadv.2008.09.002.

Ravichandran, S. *et al.* (2015) 'A novel approach for the biosynthesis of silver oxide nanoparticles using aqueous leaf extract of Callistemon lanceolatus (Myrtaceae) and their therapeutic potential', *Journal of Experimental Nanoscience*. Taylor & Francis, 8080(August), pp. 1–14. doi: 10.1080/17458080.2015.1077534.

Rhazi, M. *et al.* (2002) 'Influence of the nature of the metal ions on the complexation with chitosan.: Application to the treatment of liquid waste', *European Polymer Journal*, 38, pp. 1523–1530.

Rhoades, J. and Roller, S. (2000) 'Antimicrobial actions of degraded and native chitosan against spoilage organisms in laboratory media and foods', *Applied and Environmental Microbiology*, 66(1), pp. 80–86. doi: 10.1128/AEM.66.1.80-86.2000.

Richards, R. and Bonnemann, H. (2005) 'Synthetic Approaches to Metallic Nanomaterials', *Nanofabrication Towards Biomedical Applications: Techniques, Tools, Applications, and Impact*, pp. 1–32. doi: 10.1002/3527603476.ch1.

Salehi, R. *et al.* (2010) 'Novel biocompatible composite (Chitosan-zinc oxide nanoparticle): Preparation, characterization and dye adsorption properties', *Colloids and Surfaces B: Biointerfaces*. Elsevier B.V., 80(1), pp. 86–93. doi: 10.1016/j.colsurfb.2010.05.039.

Sanpui, P. *et al.* (2008) 'The antibacterial properties of a novel chitosan-Ag-nanoparticle composite', *International Journal of Food Microbiology*, 124(2), pp. 142–146. doi: 10.1016/j.ijfoodmicro.2008.03.004.

Santos, C. L. *et al.* (2013) 'Nanomaterials with Antimicrobial Properties : Applications in Health Sciences', *Microbial pathogens and strategies for combating them: science, technology and education*, 1, pp. 143–154.

Sanyal, M. K., Datta, A. and Hazra, S. (2002) 'Morphology of nanostructured materials', *Pure and Applied Chemistry*, 74(9), pp. 1553–1570. doi: 10.1351/pac200274091553.

Schlenoff, J. B., Ly, H. and Li, M. (1998) 'Charge and Mass Balance in Polyelectrolyte

Multilayers - Journal of the American Chemical Society (ACS Publications)', *Journal of the American Chemical …*, 7863(13), pp. 7626–7634. doi: 10.1021/ja980350.

Sehat, A. A. *et al.* (2015) 'Fast immobilization of glucose oxidase on graphene oxide for highly sensitive glucose biosensor fabrication', *International Journal of Electrochemical Science*, 10(1), pp. 272–286.

Seil, J. T. and Webster, T. J. (2012) 'Antimicrobial applications of nanotechnology: Methods and literature', *International Journal of Nanomedicine*, 7, pp. 2767–2781. doi: 10.2147/IJN.S24805.

Sezer, A. D. and Cevher, E. (1992) 'Biopolymers as Wound Healing Materials: Challenges and New Strategies', *Biomaterials Applications for Nanomedicine*, pp. 383–414. doi: 10.5772/25177.

Shen, X. S. *et al.* (2009) 'Nanospheres of silver nanoparticles: agglomeration, surface morphology control and application as SERS substrates', *Physical Chemistry Chemical Physics*. The Royal Society of Chemistry, 11(34), pp. 7450–7454. doi: 10.1039/B904712C.

Shrivastava, S. *et al.* (2010) 'Characterization of enhanced antibacterial effects of novel silver nanoparticles', *Nanotechnology*, 18(22), pp. 1–9. doi: 10.1088/0957-4484/18/22/225103.

Sirkka, T., Skiba, J. B. and Apell, S. P. (2016) 'Wound pH depends on actual wound size', p. 13.

Srivastava, S., Agrawal, A. and Kumar, S. (2013) 'Synthesis and Characterisation of Copper Oxide nanoparticles', *Journal of Applied Physics*, 5(4), pp. 61–65.

Street, E. and Lake, C. (2014) 'Aatcc t', pp. 2012–2015.

Sudheesh Kumar, P. T. *et al.* (2012) 'Flexible and microporous chitosan hydrogel/nano ZnO composite bandages for wound dressing: In vitro and in vivo evaluation', *ACS Applied Materials and Interfaces*, 4(5), pp. 2618–2629. doi: 10.1021/am300292v.

Sudheesh Kumar, P. T. *et al.* (2013) 'Evaluation of wound healing potential of β-chitin hydrogel/nano zinc oxide composite bandage', *Pharmaceutical Research*, 30(2), pp. 523–537. doi: 10.1007/s11095-012-0898-y.

Sun, K. and Li, Z. H. (2011) 'Preparations, properties and applications of chitosan based nanofibers fabricated by electrospinning', *Express Polymer Letters*, 5(4), pp. 342–361. doi: 10.3144/expresspolymlett.2011.34.

Sutherland, L. F. and D. (2012) *Nanotechnologies: Principles, Applications, Implications and Hands-on Activities*. doi: :10.2777/76945.

Talam, S., Karumuri, S. R. and Gunnam, N. (2012) 'Synthesis, Characterization, and Spectroscopic Properties of ZnO Nanoparticles', *ISRN Nanotechnology*, 2012, pp. 1–6. doi: 10.5402/2012/372505.

Tamayo, L. *et al.* (2016) 'Copper-polymer nanocomposites: An excellent and cost-effective biocide for use on antibacterial surfaces', *Materials Science and Engineering C*. Elsevier B.V., 69, pp. 1391–1409. doi: 10.1016/j.msec.2016.08.041.

Teterycz, H. *et al.* (2014) 'Deposition of Zinc Oxide on the Materials Used in Medicine. Preliminary Results', *FIBRES & TEXTILES in Eastern Europe*, 22(105), pp. 3–126.

Tikhonov, V. E. *et al.* (2006) 'Bactericidal and antifungal activities of a low molecular weight chitosan and its N-/2(3)-(dodec-2-enyl)succinoyl/-derivatives', *Carbohydrate Polymers*, 64(1), pp. 66–72. doi: 10.1016/j.carbpol.2005.10.021.

Tran, D. L. *et al.* (2011) 'Some biomedical applications of chitosan-based hybrid nanomaterials', *Advance in Natural Science: Nanoscience Nanotechnology*, 2, pp. 1–6. doi: 10.1088/2043-6262/2/4/045004.

Tran, T. H. and Nguyen, V. T. (2014) 'Copper Oxide Nanomaterials Prepared by Solution Methods, Some Properties, and Potential Applications: A Brief Review', *International Scholarly Research Notices*. Hindawi Publishing Corporation, 2014, pp. 1–14. doi: 10.1155/2014/856592.

Umesh, Kathad; Gajera, H. . (2014) 'Synthesis of copper nanoparticles by two different methods and size comparison', *Int J Pharm Bio Sci*, 5(1), pp. 978–982.

Usman, M. S. *et al.* (2012) 'Copper nanoparticles mediated by chitosan: Synthesis and characterization via chemical methods', *Molecules*, 17(12), pp. 14928–14936. doi: 10.3390/molecules171214928.

Valov, I. and Lu, W. D. (2016) 'Nanoscale electrochemistry using dielectric thin films as solid electrolytes', *Nanoscale*. The Royal Society of Chemistry, 8(29), pp. 13828–13837. doi: 10.1039/C6NR01383J.

Vaseeharan, B., Sivakamavalli, J. and Thaya, R. (2015) 'Synthesis and characterization of chitosan-ZnO composite and its antibiofilm activity against aquatic bacteria', *Journal of*

Composite Materials, 49(2), pp. 177–184. doi: 10.1177/0021998313515289.

Velasco, J. G. (1997) 'Determination of standard rate constants for electrochemical irreversible processes from linear sweep voltammograms', *Electroanalysis*, 9(11), pp. 880–882. doi: 10.1002/elan.1140091116.

Wang, X. *et al.* (2005) 'Chitosan- metal complexes as antimicrobial agent: Synthesis, characterization and Structure-activity study', *Polymer Bulletin*, 55(1–2), pp. 105–113. doi: 10.1007/s00289-005-0414-1.

Wang, Z. L. (2004) 'Zinc oxide nanostructures: growth, properties and applications', *Journal of Physics: Condensed Matter*, 16(25), pp. R829–R858. doi: 10.1088/0953-8984/16/25/R01.

Wei, D. *et al.* (2009) 'The synthesis of chitosan-based silver nanoparticles and their antibacterial activity', *Carbohydrate Research*. Elsevier Ltd, 344(17), pp. 2375–2382. doi: 10.1016/j.carres.2009.09.001.

Wicramarachchi, P. and Hettiarachchi, M. (2011) 'Synthesis of chitosan stabilised silver nanoparticles using gamma ray radiation and characterisation', *Jousrnal of Scinece*, 6, pp. 65–75.

Xiliang, Q. *et al.* (2014) 'Large-Scale Synthesis of Silver Nanoparticles by Aqueous Reduction for Low-Temperature Sintering Bonding', 2014.

Xiong, G. *et al.* (2006) 'Photoluminescence and FTIR study of ZnO nanoparticles: The impurity and defect perspective', *Physica Status Solidi (C) Current Topics in Solid State Physics*, 3(10), pp. 3577–3581. doi: 10.1002/pssc.200672164.

Yukna, J. (Souther. I. U. at C. . (2014) 'International Journal of Nano Dimension Synthesis and characterization of Copper and Copper Oxide nanoparticles by thermal decomposition method', *Thesis paper*, 5(4), pp. 321–327.

Zhang, L., Zeng, Y. and Cheng, Z. (2016) 'Removal of heavy metal ions using chitosan and modified chitosan: A review', *Journal of Molecular Liquids*. Elsevier B.V., 214, pp. 175–191. doi: 10.1016/j.molliq.2015.12.013.

Zhou, E., Hashimoto, K. and Tajima, K. (2013) 'Low band gap polymers for photovoltaic device with photocurrent response wavelengths over 1000 nm', *Polymer (United Kingdom)*. Elsevier Ltd, 54(24), pp. 6501–6509. doi: 10.1016/j.polymer.2013.09.058.

CHAPTER TWO
LITERATURE REVIEW

2.1. Modified antibacterial wound dressings

This chapter explores and reviews the literature on the use of nanoparticles and chitosan as wound healing and bactericidal agents. The evolution of nanoparticles and chitosan as modern day healing agents is highlighted and their applications are discussed. The mechanism of the nanoparticles and their use in wound gauze modification is explored with relevance to their bactericidal and wound healing potential.

Wound dressings are strategic and of imminence in the maintenance of good wound healing rate on the human body. Types of wound dressings vary according to use however any wound gauze should generally be able to prevent infection, relieve pain, retain moisture, exudate and facilitate autolytic debridement (Lionelli and Lawrence, 2003). Most textile wound dressings have excellent moisture extrusion and retention properties however this creates a lucrative growth environment for bacteria within the warm moist dressing(Sun and Li, 2011). The wound dressings have ability to keep out bacteria however they create an environment that could breed bacteria around the wound. A method to maintain the benefits of the wound dressing yet eliminating its adverse ability to harbour and breed bacteria is to modify the wound dressing thereby making it chemo-active. Making the dressing chemo-active ensures the elimination of harmful bacteria in and around the wound cavity yet maintaining the utility of the wound gauze. The agents used to modify the wound gauzes should be able to undergo their mechanism of action without detrimentally altering the normal utility of the wound gauze. Modification of wound gauzes have been done before using organic material such as collagen, chitin, chitosan and cellulose (Feng *et al.*, 2000). Metallic nanoparticles have also been used to modify wound gauzes in the presence of an adherent agent or polymer (Hajipour *et al.*, 2012). Both inorganic and organic modification agents pose distinct advantages and disadvantages. Developing hybrid wound gauze containing both antibacterial organic and inorganic material helps scale down the disadvantages of both the later and the former yet creating a beneficial synergetic effect. Bactericidal activity, curative effects and wound gauze utility is increased significantly when the wound gauze is modified using organic-inorganic hybrids or composites (Sanpui *et al.*, 2008; Ali, Rajendran and Joshi, 2011; Hajipour *et al.*, 2012; Sutherland, 2012).

2.2. Nanoparticles

Nanotechnology has been emerging as one of the most studied technology in the past

decades due to its versatility in utility and potential. Nanotechnology is a branch of science that deals with particles of about one billionth of a meter (10^{-9}M) in size and has particles within the range of 1-100nm (Xiong *et al.*, 2006) (Mansoori, 2005). The material functions on the basis of manipulating matter at molecular and atomic level such that it exhibits enhanced performance due to increased surface area ratio to volume. Matter usually has a degree of consistency in its properties throughout most sizes but this is not so for nanoparticles size. Their relatively very small size gives them the ability to have other characteristics that are not normally found in their bulk material. The nanoparticles exhibit unexpected characteristics due to their large surface area per volume ratio and also to their relatively small size which causes quantum effects to dominate (Franci *et al.*, 2015). It is however of preeminent consideration that nanoparticles do not only have unique abilities and properties due to its small particle size but also due to the various morphological states the nanoparticles can take (Wang *et al.*, 2005). Unique and profound properties such as plasmon resonance, diverse refractive index, photoluminescence properties and high transparency, give nanoparticles and their composites/hybrids a cutting edge in their application and uses (Jain, 2007). This phenomenon has caused them to possess multi-applicatory attributes with their applications ranging from electronic use, medicinal, imaging, food, fuel cells, and water and air treatment. Nanoparticles have assumed novelty in most of the areas that they are applied and they prove to have a degree of efficacy when applied within appropriate conditions and parameters.

In medicine nanoparticles has been used extensively in applications such as chemotherapy, as sensors, dialysis, therapeutic diagnosis, and drug delivery. Not all nanoparticles are biologically active and this creates a divide in nanoparticles that can be used as bactericidal or bacteriostatic agents.

2.2.1. Nanoparticles as antimicrobial agents

In the past the use of nanoparticles for bacterial control has been on a smaller scale and their properties have proved to show better signs of effectiveness than other convectional anti-bacterial methods (Seil and Webster, 2012). The nanoparticles used as bactericidal or antibiotic agents should be biologically active and can be either inorganic or organic in nature. Metallic elements such as copper, zinc, titanium and silver which have notable antibiotic properties in their bulk form have been used in the past for the treatment of mild infections and as bacterial prophylaxis agents both internally and also in the epidermal cavity (Seil and Webster, 2012). It is then expected that as these naturally antibacterial metals approach their nano size range, they should have an increased bactericidal effect since the surface area to volume ratio increase as size decreases. Other metallic elements like iron

are not bactericidal in their bulk form but yet they exhibit bactericidal effects as their size goes below 80nm and this makes them potential bactericidal agents (Alvarez and Lowry, 2009; Hajipour *et al.*, 2012). This takes into account the hypothesis that bactericidal capability of the nanoparticles is dependent on the surface area to volume ratio of the nanoparticles particles and their morphology. Therefore, these nano-scale attributes of metallic nanoparticles pose great potential for their use as modern day antibiotics. Studies show that different types of metallic nanoparticles behave differently towards the vast species of bacteria available (Hajipour *et al.*, 2012; Santos *et al.*, 2013). The bactericidal efficacy of the nanoparticles against different positive gram and negative gram bacteria have to be evaluated in order to appropriate the different metallic nanoparticles with the bacteria they can effectively combat. Metallic metals that have been investigated vastly as potential antibiotics are silver, zinc, copper, gold, aluminium, titanium and iron (Huh and Kwon, 2011; Santos *et al.*, 2013). Besides the efficacy factor, the issues of relative toxicity and also relative economics come into play. It is more favourable for the nanoparticles that are economic in terms of synthesis and production to be used as an antibiotic in order to prevent the economic cons out-weighing the advantages of the nanoparticles as bactericidal agents. Toxicity of nanoparticles is also an issue of paramount concern, since it is desired that the nanoparticles effectively combat the bacteria yet exerting minimal adverse effects on the hosts' cells and tissue. Some nanoparticles are bactericidal but however it can be aggressive in mechanism of action such that they damage the cells of the host or patient being treated. These types of nanoparticles are classified as host cytotoxic since they do not only attack the target bacteria but they also attack the cells and tissue of the host.

Metallic nanoparticles have been used in the past for trial runs as bactericidal agents due to their economic advantage and also because their methods of synthesis have been established and can be carried out economically. However, studies have been carried out in the possibility of using organic nanoparticles as bactericidal agents. Organic nanoparticles offer more advantages than the metallic agents because they are biodegradable, nontoxic and they are sustainable. Organic polymeric nanoparticles operate using various mechanisms in their way as antimicrobials. They usually eliminate and exert stasis on bacteria by releasing antimicrobial peptides, general antibiotics, alkyl pyridines and quaternary ammonium or phosphonium (Beyth *et al.*, 2015). It is proposed that the cationic species released by the organic matter attacks the peptoglycogen structure of the cell wall disrupting it, consequently causing rapture and lysis (Beyth *et al.*, 2015). Organic nanoparticles has been favoured because it has therapeutic properties which help in wound healing when applied to an open wound directly (Hajipour *et al.*, 2012). Some organic nanoparticles are not effective as metallic nanoparticles bactericidal agents but they are

effective as inhibitory agents. This means that it does not necessarily eliminate the bacteria but rather it inhibits and immobilizes bacteria from further growth and operation. These are used for sensitive cavities where mild bactericidal remedies are desired to minimise any possible damage to host tissue.

Nanoparticles have shown remarkable bactericidal and bacteriostatic effects in bacterium that has been previously resistant to conventional antibiotics (Maneerung, Tokura and Rujiravanit, 2008). This has placed them as potential bactericidal agents since they have exhibited high complementarity to present antibiotics. Assuming that the nature and structure of the metallic and organic nanoparticles used for the development of the antibiotics will make it difficult for the microorganisms to develop bactericidal resistance. The mechanism against bacteria for the various nanoparticles differs from one material to another but their bactericidal strength lies in their large surface area to volume ratio which makes the particles very reactive and also small enough to penetrate through cyto-pores of bacterial cell walls. The morphology of the particular nanoparticles has shown to affect the effectiveness and efficacy of the nanoparticles in the elimination of bacteria (Gunalan, Sivaraj and Rajendran, 2012). The bactericidal effects of nanoparticles have also been shown to be influenced by the type, dimensions and shape of the nanoparticles (Seil and Webster, 2012) The methods of administration of nanoparticles as complementary bactericides are broad due to their relative solubility and ability to be incorporated in composites and hybrids with other material. As bactericidal agents, nanoparticles have been incorporated in creams, ointments and epidermal fluids (Santos *et al.*, 2013). Metal oxide nanoparticles have been used for the modification of textiles functionalizing the textiles to be antimicrobial cloths which are used for in the specialised industry such as food manufacturing or biotechnology.

2.2.2. Zinc oxide as antimicrobial nanoparticles

Zinc oxide nanoparticles have shown to be a broad spectrum bactericidal agent in previous studies and this has made it to be considered as a potential alternative bactericidal agent (Raghupathi, Koodali and Manna, 2011). Zinc oxide in bulk form is a natural bactericidal agent that has been used in the past in epidermal creams and ointments. These bactericidal properties increase as the zinc material decreases in size. Zinc nanoparticles are favoured as bactericidal agents due to their cost effectiveness and relative efficacy against a wide range of bacteria (Huh and Kwon, 2011). Zinc nanoparticles have shown through studies that they have remarkable efficacy as a bacteriostatic and as a bactericide with different types of bacteria flora that is pathogenic to humans (Gunalan, Sivaraj and Rajendran, 2012). An *in vitro* study on the efficacy of zinc against common enteric bacteria pathogens showed notable efficacy of zinc against enteric bacteria pathogens (Faiz *et al.*, 2011). The study also

revealed the compatibility and suitability of the internal use of zinc nanoparticles in the human body. The minimum inhibitory concentrations ranged from 0.2300 to 0.4700 mg/L of zinc oxide in sterile water. The study established the approximate concentration range of zinc nanoparticles that can be introduced into the human body to combat bacteria without causing adverse effects to the human body. However internal use concentrations and open epidermal application concentrations can differ due to the different tissue of the two different applications. Spores, which are one of the major causes of bacteria resistance to antibiotics, do not affect the efficacy of zinc oxide particles thereby making the zinc oxide effective against some drug resistant bacteria (Jemimah and Arulpandi, 2014). Zinc nanoparticles behave differently with the different species of bacteria it is exposed to and this is attributed to the diverse mechanisms of action that the nanoparticles engage with different bacteria (Wang *et al.*, 2005). The type of mechanism is influenced greatly by the type and structure of the target bacteria. Zinc nanoparticles operate by mainly affecting the metabolic pathways of the bacteria cells. They induce the formation of reactive oxygen species (ROS) and they are also known for binding to membranes causing disruption and integrity in the membrane system (Jin *et al.*, 2009). It has also been observed that the efficacy of zinc oxide nanoparticles is size-based and it increases as the size of the nanoparticles decreases (Raghupathi, Koodali and Manna, 2011). Zinc has been applied in textiles before in the study of antimicrobial clothing and textiles. Deposition on zinc oxide on textiles can be done either using an alcohol solvent or by using a polymer adherent (Teterycz *et al.*, 2014). If the study to be done is specifically for zinc nanoparticles alcohol cannot be used to keep the influence of the results attributed to zinc only. The use of a polymer requires the choice of an activity neutral polymer such that results achieved during the study can be fully attributed to the activity of the zinc nanoparticles only. Polymer deposition is favoured due to its high adherence levels and minimal deposition time. A nano zinc oxide β-chitin hydrogel hybrid gauze used in an *in vivo* study using albino rats infected with *Staphylococcus aureus* and *Escherichia coli* showed that besides aiding in blood clotting on the wound, the composite gauze showed a high degree of bactericidal efficacy against the pathogens at low concentrations (Sudheesh Kumar *et al.*, 2013). The efficacy can be attributed to the synergetic effect that emerges from the combination of chitin and zinc oxide nanoparticles. The chitin seems to cover the area of bactericidal spectrum that zinc oxide does not cover and zinc oxide also does the same for chitin. This enables the two bactericidal agents to cover a wider spectrum than they would cover at individual capacities. The stability of zinc oxide and its straightforward synthesis methods add to the advantages that make zinc oxide nanoparticles a lucrative alternative bactericidal agent in wound healing.

2.2.3. Silver as antimicrobial nanoparticles

Silver has been used as a mild bactericidal agent in its bulk form in the past years. It has been used effectively against bacteria and fungi and it exhibited above average efficacies compared to other metals (Khatoon *et al.*, 2015). The activity and efficacy of silver as an antimicrobial is size dependant with the higher efficacies being experienced as the size of the silver nanoparticles decreases (Rai, Yadav and Gade, 2009). The mechanistic pathway of silver nanoparticles against bacteria varies and is dependent on bacteria species. The major mechanisms of action that silver nanoparticles uses against bacteria are attack of the cell wall and the inhibition of RNA and DNA replication (Feng *et al.*, 2000; Rai, Yadav and Gade, 2009). Silver nanoparticles are known to be abrasive to the cell wall and this gives them the ability to disrupt the proteins in the cell wall thereby causing disintegration and consequently lysis. Silver nanoparticles attach to the RNA and DNA in the bacteria cell causing irregular amino acid orientation and thereby successfully inhibiting both DNA and RNA replication. Silver nanoparticles shows bactericidal activity against both gram positive and gram negative bacterium from concentrations of 10 µg/mL and this indicates that the bactericidal spectrum of silver nanoparticles is wider than most metallic nanoparticles (Seil and Webster, 2012). Its broad spectrum trait can be enhanced by administering it alongside conventional antibiotics where the two produce synergetic bactericidal effects (Atiyeh *et al.*, 2007). Silver is ideal for prophylaxis purposes since it has a relatively low toxicity to bactericidal ratio. Silver nanoparticles can be used to coat wound gauzes as a prophylaxis antibiotic agent and studies have shown it to reduce bacterial and fungal colonies by 90% (Gouda, 2012) (Paladini *et al.*, 2016). This phenomenon can be explained chemically by understanding that silver nanoparticles have the ability to ionize and release silver ions into any cavity or medium they are in (Rai, Yadav and Gade, 2009). The silver ions are abrasive to the bacterial cell wall and interfere with DNA/RNA replication. The various advantages of silver nanoparticles make them potential alternative bacterial agents in wound healing. Cotton wound gauzes coated with silver nanoparticles prove to be a potential effective alternative to conventional untreated wound gauzes.

2.2.4. Copper as antimicrobial nanoparticles

Bulk copper exhibits antimicrobial properties though it has been noted that it has lower fervency than zinc oxide and silver (Beyth *et al.*, 2015). The mechanism of action of copper nanoparticles is suggested to operate by disruption of enzymes thereby impairing metabolically respiratory pathways leading to activator deficiency and eventually fatality of bacterial cell (Tamayo *et al.*, 2016). This disruption of enzyme activity can be attributed to the ions Cu^{2+} and Cu^{+} which are released when CuO ions dissolve in media with pH > 6. Copper

nanoparticles are active against both gram positive and gram negative bacteria though due to its low bactericidal fervency, a higher dosage of it has to be used in order to effectively immobilize and eradicate bacterial activity (Tamayo *et al.*, 2016). However copper nanoparticles are selective in its bactericidal activity as studies have shown that it exhibits significantly different efficacies for different types of bacterium at the same dosage (Applerot *et al.*, 2012). Copper nanoparticles could emerge as a lucrative bactericidal material since it is relatively cheap and less toxic than silver and zinc nanoparticles (Tamayo *et al.*, 2016). Copper nanoparticles are effective bactericide to be used in areas where mild bactericide operating conditions are required. Higher dosages of the nanoparticles can be used with relatively less adverse effects on the host's tissue and cell structure.

Table 2. 1 Summary of mechanism of action and bacterial specie response NPs.

NPs	Mechanism of action.	Responsive Species	References
ZnO	• Electrostatic interaction • Accumulation of ZnO in cytoplasm • Increase in membrane permeability	*Bacillus subtilis* *Escherichia coli* *Listeria monocytogenes* *Staphylococcus aureus (MRSE)* *S. epidermis* *S.aureus (MRSA)*	Abbasipour et al. 2014 Seil & Webster 2012 Raghupathi et al. 2011; Huh & Kwon 2011
Ag	•Electrostatic interactions caused by Ag^{+}. •Abrasive damage on cell wall. • Plasmic membrane rupture. •Disruption of biochemical processes.	*Escherichia coli* *Pseudomonas fluorescens* *S.aureus*	Hajipour et al. 2012; Franci et al. 2015; Khatoon et al. 2015
CuO	• Decreased enzymatic activity • NADPH production • Cell membrane damage	*E. coli* *S. aureus* *B. subtilis* *B. anthracis*	Beyth et al. 2015 Hajipour, Fromm & Ashkarran 2012

2.3. Chitosan

Chitosan [poly-(b-1/4)-2-amino-2-deoxy-D-glucopyranose] is a polysaccharide of acetylated chitin products that is found in nature and readily extracted from a diversity of plants and sea creatures. It's relatively abundant and its earth abundance comes second after cellulose, making it cost effective and available (Azuma *et al.*, 2015). This gives it vast applicatory status with applications in agriculture, food, cosmetics, water treatment, textile, and pharmaceutical industries. It is bactericidal, non-toxic, biocompatible and biodegradable hence a considerable choice for modern day antibiotics (Hajipour *et al.*, 2012).

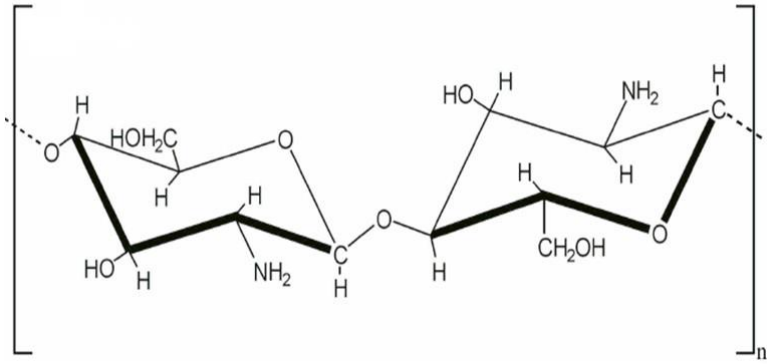

Figure 2. 1 Structure of chitosan

Medically, chitosan has been used in various applications and studies shown that it exhibits remarkable antimicrobial and hydrating effects (Sudheesh Kumar *et al.*, 2013). The polysaccharide is also a very good drug-delivery agent and has been used to deliver anti-cancer drugs, proteins and peptides, bactericidal agents and vaccines (Dash *et al.*, 2011). In wound treatment chitosan has been used as a curative bactericidal agent, membrane dressing and as structural fibre material for chitosan dressings. Studies show that chitosan is highly effective against gram positive and gram negative bacteria yet having remarkably low toxicity against mammalian cells (Tikhonov *et al.*, 2006).

2.3.1. Chitosan as a bactericidal agent

The chemical mechanism of chitosan against bacteria is not yet known with clarity, however it is suggested that the polycationic nature of chitosan is the basis of its activity. In low pH, chitosan is cationic in nature due to the acceptance of a proton, H^+, by the amine group at position 2. This characteristic gives chitosan the ability to dissolve in low pH media. If placed in a medium with a 6< pH, the amino groups on the chitosan structure are deprotonated and this makes it to lose its solubility gradually. The phenomenon is illustrated by following schematic diagram:

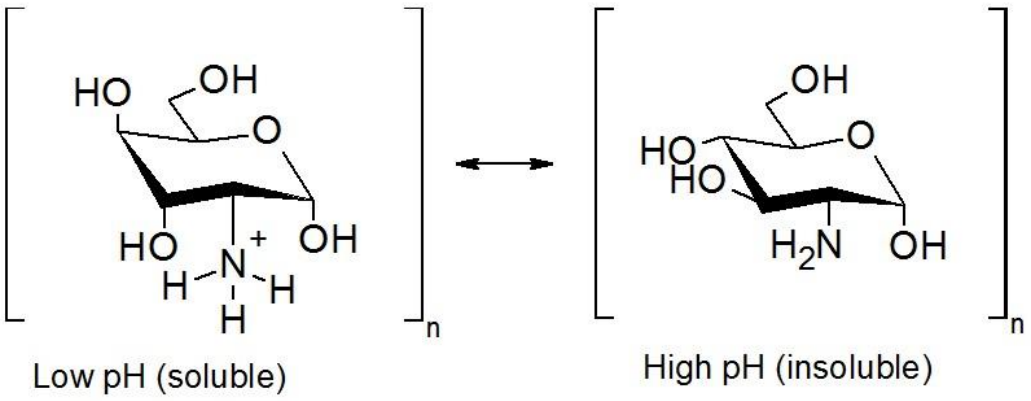

Figure 2. 2. pH influenced ionic versatility of chitosan.

It is assumed that the mechanism of action of chitosan against bacteria is initiated by the protonated amino groups attaching to the cell walls of the bacterium (Kong *et al.*, 2010). Bacteria cell walls have anionic sites in addition to the well-known hydrophilic and hydrophobic sites. The cationic sites of the chitosan attach to these anionic sites on the bacteria walls causing disintegration and consequent disruption of the cell wall (Goy, Britto and Assis, 2009). The other proposed models on the mechanism of action against bacteria is by altering properties of the cell membrane permeability which creates an internal osmotic imbalance and also by the hydrolysis of peptidoglycans along the cell wall which leads to leakage of protein and important electrolytes such as potassium (Goy, Britto and Assis, 2009). Major factors known to affect the bactericidal activity of chitosan are mainly the pH of the surrounding media, degree of deactylation and also the molecular weight of the chitosan (de Paz *et al.*, 2011). Highly quaternized chitosan is expected to exhibit increased bactericidal activity due to increased number of protonated amino groups. Some studies have shown that high molecular weight chitosan has increased bactericidal activity while low molecular chitosan has relatively lower bactericidal activity (Kong *et al.*, 2010). However other studies show no significant difference in activity between the different molecular weight chitosan (Tikhonov *et al.*, 2006). Intrinsic factors such as degree of deactylation and molecular weight are consistent hence they are not considered to influence the bactericidal activity of chitosan. This shifts the focus to extrinsic factors affecting bactericidal activity that are versatile and susceptible to change. Extrinsic factors such as temperature, pH, and electrolytic capacity have to be considered in the application of chitosan in order to achieve the desired results. It has also been discovered that chitosan is more of an inhibitor than a fully-fledged bactericidal agent (Rhoades and Roller, 2000; Goy, Britto and Assis, 2009). It is

a stronger bacteriostatic agent than it is a bactericidal agent so it can be more effective when used alongside other bactericidal nanoparticles in composites or hybrids to increase its efficacy.

Besides having bactericidal effects, chitosan is known to have wound healing capabilities towards human and animal tissue (Patrulea *et al.*, 2015). It also has good reputation as a reliable analgesic which has been used to prevent and control inflammation of tissue and cavities (Ahmed and Ikram, 2016). It has been considered for use in wound healing and acute burn healing because it has a lot of intrinsic and extrinsic characters which benefit the wound cavity as it heals. Chitosan has been in the fabrication of wound dressing scaffolds which have curative and bactericidal properties to the wound (Dai *et al.*, 2011). The use of chitosan in wound gauze dressing modification to increase antimicrobial activity and curative effects has been reported (Sudheesh Kumar *et al.*, 2013). Studies show that the modification of the wound gauze with chitosan causes an increment in the water retention capability of the wound gauze hence increasing the wound healing efficacy of the modified gauze.

2.3.2. Chitosan-metallic nanoparticles hybrids

Chitosan has high chelating tendencies and capabilities in acidic media (Kong *et al.*, 2010). The functional groups on chitosan that participate in chelating are the amine group and the hydroxyl group. The two groups act as electron donors to the incoming cationic metal and the same groups are also responsible for electrostatic forces that help stabilize the chelate structure (Mohammad, A. Al-Lohedan and N. Al-Haque, 2016). It forms chelate complexes that are stable in neutral conditions with transition metals. A hybrid of chitosan and metallic nanoparticles is of high mechanical strength due to the type of networking that is formed within the polymer (Tran *et al.*, 2011) and this prevents self-aggregation thereby ensuring internal and external robustness in the hybrid. Chitosan-metallic nanoparticles hybrids have been used to make biosensors, drug delivery hybrids and modified wound dressing amongst the vast applicatory areas. Modification of wound gauzes with metallic nanoparticles using chitosan poses a lot of benefits due to the versatility in utility of chitosan (Ali, Rajendran and Joshi, 2011). Within the wound gauze, the chitosan acts as a chelating agent binding the metallic nanoparticles together in place while creating an attachment to the fibres of the wound gauze. As a healing agent it provides a remarkable wound water retention, wound curative properties and mild bactericidal activity (Raafat and Sahl, 2009). The sensitivity of chitosan to pH environment makes it an efficient drug delivery agent with the capability of releasing the nanoparticles from the hybrid at a consistent rate if pH is lower than the pKa of chitosan (Hajipour *et al.*, 2012). The pH of normal unbroken skin ranges between pH 4-6 while the pH of an open wound ranges from pH 6.5-7.5 (Sirkka, Skiba and Apell, 2016).

During wound healing the pH of the wound begins to drop towards the pH of skin thereby lowering the pH of the wound cavity. It is expected that as pH in and around the wound begins to drop towards the pH of skin, it initiates the release of metallic cations from the chitosan chelate as they dissolve out of the chitosan chelate on the modified wound gauze. The chemistry of the body then controls the release of the healing nanoparticles into the wound cavity.

Studies have shown that chitosan-NPs modified wound gauzes have remarkable bactericidal efficacy. A chitosan-silver nanoparticles hybrid wound gauze showed enhanced bacterial inhibition capabilities against *S. aureus* bacteria (Ali, Rajendran and Joshi, 2011). The chitosan-silver nanoparticles hybrid was loaded onto polyester wound gauze and the modified wound gauze showed clear zones of inhibition which may be attributed to the synergetic effects of chitosan-Ag NPs. The modified wound gauze showed acceptable stability and robustness during utility tests. In another separate study, a cotton wound gauze fabric was loaded with a chitosan-Ag-ZnO composite using the drip and dry method and the results showed improved water retention, drying time and water absorbance (Hajipour *et al.*, 2012). The results show that modified wound gauze subjected to bactericidal efficacy tests against *Escherichia coli* and for *Staphylococcus aureus gave* efficacies 96% and 99% respectively. Chitosan and silver nanoparticles loaded polyester wound gauze indicated that the metallic nanoparticles can be dispersed from the polymer at a pH < 6.3 (Sanpui *et al.*, 2008). The wound gauze was subjected to bactericidal efficacy tests against *Escherichia coli*. It was discovered using fluorescence spectroscopy that the bacterium specie was deactivated the moment it came into contact with the chitosan-silver hybrid wound gauze. The timer tests showed that the deactivation of the bacterium took place faster than it would have taken if chitosan was being used in the absence of silver nanoparticles.

In this current study ZnO, Ag, CuO NPs were synthesized and characterised to establish their optical, morphological, and electrochemical properties. The NPs were combined with chitosan to form composites with the various NPs. The composites underwent analysis to establish any changes in their optical and electrochemical properties. The composites were used to modify common cotton wound gauzes after which the modified gauzes were subjected to bactericidal efficacy tests and utility tests.

2.4. References

Abbasipour, M. *et al.* (2014) 'Coated Cotton Gauze with Ag/ZnO/chitosan Nanocomposite as a Modern Wound Dressing', *Journal of Engineered Fibers and Fabrics*, 9(1), pp. 124–130.

AbdElhady, M. M. (2012) 'Preparation and Characterization of Chitosan/Zinc Oxide Nanoparticles for Imparting Antimicrobial and UV Protection to Cotton Fabric', *International Journal of Carbohydrate Chemistry*, 2012, pp. 1–6. doi: 10.1155/2012/840591.

Abiraman, T. *et al.* (2016) 'Antifouling behavior of chitosan adorned zinc oxide nanorods', *RSC Adv.* Royal Society of Chemistry, 6(73), pp. 69206–69217. doi: 10.1039/C6RA13321E.

Ahmed, S. and Ikram, S. (2016) 'Chitosan Based Scaffolds and Their Applications in Wound Healing', *Achievements in the Life Sciences*. Far Eastern Federal University, 10(1), pp. 27–37. doi: 10.1016/j.als.2016.04.001.

Alagumuthu, G. and Kumar, T. A. (2013) 'Synthesis and Characterization of Chitosan / TiO 2 Nanocomposites Using Liquid Phase Deposition Technique', 4(1), pp. 105–111.

Algawi, S. D. A. L. (no date) 'Copper Oxide Nanostructures ; Syntheses and Characterization', 71, pp. 0–4.

Ali, S. W., Rajendran, S. and Joshi, M. (2011) 'Synthesis and characterization of chitosan and silver loaded chitosan nanoparticles for bioactive polyester', *Carbohydrate Polymers*. Elsevier Ltd., 83(2), pp. 438–446. doi: 10.1016/j.carbpol.2010.08.004.

Alvarez, P. J. J. and Lowry, G. (2009) 'Nanomaterials with Antimicrobial Properties : Mechanisms , Implications and Applications pp I i'.

Applerot, G. *et al.* (2012) 'Understanding the antibacterial mechanism of CuO nanoparticles: Revealing the route of induced oxidative stress', *Small*, 8(21), pp. 3326–3337. doi: 10.1002/smll.201200772.

Arefi, M. R. and Rezaei-Zarchi, S. (2012) 'Synthesis of zinc oxide nanoparticles and their effect on the compressive strength and setting time of self-compacted concrete paste as cementitious composites', *International Journal of Molecular Sciences*, 13(4), pp. 4340–4350. doi: 10.3390/ijms13044340.

Atiyeh, B. S. *et al.* (2007) 'Effect of silver on burn wound infection control and healing:

Review of the literature', *Burns*, 33(2), pp. 139–148. doi: 10.1016/j.burns.2006.06.010.

Azuma, K. *et al.* (2015) *Chitin, Chitosan, and Its Derivatives for Wound Healing: Old and New Materials*, *Journal of Functional Biomaterials*. doi: 10.3390/jfb6010104.

Babu, V. S. (2010) *Solid State Devices and Technology*. 3rd edn, *Solid states devices and technology.* 3rd edn. Mumbai: Pearson.

Bagabas, A. *et al.* (2013) 'Room-temperature synthesis of zinc oxide nanoparticles in different media and their application in cyanide photodegradation', *Nanoscale Research Letters*, 8(1), p. 516. doi: 10.1186/1556-276X-8-516.

Balamurugan, B. and Mehta, B. R. (2001) 'Optical and structural properties of nanocrystalline copper oxide thin films prepared by activated reactive evaporation', *Thin Solid Films*, 396(1–2), pp. 90–96. doi: 10.1016/S0040-6090(01)01216-0.

Balu, S. S. and Bhakat, C. (2012) 'SYNTHESIS OF SILVER NANOPARTICLES BY CHEMICAL REDUCTION AND THEIR ANTIMICROBIAL ACTIVITY Materials and Methods ':, 1(6), pp. 1–5.

Bard, A. J. *et al.* (1944) *ELECTROCHEMICAL METHODS Fundamentals and Applications*, *Electrochemistry. I. Faulkner, Larry R*. doi: 10.1016/B978-0-12-381373-2.00056-9.

Benavente, M. (2008) *Adsorption of metallic ions onto chitosan: equilibrium and kinetic studies*. doi: 976–988.

Beyth, N. *et al.* (2015) 'Alternative Antimicrobial Approach: Nano-Antimicrobial Materials', *Evidence-Based Complementary and Alternative Medicine*, 2015, pp. 1–16. doi: 10.1155/2015/246012.

Biovation, L. (2010) *Testing for Antimicrobial Activity in Textiles.* Boothbay.

Bonnemann, H. and Richards, R. M. (2001) 'Nanoscopic metal particles - synthetic methods and potential applications', *Eur. J. Inorg. Chem.*, pp. 2455–2480. doi: 10.1002/1099-0682(200109)2001:10<2455::AID-EJIC2455>3.0.CO;2-Z.

Brintha, S. R. and Ajitha, M. (2015) 'Synthesis and characterization of ZnO nanoparticles via aqueous solution, sol-gel and hydrothermal methods', *IOSR Journal of Applied Chemistry*, 8(11), pp. 66–72. doi: 10.9790/5736-081116672.

Brown, J. H. (2015) 'Development and Use of a Cyclic Voltammetry Simulator To Introduce

Undergraduate Students to Electrochemical Simulations', *Journal of Chemical Education*. American Chemical Society, 92(9), pp. 1490–1496. doi: 10.1021/acs.jchemed.5b00225.

Brown, K. and Gray, S. B. (2010) 'Cyclic Voltammetric Studies of Electropolymerized Films Based on Ruthenium (II/III) Bis (1, 10phenanthroline)(4-methyl-4'vinyl-2, 2'-bipyridine).', *International Journal of Chemistry*, 2(2), pp. 3–9. Available at: http://search.ebscohost.com/login.aspx?direct=true&profile=ehost&scope=site&authtype=crawler&jrnl=19169698&AN=52739860&h=s7r8gpPlt9tlQXU1DwQKvth6GpoG/uSIl9+y7buDKd4ozaZ6T7n2jMZlVbnZRzIKzPwKahBTG9vQKJVjeYgNcA==&crl=c.

Brownson, D. A. C. and Banks, C. E. (2014) *The Handbook of Graphene Electrochemistry*, *The Handbook of Graphene Electrochemistry*. doi: 10.1007/978-1-4471-6428-9.

Brugnerotto, J. *et al.* (2001) 'An infrared investigation in relation with chitin and chitosan characterization', *Polymer*, 42(8), pp. 3569–3580. doi: 10.1016/S0032-3861(00)00713-8.

Budhiraja, N. *et al.* (2013) 'Synthesis and Optical Characteristics of Silver Nanoparticles on Different Substrates', *International Letters of Chemistry, Physics and Astronomy*, 19, pp. 80–88. doi: 10.18052/www.scipress.com/ILCPA.19.80.

Calvo, E. J. and Wolosiuk, A. (2002) 'Donnan permselectivity in layer-by-layer self-assembled redox polyelectrolye thin films', *Journal of the American Chemical Society*, 124(28), pp. 8490–8497. doi: 10.1021/ja020107h.

Cavassin, E. D. *et al.* (2015) 'Comparison of methods to detect the in vitro activity of silver nanoparticles (AgNP) against multidrug resistant bacteria', *Journal of Nanobiotechnology*. BioMed Central, 13(1). doi: 10.1186/s12951-015-0120-6.

Dai, T. *et al.* (2011) *NIH Public Access*, *Expert Rev Anti Infect Ther*. doi: 10.1586/eri.11.59.Chitosan.

Dash, M. *et al.* (2011) 'Chitosan - A versatile semi-synthetic polymer in biomedical applications', *Progress in Polymer Science (Oxford)*. Elsevier Ltd, 36(8), pp. 981–1014. doi: 10.1016/j.progpolymsci.2011.02.001.

Davis, J. and McLister, A. (2016) 'Chapter Four - Passive and Interactive Dressing Materials', in Davis, J. et al. (eds) *Smart Bandage Technologies*. Academic Press, pp. 93–144. doi: https://doi.org/10.1016/B978-0-12-803762-1.00004-7.

Debanath, M. K. and Karmakar, S. (2013) 'Study of blueshift of optical band gap in zinc oxide

(ZnO) nanoparticles prepared by low-temperature wet chemical method', *Materials Letters*. Elsevier, 111, pp. 116–119. doi: 10.1016/j.matlet.2013.08.069.

Dehaghi, S. M. *et al.* (2014) 'Removal of permethrin pesticide from water by chitosan–zinc oxide nanoparticles composite as an adsorbent', *Journal of Saudi Chemical Society*, 18(4), pp. 348–355. doi: https://doi.org/10.1016/j.jscs.2014.01.004.

Devi, H. S. and Singh, T. D. (2014) 'Synthesis of Copper Oxide Nanoparticles by a Novel Method and its Application in the Degradation of Methyl Orange', *Advance in Electronic and Electric Engineering*, 4(1), pp. 83–88.

Douglas Skoog, James Holler, S. C. (2007) 'Principles of instrumental analysis.', in Harris, D. (ed.) *Principles of instrumental analysis.* 6th edn. Belmont: Brooks/Cole, p. 371.

Durga Praveena, V. and Vijaya Kumar, K. (2013) 'Synthesis and Characterization of Chitosan based Silver Nano Composite System for Antibacterial Applications', *Proceedings of the International Conference on Advanced Nanomaterials & Emerging Engineering Technologies*, pp. 76–79.

Faiz, U. *et al.* (2011) 'Efficacy of zinc as an antibacterial agent against enteric bacterial pathogens.', *Journal of Ayub Medical College*, 23(2), pp. 18–21.

Feng, Q. L. *et al.* (2000) 'A mechanistic study of the antibacterial effect of silver ions on <I>Escherichia coli</I> and <I>Staphylococcus aureus</I>', *Journal of Biomedical Materials Research*, pp. 662–668. doi: 10.1002/1097-4636(20001215)52:4<662::aid-jbm10>3.0.co;2-3.

Fielicke, A., Rabin, I. and Meijer, G. (2006) 'Far-infrared spectroscopy of small neutral silver clusters', *Journal of Physical Chemistry A*, 110(26), pp. 8060–8063. doi: 10.1021/jp062095i.

Fievet, P. (2015) 'Donnan Potential BT - Encyclopedia of Membranes', in Drioli, E. and Giorno, L. (eds). Berlin, Heidelberg: Springer Berlin Heidelberg, pp. 1–3. doi: 10.1007/978-3-642-40872-4_1716-1.

Franci, G. *et al.* (2015) 'Silver nanoparticles as potential antibacterial agents', *Molecules*, 20(5), pp. 8856–8874. doi: 10.3390/molecules20058856.

Gliga, A. R. *et al.* (2014) 'Size-dependent cytotoxicity of silver nanoparticles in human lung cells: the role of cellular uptake, agglomeration and Ag release', *Particle and Fibre Toxicology*, 11(1), p. 11. doi: 10.1186/1743-8977-11-11.

Gogoi, S. K. *et al.* (2006) 'Green fluorescent protein-expressing Escherichia coli as a model

system for investigating the antimicrobial activities of silver nanoparticles', *Langmuir*, 22(22), pp. 9322–9328. doi: 10.1021/la060661v.

Gouda, M. (2012) 'Nano-zirconium oxide and nano-silver oxide/cotton gauze fabrics for antimicrobial and wound healing acceleration', *Journal of Industrial Textiles*, 41(3), pp. 222–240. doi: 10.1177/1528083711414960.

Goy, R. C., Britto, D. de and Assis, O. B. G. (2009) 'A review of the antimicrobial activity of chitosan', *Polímeros*, 19(3), pp. 241–247. doi: 10.1093/jac/dkg286.

Guidelli, R. *et al.* (2014) 'Defining the transfer coefficient in electrochemistry: An assessment (IUPAC Technical Report)', *Pure and Applied Chemistry*, 86(2), pp. 245–258. doi: 10.1515/pac-2014-5026.

Gunalan, S., Sivaraj, R. and Rajendran, V. (2012) 'Green synthesized ZnO nanoparticles against bacterial and fungal pathogens', *Progress in Natural Science: Materials International*. Elsevier, 22(6), pp. 693–700. doi: 10.1016/j.pnsc.2012.11.015.

Guo, S. and Dipietro, L. A. (2010) 'Factors Affecting Wound Healing', *Obstetrics & Gynecology*, (Mc 859), pp. 219–229. doi: 10.1177/0022034509359125.

Haghighat, S. and Dawlaty, J. M. (2016) 'pH Dependence of the Electron-Transfer Coefficient: Comparing a Model to Experiment for Hydrogen Evolution Reaction', *Journal of Physical Chemistry C*, 120(50), pp. 28489–28496. doi: 10.1021/acs.jpcc.6b10602.

Hajipour, M. J. *et al.* (2012) 'Coated Cotton Gauze with Ag/ZnO/chitosan Nanocomposite as a Modern Wound Dressing', *Journal of Industrial Textiles*. Elsevier Ltd, 9(6), pp. 143–154. doi: 10.1155/2015/246012.

Hajipour, M. J., Fromm, K. M. and Ashkarran, A. (2012) 'Antibacterial properties of nanoparticles', *Trends in Biotechnology*. Elsevier Ltd, 30(10), pp. 499–511. doi: 10.1016/j.tibtech.2012.06.004.

Huh, A. J. and Kwon, Y. J. (2011) '"Nanoantibiotics": A new paradigm for treating infectious diseases using nanomaterials in the antibiotics resistant era', *Journal of Controlled Release*. Elsevier B.V., 156(2), pp. 128–145. doi: 10.1016/j.jconrel.2011.07.002.

I. Markova-Deneva (2010) 'Infrared Spectroscopy Investigation of Metallic Nanoparticles Based on Copper, Cobalt, and Nickel Synthesized Through Borohydride Reduction Method', *Journal of the University of Chemical Technology and Metallurgy*, 45(4), pp. 351–378.

Ijaz, F. *et al.* (2017) ‘Green synthesis of copper oxide nanoparticles using abutilon indicum leaf extract: Antimicrobial, antioxidant and photocatalytic dye degradation activities’, *Tropical Journal of Pharmaceutical Research*, 16(4), pp. 743–753. doi: 10.4314/tjpr.v16i4.2.

ISO (2007) ‘ISO 21348 Definitions of Solar Irradiance Spectral Categories’, *Environment*, (section 5), pp. 6–7.

Jain, K. K. (2007) ‘Applications of nanobiotechnology in clinical diagnostics’, *Clinical Chemistry*, 53(11), pp. 2002–2009. doi: 10.1373/clinchem.2007.090795.

Jemimah, V. H. and Arulpandi, I. (2014) ‘Evaluation of Antimicrobial Property of Biosynthesized Zinc Oxide Nanoparticles (ZnO NPs) and its Application on Baby Diapers’, 6(2), pp. 113–119.

Jin, T. *et al.* (2009) ‘Antimicrobial efficacy of zinc oxide quantum dots against Listeria monocytogenes, Salmonella Enteritidis, and Escherichia coli O157:H7’, *Journal of Food Science*, 74(1). doi: 10.1111/j.1750-3841.2008.01013.x.

John Kotz, Paul Treichel, J. T. (2009) *Chemistry and chemical reactivity .* 2nd edn, *Chemistry and chemical reactivity .* 2nd edn. Edited by Lisa Lockwood. Belmont: Brooks/Cole.

Joseph Wang (2006) *Analytical Electrochemistry*. 3rd edn. New Jersey: John Wiley and Sons.

Jyoti, K., Baunthiyal, M. and Singh, A. (2016) ‘Characterization of silver nanoparticles synthesized using Urtica dioica Linn. leaves and their synergistic effects with antibiotics’, *Journal of Radiation Research and Applied Sciences*. Elsevier Ltd, 9(3), pp. 217–227. doi: 10.1016/j.jrras.2015.10.002.

Kalimuthu, K. *et al.* (2008) ‘Biosynthesis of silver nanocrystals by Bacillus licheniformis’, *Colloids and Surfaces B: Biointerfaces*, 65(1), pp. 150–153. doi: https://doi.org/10.1016/j.colsurfb.2008.02.018.

Kang, X. *et al.* (2009) ‘Glucose Oxidase-graphene-chitosan modified electrode for direct electrochemistry and glucose sensing’, *Biosensors and Bioelectronics*, 25(4), pp. 901–905. doi: 10.1016/j.bios.2009.09.004.

Karim-Nezhad, G. *et al.* (2009) *Kinetic Study of Electrocatalytic Oxidation of Carbohydrates on Cobalt Hydroxide Modified Glassy Carbon Electrode*, *J. Braz. Chem. Soc.* doi: 10.1590/S0103-50532009000100022.

Kayani, Z. N. *et al.* (2012) 'Synthesis and characterization of CuO nanowires by a simple wet chemical method', *International Letters of Chemistry, Physics and Astronomy*. Springer Open Ltd, 14(1), pp. 26–36. doi: 10.1186/1556-276X-7-70.

Kayani, Z. N. *et al.* (2015) 'Characterization of Copper Oxide Nanoparticles Fabricated by the Sol???Gel Method', *Journal of Electronic Materials*, 44(10), pp. 3704–3709. doi: 10.1007/s11664-015-3867-5.

Khatoon, N. *et al.* (2015) 'Biosynthesis, Characterization, and Antifungal Activity of the Silver Nanoparticles Against Pathogenic Candida species', *BioNanoScience*, 5(2), pp. 65–74. doi: 10.1007/s12668-015-0163-z.

Khorsand Zak, A. *et al.* (2011) 'Synthesis and characterization of a narrow size distribution of zinc oxide nanoparticles', *International Journal of Nanomedicine*, 6(1), pp. 1399–1403. doi: 10.2147/IJN.S19693.

Kong, M. *et al.* (2010) 'Antimicrobial properties of chitosan and mode of action: A state of the art review', *International Journal of Food Microbiology*. Elsevier B.V., 144(1), pp. 51–63. doi: 10.1016/j.ijfoodmicro.2010.09.012.

Krishna Veni (2016) 'Anti-Bacterial Coating of Chrysanthemum Extract on Bamboo Fabric for Healthcare Applications', *Journal of Textile Science & Engineering*, 6(4), pp. 6–8. doi: 10.4172/2165-8064.1000267.

Krishnamoorthy, K. and Kim, S. J. (2013) 'Growth, characterization and electrochemical properties of hierarchical CuO nanostructures for supercapacitor applications', *Materials Research Bulletin*. Elsevier Ltd, 48(9), pp. 3136–3139. doi: 10.1016/j.materresbull.2013.04.082.

Kumar, H. and Rani, R. (2013) 'Structural Characterization of Silver Nanoparticles Synthesized by Micro emulsion Route', *International Journal of Engineering and Innovative Technology*, 3(3), pp. 344–348.

Kurien, S. (2005) 'Chapter 4: ANALYSIS OF FTIR SPECTRA OF NANOPARTICLES of MgAl2O4, SrAl2O4, and NiAl2O4', 1595, pp. 64–78. Available at: http://mgutheses.in/page/?q=T 1354&search=siby+kurien&page=1&rad=sc.

Laurent, D. and Schlenoff, J. B. (1997) 'Multilayer Assemblies of Redox Polyelectrolytes', *Langmuir*, 13(6), pp. 1552–1557. doi: 10.1021/la960959t.

Laviron, E. (1979) ‘General expression of the linear potential sweep voltammogram in the case of diffusionless electrochemical systems’, *Journal of Electroanalytical Chemistry and Interfacial Electrochemistry*, 101(1), pp. 19–28. doi: https://doi.org/10.1016/S0022-0728(79)80075-3.

Laviron, E. (1979) ‘General expression of the linear potential sweep voltammogram in the case of diffusionless electrochemical systems’, *Journal of Electroanalytical Chemistry*, 101(1), pp. 19–28. doi: 10.1016/S0022-0728(79)80075-3.

Laviron, E. (1995) ‘The use of polarography and cyclic voltammetry for the study of redox systems with adsorption of the reactants. Heterogeneous vs. surface path’, *Journal of Electroanalytical Chemistry*, 382(1–2), pp. 111–127. doi: 10.1016/0022-0728(94)03684-U.

Lionelli, G. T. and Lawrence, W. T. (2003) ‘Wound dressings’, *Surgical Clinics of North America*, pp. 617–638.

Liu, B. *et al.* (2013) ‘Adsorption of heavy metal ions, dyes and proteins by chitosan composites and derivatives --- A review’, *Journal of Ocean University of China*, 12(3), pp. 500–508. doi: 10.1007/s11802-013-2113-0.

Logothetidis, S. (2012) *Nanotechnology : Principles and Applications*. doi: 10.1007/978-3-642-22227-6.

Long, J. *et al.* (2016) ‘A new class of nanocomposites of Zn–Al–Bi layered double oxides: large reversible capacity and better cycle performance for alkaline secondary batteries’, *RSC Adv.* Royal Society of Chemistry, 6(95), pp. 92896–92904. doi: 10.1039/C6RA18164C.

Lović, J. (2017) ‘Glucose Sensing Using Glucose Oxidase-Glutaraldehyde- Cysteine Modified Gold Electrode’, *International Journal of Electrochemical Science*, (July), pp. 5806–5817. doi: 10.20964/2017.07.65.

Luna, I. Z. *et al.* (2015) ‘Preparation and Characterization of Copper Oxide Nanoparticles Synthesized via Chemical Precipitation Method’, *OALib*, 2(3), pp. 1–8. doi: 10.4236/oalib.1101409.

Ma, A. *et al.* (2011) ‘Evaluation of antibacterial activity of silver nanoparticles against MSSA and MRSA on isolates from skin infections’, *Research Article Biology and Medicine*, 3(2), pp. 141–146.

Malinowska-Pańczyk, E. *et al.* (2009) ‘The combined effect of moderate pressure and

chitosan on Escherichia coli and Staphylococcus aureus cells suspended in a buffer and on natural microflora of apple juice and minced pork', *Food Technology and Biotechnology*, 47(2), pp. 202–209.

Maneerung, T., Tokura, S. and Rujiravanit, R. (2008) 'Impregnation of silver nanoparticles into bacterial cellulose for antimicrobial wound dressing', *Carbohydrate Polymers*, 72(1), pp. 43–51. doi: 10.1016/j.carbpol.2007.07.025.

Mansoori, G. A. (2005) 'Principles of Nanotechnology: Molecular Based Study of Condensed Matter in Small Systems'. doi: 10.1142/5749.

Mazloum-ardakani, M. *et al.* (2010) 'Voltammetric Determination of Dopamine at the Surface of TiO 2 Nanoparticles Modified Carbon Paste Electrode', 5, pp. 147–157.

Meftahi, A. *et al.* (2010) *The effects of cotton gauze coating with microbial cellulose*, *Cellulose*. doi: 10.1007/s10570-009-9377-y.

Mehta, B. K., Chhajlani, M. and Shrivastava, D. (2017) 'Green synthesis of silver nanoparticles and their characterization by XRD', *Frontiers of Physics and Plasma Science IOP Publishing IOP Conf. Series: Journal of Physics: Conf. Series*, 836. doi: 10.1088/1742-6596/836/1/012050.

Mohammad, F., A. Al-Lohedan, H. and N. Al-Haque, H. (2016) 'Chitosan-mediated fabrication of metal nanocomposites for enhanced biomedical applicationsf', *Advanced Materials Letters*, 8(2), pp. 89–100. doi: 10.5185/amlett.2017.6925.

Mohan, A. C. and Renjanadevi, B. (2016) 'Preparation of Zinc Oxide Nanoparticles and its Characterization Using Scanning Electron Microscopy (SEM) and X-Ray Diffraction(XRD)', *Procedia Technology*. Elsevier B.V., 24, pp. 761–766. doi: 10.1016/j.protcy.2016.05.078.

Muthukrishnan, A. M. (2015) 'Green Synthesis of Copper-Chitosan Nanoparticles and Study of its Antibacterial Activity', *Journal of Nanomedicine & Nanotechnology*, 6(1), pp. 1–6. doi: 10.4172/2157-7439.1000251.

Muzzarelli, R. (1973) *Natural chelating polymers; alginic acid, chitin, and chitosan*. 1st edn. Oxford: Pergamon press.

Muzzarelli, R. A. and Sipos, L. (1971) 'Chitosan for the collection from seawater of naturally occurring zinc, cadmium, lead and copper', *Talanta*, 18(9), p. 853—858. doi: 10.1016/0039-9140(71)80141-8.

Nam, H. C. and Schaak, R. E. (2007) ‘Shape-controlled conversion of ??-Sn nanocrystals into intermetallic M-Sn (M = Fe, Co, Ni, Pd) nanocrystals’, *Journal of the American Chemical Society*, 129(23), pp. 7339–7345. doi: 10.1021/ja069032y.

Norfazila, S. M. and Mohd, J. R. (2014) ‘Synthesis and Ultroviolet Visible Spectroscopy Studies of Chitosan Capped Gold Nanoparticles and Theri Reactions with Analytes’, *The Scientific World Journal*, 2014, p. 7. doi: http://dx.doi.org/10.1155/2014/184604.

Okumu, F. and Matoetoe, M. (2016) ‘Electrochemical Characterization of Silver-Platinum Various Ratio Bimetallic Nanoparticles Modified Electrodes’, *Journal of Nano Research*, 44, pp. 114–125. doi: 10.4028/www.scientific.net/JNanoR.44.114.

Olaniyan, O. J. *et al.* (2016) ‘Synthesis and Characterization of Chitosan-Silver Nanocomposite Film’, *Nano Hybrids and Composites*, 11, pp. 22–29. doi: 10.4028/www.scientific.net/NHC.11.22.

Ono, S. *et al.* (2015) ‘Increased wound pH as an indicator of local wound infection in second degree burns’, *Burns*. Elsevier Ltd and International Society of Burns Injuries, 41(4), pp. 820–824. doi: 10.1016/j.burns.2014.10.023.

Padil, V. and Cernik, M. (2013) *Green synthesis of copper oxide nanoparticles using gum karaya as a biotemplate and their antibacterial application*, *International journal of nanomedicine*. doi: 10.2147/IJN.S40599.

Paladini, F. *et al.* (2016) ‘In vitro assessment of the antibacterial potential of silver nano-coatings on cotton gauzes for prevention of wound infections’, *Materials*, 9(6), pp. 1–14. doi: 10.3390/ma9060411.

Panchakarla, L. S., Govindaraj, A. and Rao, C. N. R. (2007) ‘Formation of ZnO nanoparticles by the reaction of zinc metal with aliphatic alcohols’, *Journal of Cluster Science*, 18(3), pp. 660–670. doi: 10.1007/s10876-007-0129-6.

Pankratov, D. V. *et al.* (2014) ‘Impact of surface modification with gold nanoparticles on the bioelectrocatalytic parameters of immobilized bilirubin oxidase’, *Acta Naturae*, 6(20), pp. 102–106.

Patrulea, V. *et al.* (2015) ‘Chitosan as a starting material for wound healing applications’, *European Journal of Pharmaceutics and Biopharmaceutics*. Elsevier B.V., 97, pp. 417–426. doi: 10.1016/j.ejpb.2015.08.004.

Paul, H. J. and Leddy, J. (1995) 'Direct Determination of the Transfer Coefficient from Cyclic Voltammetry: Isopoints as Diagnostics', *Analytical Chemistry*, 67(10), pp. 1661–1668. doi: 10.1021/ac00106a003.

de Paz, L. E. C. *et al.* (2011) 'Antimicrobial effect of chitosan nanoparticles on Streptococcus mutans biofilms', *Applied and Environmental Microbiology*, 77(11), pp. 3892–3895. doi: 10.1128/AEM.02941-10.

Pinho, E. *et al.* (2011) 'Antimicrobial activity assessment of textiles: Standard methods comparison', *Annals of Microbiology*, 61(3), pp. 493–498. doi: 10.1007/s13213-010-0163-8.

Prodomis, M. I. *et al.* (2000) 'The Importance of Surface Coverage in the Electrochemical Study of Chemically Modified Electrodes', *Electroanalysis*, 12(18), pp. 1498–1501.

Puchalski, M. *et al.* (2007) 'The study of silver nanoparticles by scanning electron microscopy, energy dispersive X-ray analysis and scanning tunnelling microscopy', *Materials Science-Poland*, 25(2), pp. 473–478.

Raafat, D. and Sahl, H. G. (2009) 'Chitosan and its antimicrobial potential - A critical literature survey', *Microbial Biotechnology*, 2(2 SPEC. ISS.), pp. 186–201. doi: 10.1111/j.1751-7915.2008.00080.x.

Radecka, M. *et al.* (2008) 'Importance of the band gap energy and flat band potential for application of modified TiO2 photoanodes in water photolysis', *Journal of Power Sources*, 181(1), pp. 46–55. doi: https://doi.org/10.1016/j.jpowsour.2007.10.082.

Raghupathi, K. R., Koodali, R. T. and Manna, A. C. (2011) 'Size-dependent bacterial growth inhibition and mechanism of antibacterial activity of zinc oxide nanoparticles.', *Langmuir : the ACS journal of surfaces and colloids*, 27(7), pp. 4020–4028. doi: 10.1021/la104825u.

Rahman, A. *et al.* (2009) 'SYNTHESIS OF COPPER OXIDE NANO PARTICLES BY USING Phormidium cyanobacterium', *Indonesian Journal of Chemistry*, 9(3), pp. 355–360.

Rai, M., Yadav, A. and Gade, A. (2009) 'Silver nanoparticles as a new generation of antimicrobials', *Biotechnology Advances*. Elsevier Inc., 27(1), pp. 76–83. doi: 10.1016/j.biotechadv.2008.09.002.

Ravichandran, S. *et al.* (2015) 'A novel approach for the biosynthesis of silver oxide nanoparticles using aqueous leaf extract of Callistemon lanceolatus (Myrtaceae) and their therapeutic potential', *Journal of Experimental Nanoscience*. Taylor & Francis, 8080(August),

pp. 1–14. doi: 10.1080/17458080.2015.1077534.

Rhazi, M. *et al.* (2002) ‘Influence of the nature of the metal ions on the complexation with chitosan.: Application to the treatment of liquid waste’, *European Polymer Journal*, 38, pp. 1523–1530.

Rhoades, J. and Roller, S. (2000) ‘Antimicrobial actions of degraded and native chitosan against spoilage organisms in laboratory media and foods’, *Applied and Environmental Microbiology*, 66(1), pp. 80–86. doi: 10.1128/AEM.66.1.80-86.2000.

Richards, R. and Bonnemann, H. (2005) ‘Synthetic Approaches to Metallic Nanomaterials’, *Nanofabrication Towards Biomedical Applications: Techniques, Tools, Applications, and Impact*, pp. 1–32. doi: 10.1002/3527603476.ch1.

Salehi, R. *et al.* (2010) ‘Novel biocompatible composite (Chitosan-zinc oxide nanoparticle): Preparation, characterization and dye adsorption properties’, *Colloids and Surfaces B: Biointerfaces*. Elsevier B.V., 80(1), pp. 86–93. doi: 10.1016/j.colsurfb.2010.05.039.

Sanpui, P. *et al.* (2008) ‘The antibacterial properties of a novel chitosan-Ag-nanoparticle composite’, *International Journal of Food Microbiology*, 124(2), pp. 142–146. doi: 10.1016/j.ijfoodmicro.2008.03.004.

Santos, C. L. *et al.* (2013) ‘Nanomaterials with Antimicrobial Properties : Applications in Health Sciences’, *Microbial pathogens and strategies for combating them: science, technology and education*, 1, pp. 143–154.

Sanyal, M. K., Datta, A. and Hazra, S. (2002) ‘Morphology of nanostructured materials’, *Pure and Applied Chemistry*, 74(9), pp. 1553–1570. doi: 10.1351/pac200274091553.

Schlenoff, J. B., Ly, H. and Li, M. (1998) ‘Charge and Mass Balance in Polyelectrolyte Multilayers - Journal of the American Chemical Society (ACS Publications)’, *Journal of the American Chemical …*, 7863(13), pp. 7626–7634. doi: 10.1021/ja980350.

Sehat, A. A. *et al.* (2015) ‘Fast immobilization of glucose oxidase on graphene oxide for highly sensitive glucose biosensor fabrication’, *International Journal of Electrochemical Science*, 10(1), pp. 272–286.

Seil, J. T. and Webster, T. J. (2012) ‘Antimicrobial applications of nanotechnology: Methods and literature’, *International Journal of Nanomedicine*, 7, pp. 2767–2781. doi: 10.2147/IJN.S24805.

Sezer, A. D. and Cevher, E. (1992) 'Biopolymers as Wound Healing Materials: Challenges and New Strategies', *Biomaterials Applications for Nanomedicine*, pp. 383–414. doi: 10.5772/25177.

Shen, X. S. *et al.* (2009) 'Nanospheres of silver nanoparticles: agglomeration, surface morphology control and application as SERS substrates', *Physical Chemistry Chemical Physics*. The Royal Society of Chemistry, 11(34), pp. 7450–7454. doi: 10.1039/B904712C.

Shrivastava, S. *et al.* (2010) 'Characterization of enhanced antibacterial effects of novel silver nanoparticles', *Nanotechnology*, 18(22), pp. 1–9. doi: 10.1088/0957-4484/18/22/225103.

Sirkka, T., Skiba, J. B. and Apell, S. P. (2016) 'Wound pH depends on actual wound size', p. 13.

Srivastava, S., Agrawal, A. and Kumar, S. (2013) 'Synthesis and Characterisation of Copper Oxide nanoparticles', *Journal of Applied Physics*, 5(4), pp. 61–65.

Street, E. and Lake, C. (2014) 'Aatcc t', pp. 2012–2015.

Sudheesh Kumar, P. T. *et al.* (2012) 'Flexible and microporous chitosan hydrogel/nano ZnO composite bandages for wound dressing: In vitro and in vivo evaluation', *ACS Applied Materials and Interfaces*, 4(5), pp. 2618–2629. doi: 10.1021/am300292v.

Sudheesh Kumar, P. T. *et al.* (2013) 'Evaluation of wound healing potential of β-chitin hydrogel/nano zinc oxide composite bandage', *Pharmaceutical Research*, 30(2), pp. 523–537. doi: 10.1007/s11095-012-0898-y.

Sun, K. and Li, Z. H. (2011) 'Preparations, properties and applications of chitosan based nanofibers fabricated by electrospinning', *Express Polymer Letters*, 5(4), pp. 342–361. doi: 10.3144/expresspolymlett.2011.34.

Sutherland, L. F. and D. (2012) *Nanotechnologies: Principles, Applications, Implications and Hands-on Activities*. doi: :10.2777/76945.

Talam, S., Karumuri, S. R. and Gunnam, N. (2012) 'Synthesis, Characterization, and Spectroscopic Properties of ZnO Nanoparticles', *ISRN Nanotechnology*, 2012, pp. 1–6. doi: 10.5402/2012/372505.

Tamayo, L. *et al.* (2016) 'Copper-polymer nanocomposites: An excellent and cost-effective biocide for use on antibacterial surfaces', *Materials Science and Engineering C*. Elsevier B.V., 69, pp. 1391–1409. doi: 10.1016/j.msec.2016.08.041.

Teterycz, H. *et al.* (2014) ‘Deposition of Zinc Oxide on the Materials Used in Medicine. Preliminary Results’, *FIBRES & TEXTILES in Eastern Europe*, 22(105), pp. 3–126.

Tikhonov, V. E. *et al.* (2006) ‘Bactericidal and antifungal activities of a low molecular weight chitosan and its N-/2(3)-(dodec-2-enyl)succinoyl/-derivatives’, *Carbohydrate Polymers*, 64(1), pp. 66–72. doi: 10.1016/j.carbpol.2005.10.021.

Tran, D. L. *et al.* (2011) ‘Some biomedical applications of chitosan-based hybrid nanomaterials’, *Advance in Natural Science: Nanoscience Nanotechnology*, 2, pp. 1–6. doi: 10.1088/2043-6262/2/4/045004.

Tran, T. H. and Nguyen, V. T. (2014) ‘Copper Oxide Nanomaterials Prepared by Solution Methods, Some Properties, and Potential Applications: A Brief Review’, *International Scholarly Research Notices*. Hindawi Publishing Corporation, 2014, pp. 1–14. doi: 10.1155/2014/856592.

Umesh, Kathad; Gajera, H. . (2014) ‘Synthesis of copper nanoparticles by two different methods and size comparison’, *Int J Pharm Bio Sci*, 5(1), pp. 978–982.

Usman, M. S. *et al.* (2012) ‘Copper nanoparticles mediated by chitosan: Synthesis and characterization via chemical methods’, *Molecules*, 17(12), pp. 14928–14936. doi: 10.3390/molecules171214928.

Valov, I. and Lu, W. D. (2016) ‘Nanoscale electrochemistry using dielectric thin films as solid electrolytes’, *Nanoscale*. The Royal Society of Chemistry, 8(29), pp. 13828–13837. doi: 10.1039/C6NR01383J.

Vaseeharan, B., Sivakamavalli, J. and Thaya, R. (2015) ‘Synthesis and characterization of chitosan-ZnO composite and its antibiofilm activity against aquatic bacteria’, *Journal of Composite Materials*, 49(2), pp. 177–184. doi: 10.1177/0021998313515289.

Velasco, J. G. (1997) ‘Determination of standard rate constants for electrochemical irreversible processes from linear sweep voltammograms’, *Electroanalysis*, 9(11), pp. 880–882. doi: 10.1002/elan.1140091116.

Wang, X. *et al.* (2005) ‘Chitosan- metal complexes as antimicrobial agent: Synthesis, characterization and Structure-activity study’, *Polymer Bulletin*, 55(1–2), pp. 105–113. doi: 10.1007/s00289-005-0414-1.

Wang, Z. L. (2004) ‘Zinc oxide nanostructures: growth, properties and applications’, *Journal*

of Physics: Condensed Matter, 16(25), pp. R829–R858. doi: 10.1088/0953-8984/16/25/R01.

Wei, D. *et al.* (2009) 'The synthesis of chitosan-based silver nanoparticles and their antibacterial activity', *Carbohydrate Research*. Elsevier Ltd, 344(17), pp. 2375–2382. doi: 10.1016/j.carres.2009.09.001.

Wicramarachchi, P. and Hettiarachchi, M. (2011) 'Synthesis of chitosan stabilised silver nanoparticles using gamma ray radiation and characterisation', *Jousrnal of Scinece*, 6, pp. 65–75.

Xiliang, Q. *et al.* (2014) 'Large-Scale Synthesis of Silver Nanoparticles by Aqueous Reduction for Low-Temperature Sintering Bonding', 2014.

Xiong, G. *et al.* (2006) 'Photoluminescence and FTIR study of ZnO nanoparticles: The impurity and defect perspective', *Physica Status Solidi (C) Current Topics in Solid State Physics*, 3(10), pp. 3577–3581. doi: 10.1002/pssc.200672164.

Yukna, J. (Souther. I. U. at C. . (2014) 'International Journal of Nano Dimension Synthesis and characterization of Copper and Copper Oxide nanoparticles by thermal decomposition method', *Thesis paper*, 5(4), pp. 321–327.

Zhang, L., Zeng, Y. and Cheng, Z. (2016) 'Removal of heavy metal ions using chitosan and modified chitosan: A review', *Journal of Molecular Liquids*. Elsevier B.V., 214, pp. 175–191. doi: 10.1016/j.molliq.2015.12.013.

Zhou, E., Hashimoto, K. and Tajima, K. (2013) 'Low band gap polymers for photovoltaic device with photocurrent response wavelengths over 1000 nm', *Polymer (United Kingdom)*. Elsevier Ltd, 54(24), pp. 6501–6509. doi: 10.1016/j.polymer.2013.09.058.

CHAPTER THREE
RESEARCH RESULTS
SYNTHESIS AND CHARACTERIZATION OF NANOPARTICLES

3.1. Introduction

This chapter focuses on the synthesis of the silver, zinc oxide, and copper oxide nanoparticles (NPs) via the chemical reduction method and characterisation of these nanoparticles. This part explores parameters such as morphology, optical activity, and electronic bandwidth which give the nanoparticles uniqueness over their bulk form. These studies also give an insight in their potential bactericidal applications.

Diverse methods of NPs synthesis exist however it is the purpose of the NPs that greatly influences the method of synthesis. Metallic NPs synthesis methods that give cost effective results at lab-scale are the ones that makes use of metal precursors. Various methods of NPs synthesis have been developed over the years with the focus of improvement being on cost effectiveness, environmental consciousness, nanoparticle size and efficiency of synthesis (Nam and Schaak, 2007). The synthetic approaches can be classified into three major groups which are chemical synthesis, physical synthesis and biological synthesis (Logothetidis, 2012). The method classes have their different advantages and disadvantages though choice of method is usually made with regard of desired outcome.

Chemical reduction method is a controlled wet synthesis process used to reduce metallic ions in solution leading to their nucleation and aggregation thereby forming NPs within the media of reaction. This method of synthesis makes use of a metal precursor and a reducing agent with the addition of a stabilizing agent in the media if required (Richards and Bonnemann, 2005). The process generally follows three basic chemical steps namely, the reduction phase, nucleation phase and lastly the growth phase. Initially during the reduction phase the metallic salt is reduced to produce atom with zero-valence. The atoms then form clusters by collisions between the metallic atoms within the media leading to the formation of a nucleic region on which further growth begins to occur on (Bonnemann and Richards, 2001). The need for a stabilizing agent depends on the type of metallic species being formed and its relative stability within the media of formation. Destabilization is usually caused by electrostatic or columbic repulsive forces between the metallic atoms which leads to dwarfed growth after nucleation (Fielicke, Rabin and Meijer, 2006). This can consequently cause

oxidation of the metal atoms depending on the oxidation potential of the species and can eventually cause agglomeration.

3.1.1. Synthesis of Zinc nanoparticles (Zn NPs)

Several synthesis methods such as chemical vapour deposition, physical vapour deposition, metal-organic vapour, phase epistaxis exist for zinc oxide. The chemical reduction method is favoured due to its cost effectiveness, systematic clarity, and lab ready method. Figure 3.1 below shows the schematic flow process of the synthesis.

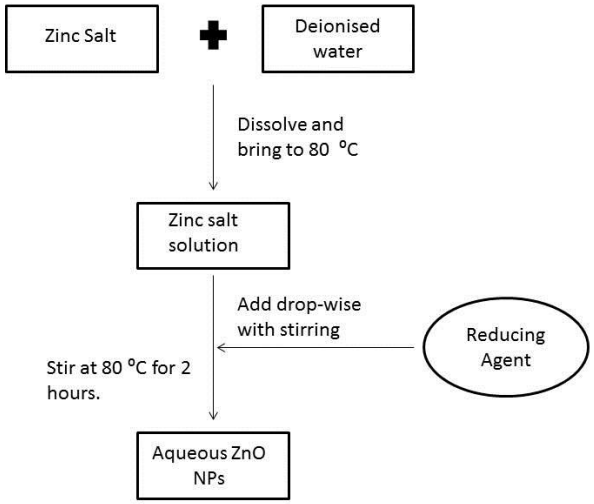

Figure 3. 1. Synthesis of ZnO NPs via chemical reduction.

The chemical reduction method was chosen for this research because the method requires less stringent reaction conditions and has the capability of producing NPs of desired morphology. The type and frequency of morphology present in zinc oxide NPs is dependent on the alcohol to water ratio in the reaction medium and the temperatures that are used during regulation. A 50-50 mixture of alcohol and a constant temperature of 80 ºC tends to form spherical and hexagonal NPs (Panchakarla, Govindaraj and Rao, 2007).

An increment of the alcohol present in the medium of reaction causes the formation of more zinc oxide nano-rods. The production of the zinc oxide via sol-gel method using zinc acetate and sodium hydroxide can be defined by three chemical steps as shown by the following reaction equations:

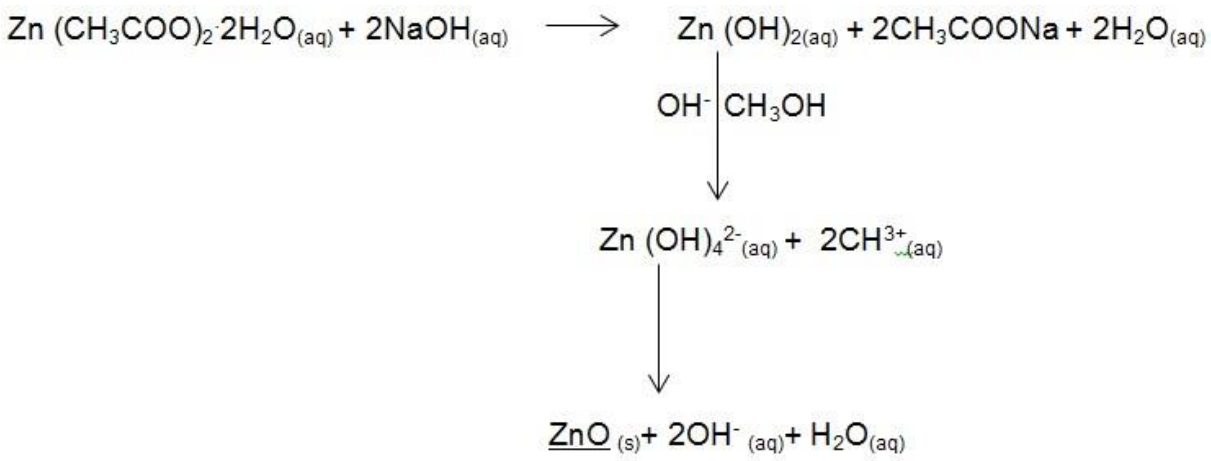

Equation 3. 1 Reaction sequence for synthesis of ZnO NPs via chemical reduction.

3.1.2. Synthesis of copper nanoparticles (Cu NPs)

Copper NPs can be synthesised by various methods such as aqueous methods, colloidal synthesis, evaporation, extract, and metallic vapour condensation. The major challenge that is usually faced in the synthesis of copper material is its ability to rapidly oxidise soon after its formation (Umesh, Kathad; Gajera, 2014). However copper oxide NPs exhibit remarkable attributes that are similar to the copper metal NPs. In this research copper (II) oxide (cupric oxide) was synthesised using the inert chemical reduction where copper (II) chloride reacts with potassium hydroxide under organic solvents. The reaction between KOH and $CuCl_2$ is vigorous in air so an inert environment has to be created to allow the formation of nano-size material. A 50-50 mixture of benzene and hexane is usually used as media for the refluxing of the two reagents to form NPs. The copper salt and the KOH are mixed evenly and submerged in the organic solvent mixture and refluxed creating an inert environment. As the refluxing begins, the first reaction to occur is the hydrolysis of the copper chloride to form copper hydroxide within the media as illustrated by equation 3.2. As the refluxing proceeds, the unstable copper hydroxide is slowly converted into cupric oxide. Calcination is required to form the NPs and it has been discovered that calcination parameters affect the size, morphology and lattice structure of the CuO NPs that is formed (Srivastava, Agrawal and Kumar, 2013).Therefore it is imperative that the parameters of calcination be comprehended in order to produce the desired CuO NPs. The overall reaction can be summarised by the following equation.

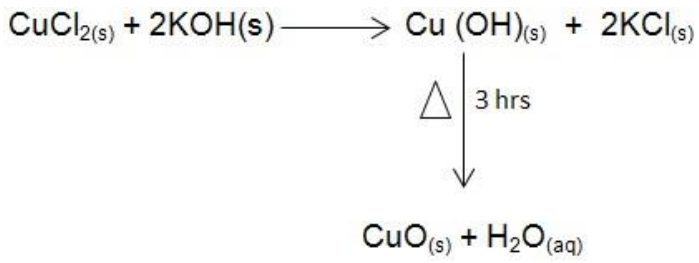

Equation 3. 2 Synthesis of CuO NPs via inert chemical reduction.

3.1.3. Synthesis of Silver nanoparticles (Ag NPs)

Several methods of silver NPs exist though the ones with the lowest production costs are being more common. Biological or green methods have become more favoured due to their relative low cost as well as their environmentally friendly nature (Ravichandran *et al.*, 2015). However, some of the green methods used are inadequate in the area of controlling morphology and the size of the NPs produced. More research is still yet to be done in the area. The conventional method for the synthesis for silver NPs that was used in this research was the chemical reduction which uses silver nitrate as a precursor and sodium triacetate as a reducing/stabilizing agent. The method is alternatively called the colloidal synthesis method. It is imperative that the reaction takes place in an alcoholic medium because in alcoholic medium the reaction is slow and controllable (Balu and Bhakat, 2012). During the synthesis reaction, aqueous silver ions in solution are reduced by the citrate ion forming metallic silver solid (Equation 3.3).

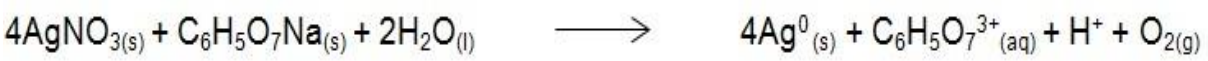

Equation 3. 3 Synthesis of Ag NPs via chemical reduction.

3.2. Characterisation of nanoparticles.

3.2.1. X-ray Diffraction

X-ray diffraction is an indispensable method of characterisation which is able to give substantial information about the crystallographic structure and chemical composition of synthetic and natural materials. It is a laboratory rapid and versatile technique that is useful in the investigation of the crystallinity and atomic structure of materials. During XRD studies of a material, the crystalline material in solid form is bombarded with an X-ray beam which is diffracted in numerous angles by crystal plane atoms within the material. A particular set of crystal planes with a specific interplanar spacing gives rise to diffraction at a specific one

angle. The angle can be elaborated using the Bragg's law (equation 3.4), where the intensities of the diffracted X-ray are plotted against Bragg's angles to produce a diffractogram.

$$N\lambda = 2d \sin\theta$$

Equation 3. 4 Bragg's law equation

Where: λ is wavelength of X-rays, d is plane spacing within the crystal, and θ is angle of diffraction. Diffraction peaks in the diffractogram are indicative of densities of the abundance of the particular crystal facets in the lattice of the analyte material. The diffractograms are unique for different material therefore they can be used for qualitative analytical investigations in material identification. In this section of research, XRD was used to characterise the NPs and to also study their crystallinity.

3.2.2. UV-Visible spectroscopy

Most metals and their oxides absorb light at specific wavelengths and this enables them to be characterised using UV-Visible spectroscopy. Since the absorbance of the metals and their oxides is also affected by size and shape, this means that the bulk material and NPs of a particular metal absorb at different wavelengths thereby making their identification using UV-Visible possible. All the NPs used in this research study are transition elements and therefore absorb in the visible region as a result of their d-orbital transitions. UV-Vis can be used to distinguish between the bulk and NPs of the same species because NPs usually exhibit a blue-shift in their SPR (Debanath and Karmakar, 2013). A blue-shift is a decrease in wavelength and it can be used to investigate the changes that have taken place in a substance. It is expected that NPs will absorb at a much lower wavelength and exhibit a larger optical band gap. This phenomenon makes it possible to distinguish between NPs and their bulk form using UV-Visible spectroscopy thereby confirming the successful synthesis of NPs. The UV-Visible spectra of Ag, CuO, and ZnO NPs were recorded in the wavelength range of 300-500nm.

3.2.3. FTIR studies

Fourier Transform Infrared spectroscopy (FTIR) is a paramount technique that characterises matter at molecular and atomic scale. FTIR can reveal the type of bonds and the particular elements that are involved in the bonding by the singular resonant vibrations that the part or wings of the molecule/element undergoes. The FTIR spectra contain a large number of bands making it virtually impossible for two molecules or two elements to have the same

spectra (Kurien, 2005). Inorganic analytes possess a unique spectrograph which occurs in the fingerprint region and this is used to identify the species involved. This is different from element to element and this gives the ability to identify different inorganic species. The large spectrum of bands also makes it possible to distinguish NPs of a particular element from its bulk material. The two differ in surface to volume ratio hence different electron densities and this causes them to give different spectra in FTIR. This makes FTIR an efficient tool in the confirmation and identification of NPs.

3.2.4. Transmission electron microscopy studies

The size and morphological properties of the synthesized NPs was studied using the transmission electron microscopy (TEM). It is of importance that the morphological properties of the nanoparticles are studied because the properties have a great influence and dictation on the chemical and physical properties of the NPs (Sanyal, Datta and Hazra, 2002).The TEM characterisation in this chapter also investigated the relationship between the synthesis pathway that is used and the NPs morphology that is as a result of that procedure. TEM was also used to determine the size of the NPs using scale calibration of the pictograms.

3.2.5. Electrochemical studies

Electrochemical properties of the NPs were investigated using the cyclic voltammetry method (CV). Cyclic voltammetry is rapid technique that is mostly used to gather qualitative information on the electrochemical reactions of a particular analyte. The technique has the ability to provide substantial information on the adsorption processes, thermodynamics of redox processes and electron transfer processes (Joseph Wang, 2006). These processes give information that can assist in determining or predicting the chemical or physical behaviour of a particular substance. This then gives an insight on the potential the substance contains with regard to its intended use. In this research the electron transfer mechanism, electronic band gap energy, analytical confirmation was undertaken by cyclic voltammetry.

3.2.6. Band gap energies

The band gap can be simply defined as the electronic difference between the HOMO and LUMO in an atom. By principle, reduction operates by adding an atom to the Lowest (in energy) Unoccupied Molecular Orbital and oxidation is the detachment of an electron from the Highest (in energy) Occupied Molecular Orbital in the atom (Zhou, Hashimoto and Tajima, 2013). The band gap energy can either be determined optically using spectrochemical methods or electronically using electrochemical methods. For most metallic elements the optical and electronic band gaps are similar though the electronic band gap energy is usually higher than the optical band gap energy. This is because in electronic band

gap measurement the electron is ejected from the valence band and in optical band gap measurement it involves the excitation of the electron from the valence band to the conduction band. Usually metals with a higher, band gap >4.0eV, are considered as insulators and are known to be of low chemical reactivity (Babu, 2010).

The Ag, CuO, and ZnO NPs were synthesized using the chemical reduction method and confirmed using UV-Visible spectroscopy. The optical properties of the NPs were investigated using the FTIR and UV-Visible spectroscopy whereas the electrochemical behaviour was investigated using cyclic voltammetry. Optical and electronic band gap energies were determined using UV-Visible and cyclic voltammetry respectively.

3.3. Experimental

3.3.1. Reagents

Zinc acetate; $Zn(CH_3COO)_2$ (Aldrich 98%), Potassium hydroxide; KOH (SaarChem 99%), Silver nitrate; $AgNO_3$ (Aldrich 99.9%), Sodium citrate; $Na_3C_6H_5O_7$ (99.9%), Copper (II) chloride; $CuCl_2$ (SaarChem 99%)

3.3.2. Synthesis of NPs

3.3.2.1. Copper NPs

The copper oxide NPs was synthesized using a prescribed sol gel method (Srivastava, Agrawal and Kumar, 2013).9.7g of copper (II) chloride was refluxed with 8g of KOH in a 50-50 hexane-benzene mixture for 2hrs 30 minutes. The copper oxide powder was separated by filtration and was washed with methanol until the pH was neutral. The copper oxide powder was dried at 120 ºC for 15 hours.

3.3.2.2. Zinc NPs

100 ml of 0.2 M zinc acetate in a 50-50 water-ethanol solution was brought to boil in an Erlenmeyer flask with vigorous stirring. An aliquot of 10 ml of 0.3 M KOH was added drop wise to the zinc acetate solution. The solution was brought to 90 ºC and maintained at the temperature for 2 hours. The product was then centrifuged and washed with a 50-50 ethanol-water solution. The resultant hydrated powder was then dried at 70 ºC for 13 hours.

3.3.2.3. Silver NPs

A 20ml solution of 0.0002487 M silver nitrate in a 50-50 ethanol-water solution was brought to boil in a foil covered Erlenmeyer flask. After boil had commenced, a 2.5 ml aliquot of 1% sodium citrate was added drop wise with magnetic stirring in a foil covered flask. The solution

was stirred and maintained at 80 ºC for 15 mins. The product was washed by centrifugation using a 50-50 water-ethanol mixture. The product was stored in a translucent container.

3.3.3. Characterization

3.3.3.1. UV-Visible spectroscopy

A Cary IE Varian dual-beam spectrometer was used for the absorption investigation of the three NPs in the wavelength range of 200-600 nm. Copper and zinc were dissolved in distilled water to enable measurement of absorption. All NPS was placed in 1 cm quartz cuvettes for absorption measurements.

3.3.3.2. FTIR spectroscopy

FTIR investigations were done using a PerkinElmer Spectrum Two apparatus in the wavelength range of 600 to 3000 cm^{-1}. The two powdered samples were placed on the diamond eye and pressed down using the pressure applicator. The silver gelatinous fluid was dropped using a pipette dropper and analysed.

3.3.3.3. X-ray Diffraction

XRD investigations were carried out using a Bruker AXS D8 Advance diffractometer. The measurement was recorded by Cu Kα radiation operated at 40 kV and 60 mA in the range of 30° to 80°.

3.3.3.4. TEM measurements

Morphological studies and particle distribution were conducted using a Tecnai G2F20 X-Twin MAT (US). Chemical compositions of the NPs were determined by an EDX analyzer that is attached to the TEM apparatus. Analysis was done by preparing liquid slurry and dropping it on a carbon-coated standard copper grid that operated at 10 kV.

3.3.3.5. Cyclic voltammetry

The electrochemical activity of zinc oxide and silver NPs was investigated by drop coating them onto the Glassy Carbon Electrode (GCE) and drying them at room temperature for 18hrs before studying the film using cyclic voltammetry. The copper oxide NPs were introduced into the supporting electrolyte media for analysis and studied using cyclic voltammetry. Interval cleaning and polishing of the GCE was done in between different modifications of the GCE and analysis. After every run the GCE was gently rubbed on a filter paper to remove the modification film and then placed in a 50-50% ethanol water solution and sonicated for 10mins at 25°C and low sonication power. After this the GCE would be rinsed with distilled water and polished with 1, 0.3 and 0.05 µm alumina slurry for 15mins per

polishing station. The slurry was rinsed off the GCE then ultra-sonication with ethanol water solution followed for 20 minutes. Reference electrode Ag/AgCl (3 M NaCl) and counter electrode, platinum wire was rinsed thoroughly with distilled water for 3 minutes after every run.

3.4. Results and discussion

The inert chemical reduction process produced a black powder of CuO NPs after annealation and it is in line with other results that were obtained using the same synthesis method (Srivastava, Agrawal and Kumar, 2013). Fine powder of zinc oxide NPs was obtained and silver NPs produced were gelatinous yellow-grey in appearance. The nanoparticles were confirmed by UV-visible with characteristic peaks being observed at 420nm, 305nm, 375nm for Ag, CuO, and ZnO respectively (Khorsand Zak *et al.*, 2011; Talam, Karumuri and Gunnam, 2012; Srivastava, Agrawal and Kumar, 2013; Jyoti, Baunthiyal and Singh, 2016).

3.4.1. UV-Vis spectroscopy studies

The optical absorption spectra for all the NPs showed plasmon bands within the wavelength range of investigation. For Ag NPs a relatively single, weak, broad surface plasmon resonance (SPR) was observed at 420 nm confirming the presence of Ag NPs (Figure 3.2). Previous studies suggest that the SPR for Ag NPs usually falls in the range of 410-450nm wavelength and usually signify the presence of spherically shaped Ag NPs (Jyoti, Baunthiyal and Singh, 2016). The broad peak is attributed to the polydispersion and wide size distribution within the Ag NPs. It is suggested by other studies that a sharp peak indicates monodispersion and narrow size distribution of the Ag NPs whereas a broad peak is as a result of polydispersion and wide size distribution (Shrivastava *et al.*, 2010). CuO NPs exhibited an excitonic SPR of 305nm which corresponds to CuO NPs (Figure 3.2). Similar results were obtained elsewhere during the optical characterisation of copper NPs (Rahman *et al.*, 2009). Past work has shown the range of CuO NPs to fall within the range of 250 to 350nm (Algawi, no date). The absorption of the copper NPs was consistent from 500nm to 350nm and an absorption tail started from 350 nm. This phenomenon is due to change in the absorption range from particle NPs to the bulk NPs which is as a result of light scattering by the agglomerated particles. Bulk normal copper usually has an SPR in the range of 500 to 600 nm with the other oxide of copper Cu_2O falling within the same range (Rahman *et al.*, 2009).

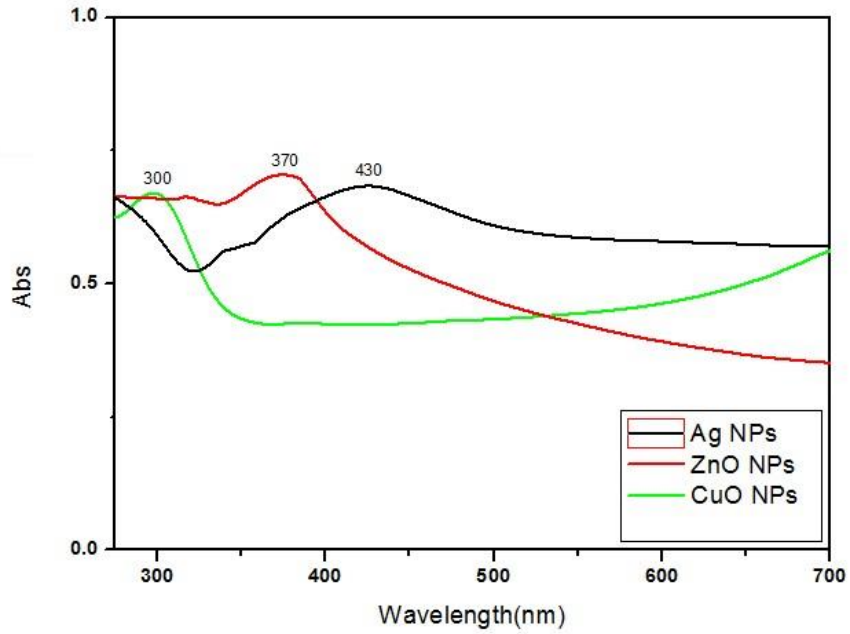

Figure 3. 2. Absorbance spectra of Ag, ZnO, and CuO NPs.

The SPR of copper obtained from the UV-Visible spectra indicates dominant presence of cupric oxide within the copper NPs than the cuprous oxide.

A characteristic peak due to the plasmon band of zinc oxide NPs was obtained at 375 nm. The surface plasmon resonance was observed as a single peak of medium strength with weak shoulder. Optical characterisation of ZnO NPs by Zak and co. gave similar results (Khorsand Zak *et al.*, 2011). The SPR for the ZnO oxide NPs is attributed to the electron transition, O_{2p} to Zn_{3d} , which is from the valence band to the conduction band. The peak broadness may indicate that the size distribution of the NPs is not narrow.

3.4.2. FTIR studies

FTIR was conducted on the synthesized NPs in a bid to comprehend the chemical bonds within the NPs. Figure 3.4 shows the overlain spectrum recorded in the wavelength range of 200 to 3000 cm^{-1}. FTIR analysis of metals give characteristic peaks that usually appear within the fingerprint region which is below 1000 cm^{-1} (Srivastava, Agrawal and Kumar, 2013). This ascribed to the vibrational and stretch mechanisms that metals undergo.

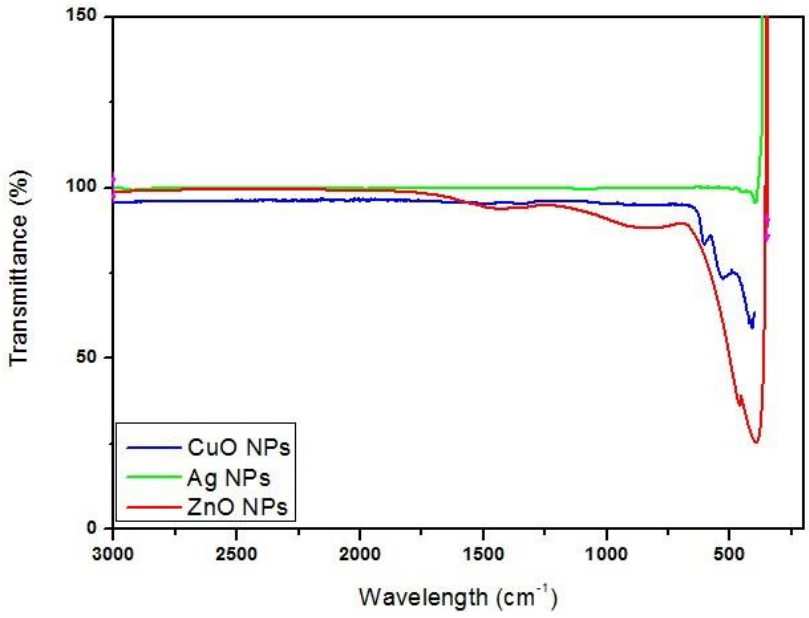

Figure 3. 3. FTIR spectra of CuO, Ag, and ZnO NPs.

Copper characteristic peaks where recorded at 490 cm^{-1}, 520 cm^{-1} and 620 cm^{-1}(Figure 3.4). The peaks at 490 cm^{-1} and 520 cm^{-1} can be attributed to the vibrational stretch of the Cu-O bond along the plane therefore signifying the presence of cupric oxide, CuO similar observations have been made (Kayani *et al.*, 2012) . The high frequency peak at 620 cm^{-1} signifies another IR active mode which gives a sign of the presence of another phase. That peak is attributed to the presence of cuprous oxide, Cu_2O. Literature submits that presence of an IR mode in the range of 605 cm^{-1} to 650 cm^{-1} for the FTIR analysis of copper NPs signifies the presence of copper (I) oxide (Kayani *et al.*, 2012) and this confirms the presence of cuprous oxide. No other peaks are visible due to the fact that the NPs were washed before calcination. The FTIR spectrum of copper NPs ascertained the purity of the material and also showed that the copper NPs contained both cupric and cuprous oxides.

For any functional effect that was attributed to the copper NPs it was taken into consideration that it was as a result of the combined action of the two copper oxides present. A characteristic peak for Ag NPs was observed at 490 cm^{-1} (Figure 3.4). This peak is attributed to the stretching of the Ag-Ag group. The peak of the Ag NPs is narrow signifying that the Ag NPs are polydispersed. Literature suggests IR mode for silver is usually in the range of 400 cm^{-1} and 700 cm^{-1} which comes about by the stretching and deformation vibration of the Ag-Ag bond(Kumar and Rani, 2013).

A characteristic peaks for zinc was observed at 430 cm^{-1} and 500 cm^{-1}. The peak at 430 cm^{-1} is attributed by the vibrational stretch of the metal-oxide along the plane. The peak is sharp and intense due to the Zn-O vibrational stretches. The peak also corresponds to the E_2 of hexagonal ZnO since the oxide is Raman active. The band at 500 cm^{-1} can be related to an oxygen deficient complex in ZnO. This can be caused by bulk defects in the structure of the metal oxide (Xiong *et al.*, 2006). Another single distinct peak is observed at 560cm^{-1}. Previous work has shown the Zn-O stretch for zinc nano-rods can be identified in the range of 400-550 cm^{-1} (Kamellia Nejati, 2011). The peak at 560 cm^{-1} is an indication of presence nano-rods which were also observed in TEM pictorials. The FTIR metal oxide frequencies for each of the metal oxides fall in within other reported study values(I. Markova-Deneva, 2010).

3.4.3. X-ray Diffraction studies (XRD)

Figure 3.2 shows the XRD diffractograms of the Ag, ZnO, and CuO NPs. The diffraction patterns for all the NPs showed exhibited sharp narrow peaks with a few weak broad peaks being seen.

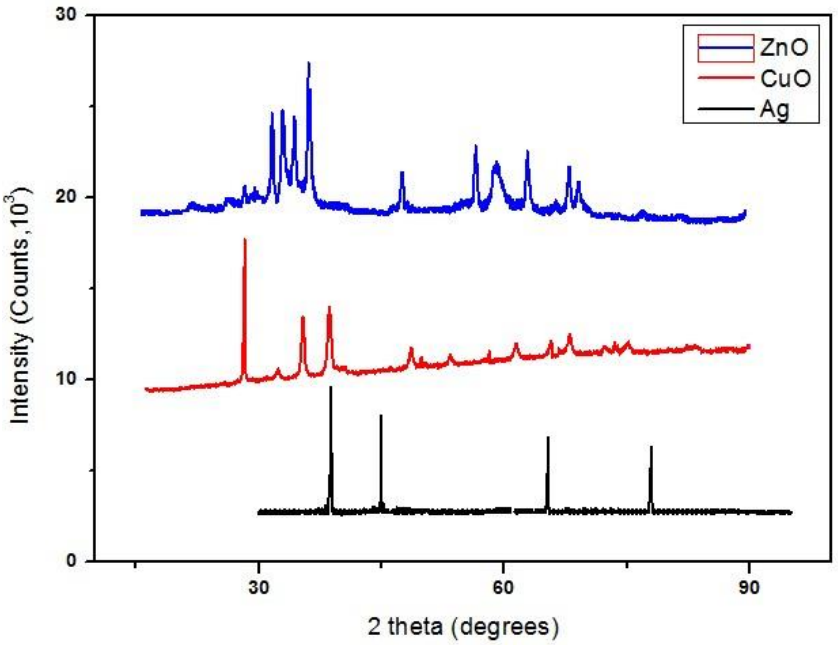

Figure 3. 4 X-ray diffraction patterns of Ag, ZnO, and CuO NPs.

The XRD pattern for the Ag NPs shows distinct narrow, sharp peaks in the diffractogram (Figure 3.2). The general appearance of the peaks indicates that the Ag particles are of high crystallinity. The XRD peaks for Ag NPs appear at 38.5°,45°,67°,78° and these peaks correspond to the (hkl) values of (111), (200), (220), (311) respectively. The peaks and their corresponding (hkl) values are characteristic of a face-centred cubic structure being the

dominant crystal structure within the Ag NPs as similarly reported (Jyoti, Baunthiyal and Singh, 2016; Mehta, Chhajlani and Shrivastava, 2017).

The XRD pattern for CuO NPs in figure 3.2 shows three sharp narrow peaks of relatively high intensity and also a number of broad low intensity peaks. The sharp narrow peak of the highest intensity at 29.4°, is due to the reflection along the (110) plane caused by the structure of the cuprous oxide, Cu2O. The two narrow peaks at 36.1° and 39° match the reflections of the planes at (-111) and (111) respectively and these are due to the cupric structure within the CuO. The other smaller peaks at 49°,66°,61° and 43° correspond to the (hkl) values of (202), (220), (113), and (200) respectively which are characteristic of the reflection in the planes of copper oxide. The (hkl) values indicate that the crystal structure of the CuO NPs is base-centred monoclinic as similarly reported (Padil and Cernik, 2013; Kayani *et al.*, 2015). The information obtained also indicates that both the two types of copper oxide, cupric and cuprous, maybe present in the CuO NPs. Reports indicate that during the formation of CuO NPs via chemical reduction, there is formation of both CuO and Cu_2O (Kayani *et al.*, 2015) .

Relatively broad distinct peaks were observed for the ZnO XRD diffractogram. The broadness in nature of the peaks gives an indication that the ZnO is within the nanometre range of size (Mohan and Renjanadevi, 2016). Peaks were observed at 34.5°,31.8°,36°,47.6°,56.7°,62.9°,68° and 67.3° and they corresponding to the (hkl) values of (002), (100), (101), (102), (110), (103), (201), (112) respectively. These values are similar to other reported values (Khorsand Zak *et al.*, 2011; Talam, Karumuri and Gunnam, 2012) . The values give an indication that the crystal structure of the ZnO NPs is hexagonal as indicated by similar work (Arefi and Rezaei-Zarchi, 2012).

3.4.4. Transmission Electron microscopy (TEM)

TEM images of synthesized NPs show single particles as well as tendency to agglomerate to create the nano-clusters (Figure 3.5). Agglomeration could have been caused by various factors such as presence of a capping agents, temperature fluctuations, and uneven stirring of media during synthesis. Capping agents are usually introduced to nanoparticles during synthesis to stabilize the nanoparticles in solution. The NPs size distribution for all the NPs indicate that all the NPs fell within the nano-range of > 100nm (Table 3.1).

TEM characterization of Ag NPs show spherical shaped NPs being dominant in the sample. In this case the agglomeration was caused by the citrate from the sodium citrate that was used during the synthesis of the silver NPs. Sodium citrate acts as both a reducing agent and a capping agent in Ag NPs synthesis protocols (Gliga *et al.*, 2014). Even though the aqueous

silver NPs was washed after synthesis, some of the capping agent tends to remain attached to the metal causing the phenomenon of agglomeration. The agglomeration of citrate capped Ag NPs increases with the concentration of the capping agent (Shen *et al.*, 2009). Higher temperatures are also known to increase the occurrence and prevalence of agglomeration of the silver NPs.

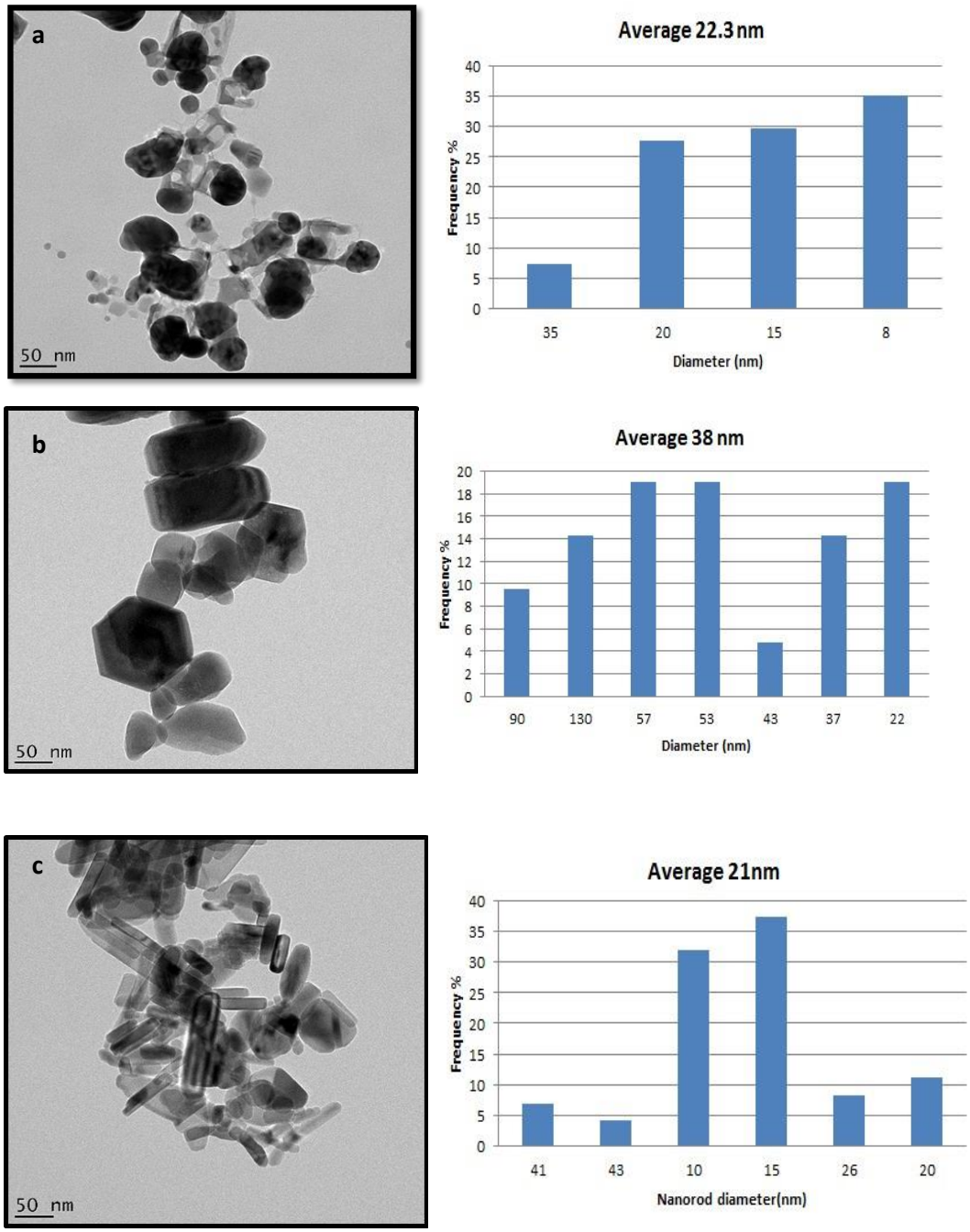

Figure 3. 5. TEM pictograms and size distribution of a) Ag b) CuO and c) ZnO NPs.

Table 3. 1. Average sizes and shapes of NPs from TEM.

	Mean diameter ± SD (nm)	Dominant Shapes	Dispersion
Ag NPs	22 ± 9	Spherical	Polydispersed
CuO NPs	38 ± 29	Hexagonal and spherical	Polydispersed
ZnO NPs	21 ± 14	Rod and spherical	Monodispersed

Temperatures around 20 ºC during synthesis give NPs with less agglomeration and particle dispersion though this is coupled up with a large distribution of bigger NPs size (Xiliang *et al.*, 2014). Temperatures above 50 ºC produce NPs of a smaller size though at these temperatures the agglomeration and particle size dispersion is pronounced (Xiliang *et al.*, 2014). In this research temperatures of 60 ºC were used in order to produce NPs of sizes 30 nm > coupled standard particle dispersion. The histogram for particle size distribution for silver (Figure 3.2a) shows that 70% of the NPs that were produced were 20 nm > in size. The TEM picture of silver nanoparticles showed spherical nanoparticles and irregular particles of between 8 and 35nm after scale calibration. Similar results were reported elsewhere (Guzman MG, 2008). The relatively smaller standard deviation (Table 3.1) shows that the reaction rate throughout the synthesis media was consistent. This can be attributed to the continuous stirring that took place during the synthesis protocol. Stirring causes equal distribution of both the silver salt and the citrate throughout the media thereby causing the reduction reaction to take place at more or less the same rate within the media.

Copper nanoparticles show the presence predominantly rod and spherically shaped NPs. It can be seen that a much higher proportion of rod-shaped particles were produced in comparison to the other shapes. The wide variance in the shapes of the NPs formed shows that the rate of reaction in the copper synthesis media varied. During the synthesis of the copper NPs, the stirring rod within the media decreased in speed due to the solid Cu NPSs which was being formed and settling at the bottom of the flask. As the speed of the stirring rod decreased, the distribution of the copper salt and reducing agent around the flask became uneven thereby causing the formation of various Cu NPs shapes and sizes during the nucleation stage. This caused the wide size distribution of the copper nanoparticles of between 22 nm to 130 nm with an average diameter of 38 nm (Table 3.1). The standard

deviation is relatively high showing that there is big size variation in the NPs that was formed thereby confirming the unevenness of reaction rates the nucleation stage of the synthesis. The rate at which the reaction of synthesis takes place is of high influence to the type of shape and size of the NPs that is formed (Tran and Nguyen, 2014) .

Zinc NPs that were formed were predominantly rod-shaped as shown by the TEM pictogram. Previous studies have shown that zinc NPs synthesized with ethanol as a solvent form rod shaped particles and using water as a solvent forms spherically shaped zinc nanoparticles (Bagabas *et al.*, 2013). The synthesis method used in this study produced spherical and rod shaped particles as expected due to the 50-50 ethanol-water solvent that was used. Previous work reported the same after the use of the same type of solvent (Avnish K, 2001). The standard deviation of the Zn NPs shows a wide size distribution with respect to the diameter of the nano-rods. The histogram for the NPs diameter distribution (Figure 3.2c) shows that the size range of the NPs had a higher frequency between 10 and 15 nm and the average diameter of the NPs was 21 nm. The wide range of nanoparticle diameter is suspected to have been caused by inconsistent heating by the water bath during the reaction. The heating temperature during synthesis plays a significant role in the size and morphology of NPs that will be produced.

3.4.4.1. Energy dispersive x-ray spectroscopy studies

The elemental composition for the various NPs was undertaken using energy dispersive x-ray (EDX) in the range of 0 to 20keV. In the spectrum for Ag NPs, it was observed that there were four distinct peaks of different species. These peaks observed were Cu, Ag and C. The Ag peaks between 2 and 5keV corresponds to Ag NPs and are of the K and L assignments (Figure 3.7a) (Puchalski *et al.*, 2007). Similar results are not observed with bulk silver nitrate (Kalimuthu *et al.*, 2008). The intensity of the peaks is weak due to the nature of the sample which was made up of Ag NPs spatially dispersed in a gelatinous fluid. The more abundant peak at 8.5keV is that of Cu and that of carbon at 0.5keV is from the carbon coated sample holder used during analysis. The ZnO NPs EDX spectrum (Figure 3.7b) showed strong peaks of Zn accompanied by weak signal peaks of O, C, Na, and Cu. The strong peak obtained between 0 to 3kV for Zn is characteristic of Zn NPs and similar results have been reported elsewhere (Brintha and Ajitha, 2015). The weak carbon and copper peaks were from the sample grid that was used in the analysis. The EDX spectra for CuO NPs (Figure 3.7c) revealed the presence of both copper and oxygen with characteristic peaks in the range of 0 to 2keV.

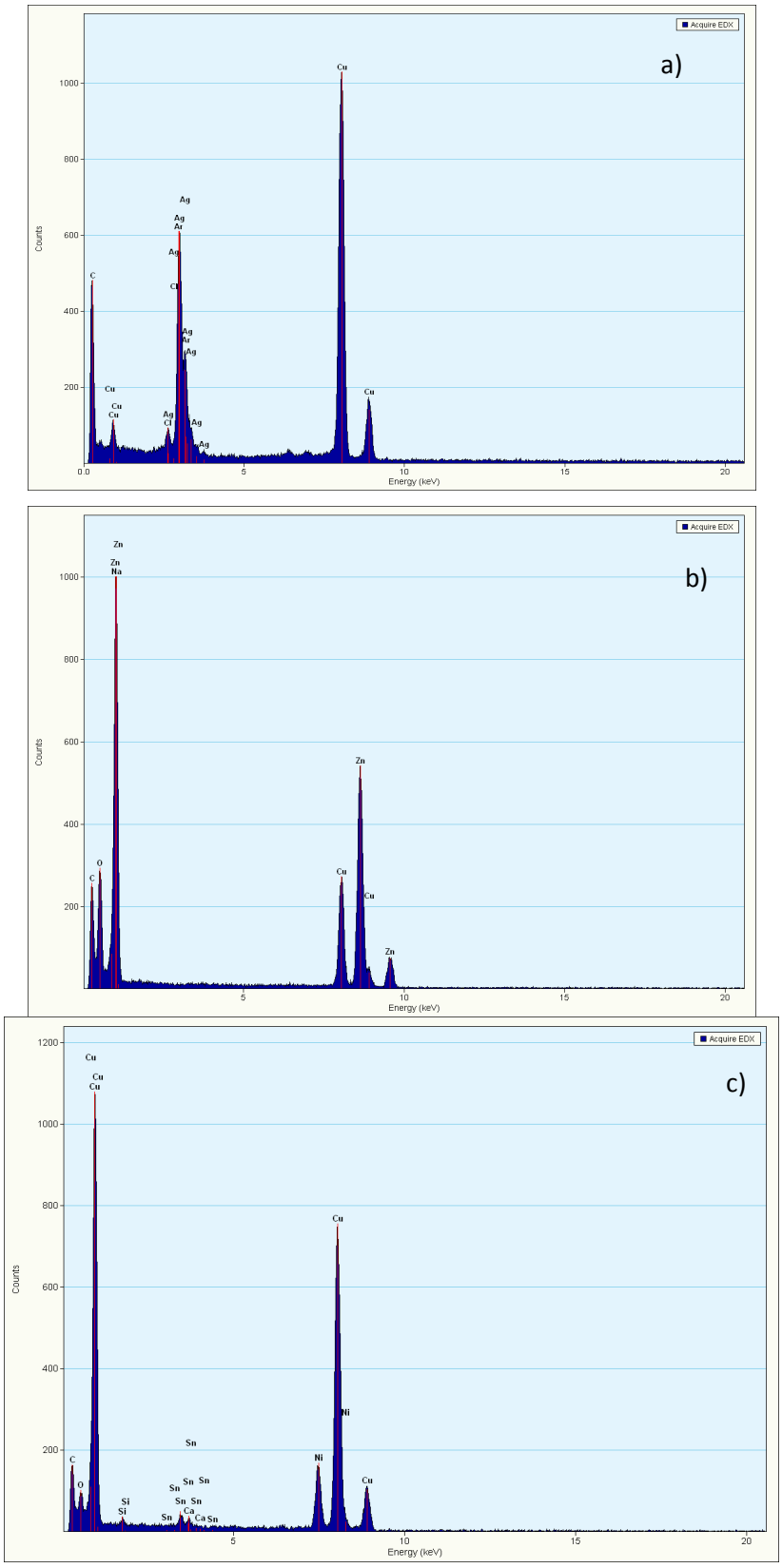

Figure 3. 6 EDX spectra obtained for a) Ag NPs b) ZnO NPs and c) CuO NPs

The peaks positions observed for copper are consistent with copper oxide assignment and the shape of the peaks indicate that the NPs are predominantly crystalline in nature(Ijaz *et al.*, 2017)(Devi and Singh, 2014; Luna *et al.*, 2015). All the EDX spectra showed that the samples were composed of the synthesized NPs.

3.4.5. Electrochemical studies using Cyclic Voltammetry.

3.4.5.1. Characterisation of Ag, CuO and ZnO modified GCE

The voltammograms of all the NPs showed characteristic oxidation and reduction peaks indicating electroactivity of the NPs. Peaks for both Ag and ZnO NPs were broad indicating that the redox reactions taking place were occurring at a slow rate. The voltammetry of the GCE/Ag NPs modified electrode gave an anodic at 250mV and a cathodic peak at -500mV (Figure 3.7). Both peaks are not present on the bare GCE electrode voltammogram and this suggests that these peaks are a response due to Ag NPs film on the GCE. On visual assessment of the voltammogram of the Ag NPs, it can be seen that the reduction peak is much more broad than the oxidation peak hence it can be considered that the reduction of Ag^{+} to Ag is much slower than the oxidation of Ag. A study conducted elsewhere produced the same peaks in a similar potential range. During the forward sweep the Ag ions are oxidised thereby losing an electron giving rise to the oxidation signal and in the reverse sweep Ag^{+} ions are reduced giving rise to the anodic peak.

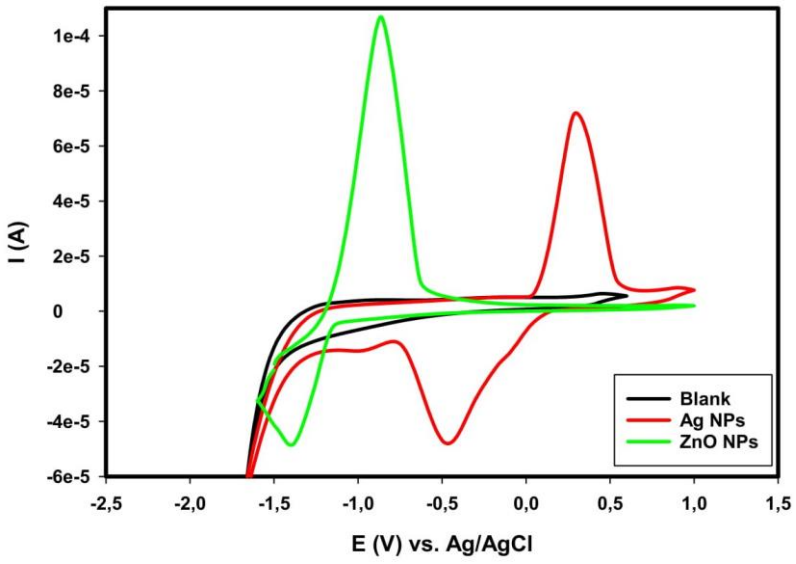

Figure 3. 7 Cyclic voltammogram of ZnO and Ag NPs modified GCE in 0.1mM HCl, pH 4.5.Scan rate 40mVs^{-1}.

The modified GCE/Zn NPs electrode produced a voltammogram with oxidation and reduction peaks at -810mV (peak A) and -1400mV (peak a) respectively as shown by Figure 3.7. The zinc oxide partially dissolves in the HCl supporting electrolyte thereby forming an aqueous

zinc ion. Zn^{+} is responsible for the peak at -810mV and this corresponds to the oxidation of Zn^{+} to Zn^{2+} by the loss of an electron at the GCE surface. Reduction of Zn^{+} at the surface of the GCE is signified by the peak at -1400mV with the broadness of the peak showing that the reduction of zinc is a much slower reaction than its oxidation. The two peaks do not exist on the bare GCE voltammogram (Figure 3.7) thereby it can be concluded that the peaks given by the GCE/Zn NPs modified electrode correspond to the redox operation of zinc NPs. Similar reports were made during the electrochemical analysis of zinc NPs(Long *et al.*, 2016).

The introduction of a drop of 6mM of Cu NPs in the supporting electrolyte produced two characteristic peaks during both the cathodic sweep and the anodic sweep (Figure 3.8). Both sweeps had one narrow high response peak and one broader low response peak. The sharp peaks indicated that the electron transfer reaction taking place happened at a faster rate and the broader peaks indicate that the reaction taking place there was at a relatively slower rate.

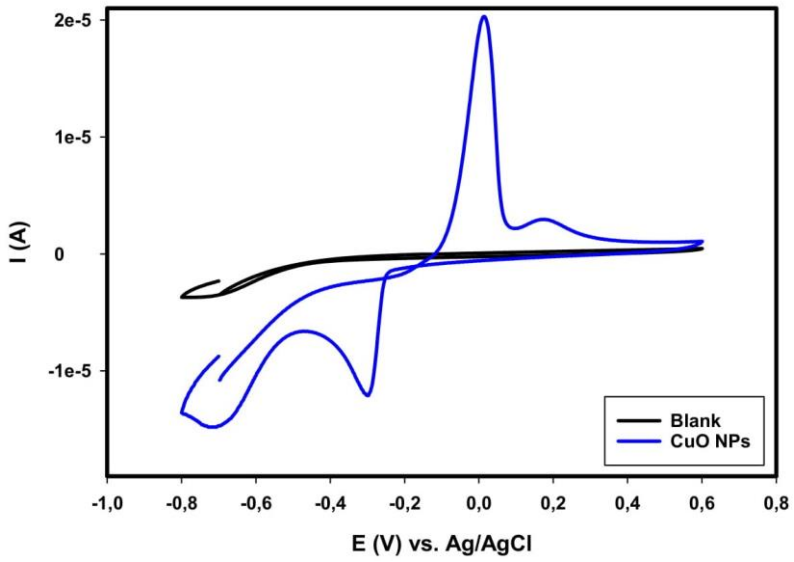

Figure 3. 8 Cyclic Voltammogram of CuO NPs in HCL 0.1mM, pH 4.5. Scan rate 40mVs^{-1}

As copper is introduced into the supporting electrolyte it dissolves forming copper (I) chloride as shown by the equation on the voltammogram. As the anodic sweep proceeds it causes the oxidation of Cu^{+} to Cu^{2+} at peak E_{pa1}=90mV. The peak is attributed to the Cu^{+}/Cu^{2+} redox couple. The peak is absent on the bare GCE voltammogram (blank) of the media. The peak at E_{pa2}=180mV, can be attributed to the Cu/Cu^{+} redox couple. The redox process is attributed to the oxidation of elemental Cu NPs that are present in the solution. The low surface area of the peak shows that the specie responsible for the peak is of less abundance in the media than of Peak A. Similar reports have been made in studies conducted elsewhere (Valov and Lu, 2016). Peak a, E_{pc1}=-310mV, is the peak attributed to the transition of Cu^{2+} to Cu^{+}

(Equation 3.8). The Cu^{+}/Cu reduction couple is represented by peak b at E_{pc2} = -800mV in the anodic sweep direction. The absence of all four peaks in the bare GCE voltammogram attributes the peaks that are visible in the Cu NPs voltammogram to the presence of Cu NPs. Similar results have been reported in other separate studies (Krishnamoorthy and Kim, 2013; Yukna, 2014). The shapes of the peaks show that during analysis the oxidation of Cu^{+} was relatively faster than the oxidation of Cu^{0} and the reduction of Cu^{2+} was faster than the reduction of Cu^{+} in the cathodic sweep.

3.4.5.2. Electron-transfer kinetics studies

In a bid to study the electron-transfer kinetics of the metallic NPs, voltammograms at various scan rates between 20 to 80mVs^{-1} produced using 0.1mM HCl supporting electrolyte.

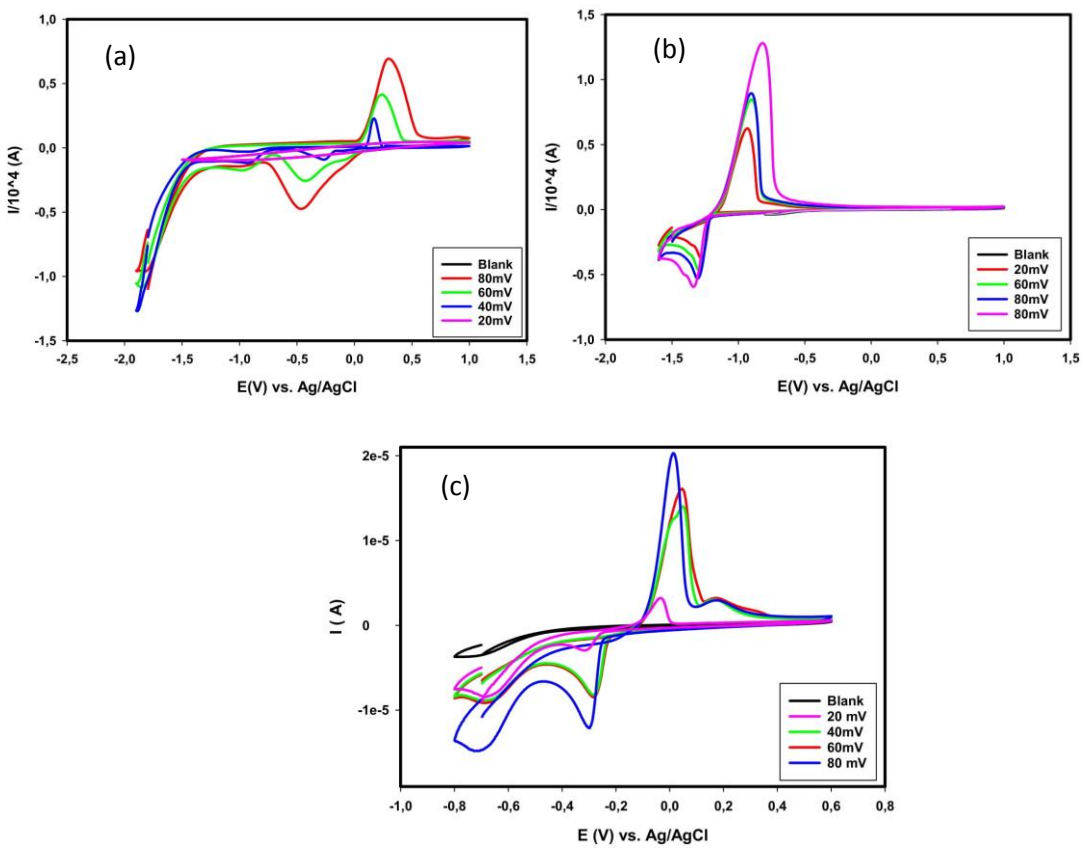

Figure 3. 9. Voltammograms of a) Ag b) ZnO and c) CuO NPs in 0.1mM HCl, pH 4. scan rates 20 to 80 mV.

It can be seen in Figure 3.2 that both the cathodic and anodic peaks shifted towards the positive side as the scan rate was increased. The positive shift in potential with increase in scan rate is less observed in the copper voltammogram compared to the voltammograms of

ZnO and Ag NPs. This is due to the fact that the CuO NPs were not drop coated onto the GCE during analysis but rather they were introduced into the supporting electrolyte for analysis. The shift towards the more positive potential with increasing scan rate is attributed to kinetic limitation which can be caused by various factors such as interference of the analyte film by supporting electrolyte species, uneven reaction site distribution of the film and electrostatic factors on the surface of the modified electrode (Bard *et al.*, 1944). The peaks of the analysis of CuO NPs indicate that there is no kinetic limitation during its analysis and this can be explained by the fact that there was no drop coated film on the GCE and the NPs were delocalised within the supporting electrolyte media.

To determine the nature of reaction taking place at the electrodes plots of Ipa vs. V and Ipa vs. $V^{1/2}$ can be made, where Ipa is the anodic current and V is the scan rate and $V^{1/2}$ is the square root of scan rate. Generally a linear plot of anodic peak versus scan rate (V) indicates that the process is adsorption controlled whereas a linear plot of anodic peaks versus the square root of the scan rate ($V^{1/2}$) indicates that the process is diffusion controlled (Sehat *et al.*, 2015).

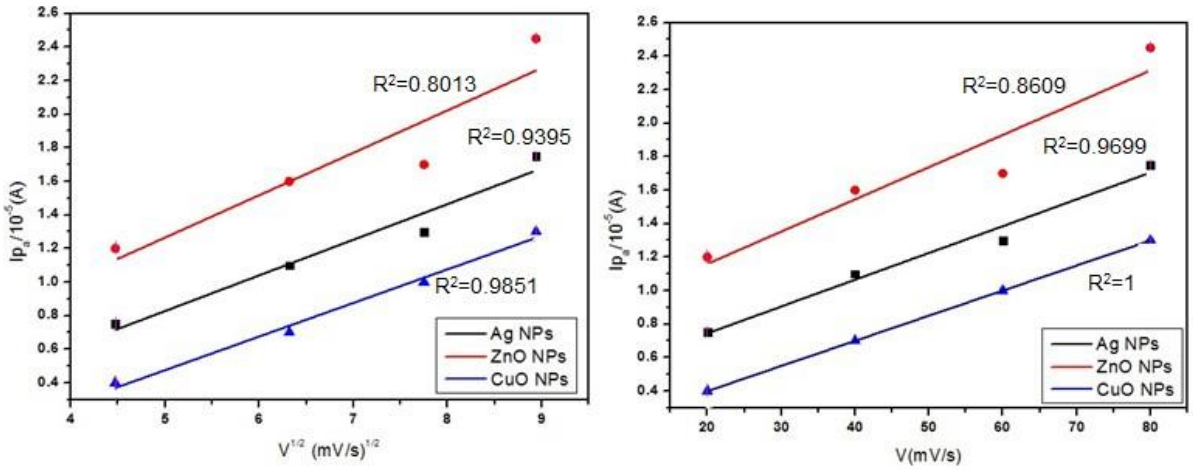

Figure 3. 10. Voltammograms of Ipa vs. a) square root of scan rate in the range of 20-80mVs^{-1}. b) Scan rates in 0.1mM HCl, pH 4.5.

From the plots of anodic peaks versus the scan rates (Figure 3.10), it can be seen that there is a linear increase of the anodic peaks versus $V^{1/2}$ in the scan rate range of 20 to 80mV/s for all the three NPs. However, a perfect linearity is observed between Ipa and V for CuO where the correlation coefficient is ideal, R^2=1. CuO also possesses a relatively stronger correlation between the Ipa and the Scan rate, V. This indicates that both diffusion and adsorption processes are taking place though the dominant process occurring is adsorption controlled. This can be explained by the fact that a drop coat film was not used in the analysis of the

CuO NPs since it was introduced into the electrolyte in solution. Ag NPs possesses a much stronger linearity and correlation in the plot of V vs. Ipa than Ipa vs. $V^{1/2}$ indicating that though both processes of diffusion and adsorption are taking place, the dominant process taking place is adsorption controlled. ZnO NPs exhibit weak correlation for both Ipa vs. V and Ipa vs. $V^{1/2}$ plots with the better correlation being in the Ipa vs. V plot. This signifies the kinetic limitations that maybe present on the drop coat film and this can be linked to the broad peaks experienced both during the cathodic and anodic sweep which indicated that the processes of reduction and oxidation took place at much slower rates. However, the dominant process taking place at the electrode is the adsorption process.

The relationship between redox peak potentials and the scan rate can be used to calculate electrochemical parameters by applying Laviron's equations using the data from the voltammograms (E Laviron, 1979).

$$E_{pa} = E^0 + \frac{2.3RT}{(1-\propto)nF}\log v \quad \text{.....3.4a}$$

$$E_{pc} = E^0 - \frac{2.3RT}{\alpha nF}\log v \quad \text{.....3.4b}$$

$$\text{Log } k_s = \alpha\log(1-\alpha) + (1-\alpha)\log\alpha - \log\left(\frac{RT}{nF}\right) - (1-\alpha)\alpha nF\frac{\Delta Ep}{2.3RT} \quad \text{.....3.4c}$$

Equation 3. 5 Laviron's equations

Where E_{pc} and E_{pa} are the cathodic and anodic peak potentials, respectively, α is the electron transfer coefficient, k_s is standard rate constant for surface reaction, v is the scan rate, R is the universal gas constant (8.314 J mol^{-1} K^{-1}), T is absolute temperature (273.15 K), F the Faraday constant (96 485 C/mol), E^0 is the formal potential and n is the electron transfer number. Using the above equation, if the E^0 is known, Ep is in linear with ln v then the αn value can be calculated from the slope and k_s from the intercept. The E^0 value can be deduced from the intercept of Ep vs. v plot on the ordinate by extrapolating the line to v = 0, when v was approached to zero, then Ep was approached to E^0 .

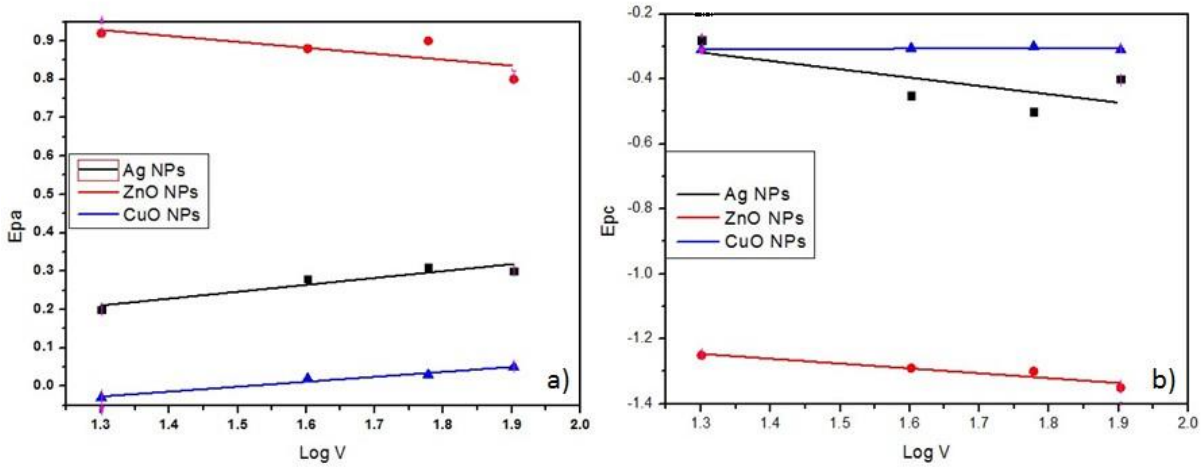

Figure 3. 11. Variation of (a) Epa versus logarithm of scan rate and (b) Epc versus logarithm of scan rate (log V) for the NPs in 0.1mM HCl, pH 4.5.

The values of α and k_s were calculated using Laviron's equations (Equation3.4a-c) and are as shown in table 3.2 and the plots from figure 3.11.

Table 3. 2 The electrochemical parameters of Ag, ZnO and CuO NPs using Laviron's equation (Equation 3.4a-c)

NPs	ΔE^0_p(mV)	nα	α	$k_s(s^{-1})$
Ag	330	1.107	0.6	0.026
ZnO	38	1.21	0.6	0.28
CuO	200	0.396	0.1	2.43

The charge transfer coefficient values (α) imply the fractionalisation of interfacial potential on the electrolyte-electrode interface, which is involved in lowering the free energy barrier for the electrochemical reaction to take place. The values of α that range between 0.5 and 0.7 indicate that the charge transfer kinetics occurring at the electrode are in the proximity of ideal unity which is α = 0.5 (Guidelli *et al.*, 2014). The calculated value of the heterogeneous rate constant, k_s, was found to be in the range of 0.02 to 2.43 s^{-1}. The values were 0.026,0.28, and 2.43 s^{-1} for Ag, ZnO and CuO NPs respectively and they were in the range of other reported values (Pankratov *et al.*, 2014). The higher heterogeneous constant value, k_s, for CuO NPs indicate that the NPs are more functionalised and provide a relatively faster electron transfer rate at the surface of the electrode as previously suggested (Kang *et al.*, 2009). Literature also states that if k_s > 0.020 cm/s it indicates that the reaction is reversible. Since all the results fall in this range, it suggests that the redox reaction of all the NPs under

study are reversible (Laviron, 1995; Brownson and Banks, 2014). The smaller values obtained for ZnO and Ag NPs may indicate that other clusters of the nanomaterial were not directly adsorbed onto the electrode during the sweeps (Prodomis *et al.*, 2000). The peak separation value, ΔE^0_p, for ZnO can be seen that its relatively smaller than the values for Ag and CuO NPs. This can be an indication of a faster electron transfer rate for the redox reaction of ZnO NPs. It can be observed visibly from the voltammogram of ZnO NPs in figure 3.7 that the distance between the E_{pa} and E_{pc} peaks is relatively shorter than for the other two NPs.

3.4.5.3. Band gap energies

The electronic band gaps (E_g) of the Ag, CuO, and ZnO NPs were determined by using HOMO and LUMO values calculated using oxidation and reduction onset values. The HOMO is expressed as I_P, which is defined as the ionisation potential and LUMO as E_a which is electron affinity. The LUMO and HOMO values can be attained by making use of the following equation:

$E_g = (I_p - E_a)$ eV

Equation 3.4. Electrochemical band gap energy equation.

Where $E_a(E_{ox})$ is the electron affinity, $I_p(-E_{red})$ is the ionisation potential; E_{ox} and E_{red} are the onset oxidation and reduction potentials. The band gaps were reported as E_g which is the difference between the HOMO and LUMO (Equation 3.4).

Table 3. 3. Electronic and optical band gaps of NPs.

	Electronic Band Gap			**Optical Band Gap**	
	I_p ($-E_{red}$)	E_a (E_{ox})	E_{eg} (eV)	λ_{max}(nm)	E_{og}(eV)
ZnO NPs	-5.11	-3.2	3.71	420	2.95
Ag NPs	-4.80	-3.3	1.50	305	4.06
CuO NPs	-4.48	-5.51	1.03	375	3.30

The electrochemical band gap for Cu NPs was found to be 1.03 eV and this can confirm the presence of monoclinic CuO NPs. Bulk CuO has an electronic band gap of 2.0 eV and the band gap decreases as the size of the CuO decreases (Balamurugan and Mehta, 2001). The phenomenon is of the band gap increasing with decrease in particle size can be attributed to the quantum confinement effect (Yukna, 2014).Similar results were recorded in separate studies (Srivastava, Agrawal and Kumar, 2013).Zinc NPs had a band gap of 3.71 eV which is within the range of other previous studies that have been conducted separately. Similar studies showed that the electronic band gap of ZnO NPs is within the range of 3.30 eV and 3.60eV (Talam, Karumuri and Gunnam, 2012)(Debanath and Karmakar, 2013). The electronic band gap of silver was found to be 1.50 eV which is higher than the 0 eV expected for bulk silver. The band gap is a confirmation of the presence of NPs since the band gap of bulk Ag NPs is expected to be in the range of 0 eV(Kumar and Rani, 2013). The similar results have been obtained in separate studies (Okumu and Matoetoe, 2016).

The optical band gap energies were calculated using the optical band energy equation (Equation 3.8) (Budhiraja *et al.*, 2013) making use of the wavelength data obtained in section 3.3.3 .

$$E_{obg} = \frac{1240}{\lambda} \qquad \text{(Equation 3.5)}$$

Equation 3. 6 Optical band gap energy equation

The optical band gaps of the three NPs fall within the range of the expected band gaps for NPs (Table 3.2). Materials with a narrow band of the range 1 - 4eV are semi-conductors with respect to electrical conductivity and also have vibrational modes of energy. This means that their valence and conduction states possess a narrow orbital overlap therefore it is easy to excite an electron to a higher state (Radecka *et al.*, 2008). This means that they have a relatively higher reactivity compared to material that has a band gap energy >4.0 eV. The relative band gap energies in table 3.4 indicate that the Ag NPs are expected exhibit a relatively higher reactivity. Researchers suggest that the band gap energy of NPs or material can give an indication on the general reactivity potential of the material (John Kotz, Paul Treichel, 2009).

3.5. Conclusion

As previously outlined, part of the objectives of this study was to synthesis and characterise Ag, CuO and ZnO NPs, which was achieved within this chapter. The three NPs were synthesised successfully using the chemical reduction method. The XRD, UV-Visible and cyclic voltammetry all confirmed the formation of nanoparticles. The average sizes of the

synthesized NPs were found to be 22.3, 38.0, 21.0 nm for Ag, Cu and Zn NPs respectively. The crystal structures determined using XRD were face-centred cubic, base-centred monoclinic and hexagonal for Ag, CuO and ZnO NPs respectively. The electronic and optical band gap energies of the NPs were in the range of 1 to 5eV which falls in the expected range for the NPs and categorises all the NPs as semi-conductors. The copper NPs showed the existence of both CuO and Cu_2O by UV-Visible and cyclic voltammetry characterisation. The electrochemical studies indicated that both the adsorption controlled and diffusion controlled electron transfer processes were taking place in the electrochemical activity of all the NPs with the adsorption controlled being significantly dominant in the Ag NPs. The heterogeneous state constant, k_s , values showed that Ag NPs had a faster electron transfer rate relative to the ZnO and CuO NPs indicating superior electrochemical activity.

From these results, the NPs were successfully synthesized and all the investigations indicate that the synthesized nanoparticles are within the required parameters suitable for use for the intended purpose.

3.6. References

Abbasipour, M. *et al.* (2014) 'Coated Cotton Gauze with Ag/ZnO/chitosan Nanocomposite as a Modern Wound Dressing', *Journal of Engineered Fibers and Fabrics*, 9(1), pp. 124–130.

AbdElhady, M. M. (2012) 'Preparation and Characterization of Chitosan/Zinc Oxide Nanoparticles for Imparting Antimicrobial and UV Protection to Cotton Fabric', *International Journal of Carbohydrate Chemistry*, 2012, pp. 1–6. doi: 10.1155/2012/840591.

Abiraman, T. *et al.* (2016) 'Antifouling behavior of chitosan adorned zinc oxide nanorods', *RSC Adv.* Royal Society of Chemistry, 6(73), pp. 69206–69217. doi: 10.1039/C6RA13321E.

Ahmed, S. and Ikram, S. (2016) 'Chitosan Based Scaffolds and Their Applications in Wound Healing', *Achievements in the Life Sciences*. Far Eastern Federal University, 10(1), pp. 27–37. doi: 10.1016/j.als.2016.04.001.

Alagumuthu, G. and Kumar, T. A. (2013) 'Synthesis and Characterization of Chitosan / TiO 2 Nanocomposites Using Liquid Phase Deposition Technique', 4(1), pp. 105–111.

Algawi, S. D. A. L. (no date) 'Copper Oxide Nanostructures ; Syntheses and Characterization', 71, pp. 0–4.

Ali, S. W., Rajendran, S. and Joshi, M. (2011) 'Synthesis and characterization of chitosan and silver loaded chitosan nanoparticles for bioactive polyester', *Carbohydrate Polymers*.

Elsevier Ltd., 83(2), pp. 438–446. doi: 10.1016/j.carbpol.2010.08.004.

Alvarez, P. J. J. and Lowry, G. (2009) 'Nanomaterials with Antimicrobial Properties : Mechanisms , Implications and Applications pp l i'.

Applerot, G. *et al.* (2012) 'Understanding the antibacterial mechanism of CuO nanoparticles: Revealing the route of induced oxidative stress', *Small*, 8(21), pp. 3326–3337. doi: 10.1002/smll.201200772.

Arefi, M. R. and Rezaei-Zarchi, S. (2012) 'Synthesis of zinc oxide nanoparticles and their effect on the compressive strength and setting time of self-compacted concrete paste as cementitious composites', *International Journal of Molecular Sciences*, 13(4), pp. 4340–4350. doi: 10.3390/ijms13044340.

Atiyeh, B. S. *et al.* (2007) 'Effect of silver on burn wound infection control and healing: Review of the literature', *Burns*, 33(2), pp. 139–148. doi: 10.1016/j.burns.2006.06.010.

Azuma, K. *et al.* (2015) *Chitin, Chitosan, and Its Derivatives for Wound Healing: Old and New Materials*, *Journal of Functional Biomaterials*. doi: 10.3390/jfb6010104.

Babu, V. S. (2010) *Solid State Devices and Technology*. 3rd edn, *Solid states devices and technology.* 3rd edn. Mumbai: Pearson.

Bagabas, A. *et al.* (2013) 'Room-temperature synthesis of zinc oxide nanoparticles in different media and their application in cyanide photodegradation', *Nanoscale Research Letters*, 8(1), p. 516. doi: 10.1186/1556-276X-8-516.

Balamurugan, B. and Mehta, B. R. (2001) 'Optical and structural properties of nanocrystalline copper oxide thin films prepared by activated reactive evaporation', *Thin Solid Films*, 396(1–2), pp. 90–96. doi: 10.1016/S0040-6090(01)01216-0.

Balu, S. S. and Bhakat, C. (2012) 'SYNTHESIS OF SILVER NANOPARTICLES BY CHEMICAL REDUCTION AND THEIR ANTIMICROBIAL ACTIVITY Materials and Methods ':, 1(6), pp. 1–5.

Bard, A. J. *et al.* (1944) *ELECTROCHEMICAL METHODS Fundamentals and Applications*, *Electrochemistry. I. Faulkner, Larry R*. doi: 10.1016/B978-0-12-381373-2.00056-9.

Benavente, M. (2008) *Adsorption of metallic ions onto chitosan: equilibrium and kinetic studies*. doi: 976–988.

Beyth, N. *et al.* (2015) ‘Alternative Antimicrobial Approach: Nano-Antimicrobial Materials’, *Evidence-Based Complementary and Alternative Medicine*, 2015, pp. 1–16. doi: 10.1155/2015/246012.

Biovation, L. (2010) *Testing for Antimicrobial Activity in Textiles.* Boothbay.

Bonnemann, H. and Richards, R. M. (2001) ‘Nanoscopic metal particles - synthetic methods and potential applications’, *Eur. J. Inorg. Chem.*, pp. 2455–2480. doi: 10.1002/1099-0682(200109)2001:10<2455::AID-EJIC2455>3.0.CO;2-Z.

Brintha, S. R. and Ajitha, M. (2015) ‘Synthesis and characterization of ZnO nanoparticles via aqueous solution, sol-gel and hydrothermal methods’, *IOSR Journal of Applied Chemistry*, 8(11), pp. 66–72. doi: 10.9790/5736-081116672.

Brown, J. H. (2015) ‘Development and Use of a Cyclic Voltammetry Simulator To Introduce Undergraduate Students to Electrochemical Simulations’, *Journal of Chemical Education*. American Chemical Society, 92(9), pp. 1490–1496. doi: 10.1021/acs.jchemed.5b00225.

Brown, K. and Gray, S. B. (2010) ‘Cyclic Voltammetric Studies of Electropolymerized Films Based on Ruthenium (II/III) Bis (1, 10phenanthroline)(4-methyl-4’vinyl-2, 2’-bipyridine).’, *International Journal of Chemistry*, 2(2), pp. 3–9. Available at: http://search.ebscohost.com/login.aspx?direct=true&profile=ehost&scope=site&authtype=crawler&jrnl=19169698&AN=52739860&h=s7r8gpPlt9tlQXU1DwQKvth6GpoG/uSIl9+y7buDKd4ozaZ6T7n2jMZlVbnZRzIKzPwKahBTG9vQKJVjeYgNcA==&crl=c.

Brownson, D. A. C. and Banks, C. E. (2014) *The Handbook of Graphene Electrochemistry*, *The Handbook of Graphene Electrochemistry*. doi: 10.1007/978-1-4471-6428-9.

Brugnerotto, J. *et al.* (2001) ‘An infrared investigation in relation with chitin and chitosan characterization’, *Polymer*, 42(8), pp. 3569–3580. doi: 10.1016/S0032-3861(00)00713-8.

Budhiraja, N. *et al.* (2013) ‘Synthesis and Optical Characteristics of Silver Nanoparticles on Different Substrates’, *International Letters of Chemistry, Physics and Astronomy*, 19, pp. 80–88. doi: 10.18052/www.scipress.com/ILCPA.19.80.

Calvo, E. J. and Wolosiuk, A. (2002) ‘Donnan permselectivity in layer-by-layer self-assembled redox polyelectrolye thin films’, *Journal of the American Chemical Society*, 124(28), pp. 8490–8497. doi: 10.1021/ja020107h.

Cavassin, E. D. *et al.* (2015) ‘Comparison of methods to detect the in vitro activity of silver

nanoparticles (AgNP) against multidrug resistant bacteria', *Journal of Nanobiotechnology*. BioMed Central, 13(1). doi: 10.1186/s12951-015-0120-6.

Dai, T. *et al.* (2011) *NIH Public Access*, *Expert Rev Anti Infect Ther*. doi: 10.1586/eri.11.59.Chitosan.

Dash, M. *et al.* (2011) 'Chitosan - A versatile semi-synthetic polymer in biomedical applications', *Progress in Polymer Science (Oxford)*. Elsevier Ltd, 36(8), pp. 981–1014. doi: 10.1016/j.progpolymsci.2011.02.001.

Davis, J. and McLister, A. (2016) 'Chapter Four - Passive and Interactive Dressing Materials', in Davis, J. et al. (eds) *Smart Bandage Technologies*. Academic Press, pp. 93–144. doi: https://doi.org/10.1016/B978-0-12-803762-1.00004-7.

Debanath, M. K. and Karmakar, S. (2013) 'Study of blueshift of optical band gap in zinc oxide (ZnO) nanoparticles prepared by low-temperature wet chemical method', *Materials Letters*. Elsevier, 111, pp. 116–119. doi: 10.1016/j.matlet.2013.08.069.

Dehaghi, S. M. *et al.* (2014) 'Removal of permethrin pesticide from water by chitosan–zinc oxide nanoparticles composite as an adsorbent', *Journal of Saudi Chemical Society*, 18(4), pp. 348–355. doi: https://doi.org/10.1016/j.jscs.2014.01.004.

Devi, H. S. and Singh, T. D. (2014) 'Synthesis of Copper Oxide Nanoparticles by a Novel Method and its Application in the Degradation of Methyl Orange', *Advance in Electronic and Electric Engineering*, 4(1), pp. 83–88.

Douglas Skoog, James Holler, S. C. (2007) 'Principles of instrumental analysis.', in Harris, D. (ed.) *Principles of instrumental analysis.* 6th edn. Belmont: Brooks/Cole, p. 371.

Durga Praveena, V. and Vijaya Kumar, K. (2013) 'Synthesis and Characterization of Chitosan based Silver Nano Composite System for Antibacterial Applications', *Proceedings of the International Conference on Advanced Nanomaterials & Emerging Engineering Technologies*, pp. 76–79.

Faiz, U. *et al.* (2011) 'Efficacy of zinc as an antibacterial agent against enteric bacterial pathogens.', *Journal of Ayub Medical College*, 23(2), pp. 18–21.

Feng, Q. L. *et al.* (2000) 'A mechanistic study of the antibacterial effect of silver ions on <I>Escherichia coli</I> and <I>Staphylococcus aureus</I>', *Journal of Biomedical Materials Research*, pp. 662–668. doi: 10.1002/1097-4636(20001215)52:4<662::aid-jbm10>3.0.co;2-3.

Fielicke, A., Rabin, I. and Meijer, G. (2006) 'Far-infrared spectroscopy of small neutral silver clusters', *Journal of Physical Chemistry A*, 110(26), pp. 8060–8063. doi: 10.1021/jp062095i.

Fievet, P. (2015) 'Donnan Potential BT - Encyclopedia of Membranes', in Drioli, E. and Giorno, L. (eds). Berlin, Heidelberg: Springer Berlin Heidelberg, pp. 1–3. doi: 10.1007/978-3-642-40872-4_1716-1.

Franci, G. *et al.* (2015) 'Silver nanoparticles as potential antibacterial agents', *Molecules*, 20(5), pp. 8856–8874. doi: 10.3390/molecules20058856.

Gliga, A. R. *et al.* (2014) 'Size-dependent cytotoxicity of silver nanoparticles in human lung cells: the role of cellular uptake, agglomeration and Ag release', *Particle and Fibre Toxicology*, 11(1), p. 11. doi: 10.1186/1743-8977-11-11.

Gogoi, S. K. *et al.* (2006) 'Green fluorescent protein-expressing Escherichia coli as a model system for investigating the antimicrobial activities of silver nanoparticles', *Langmuir*, 22(22), pp. 9322–9328. doi: 10.1021/la060661v.

Gouda, M. (2012) 'Nano-zirconium oxide and nano-silver oxide/cotton gauze fabrics for antimicrobial and wound healing acceleration', *Journal of Industrial Textiles*, 41(3), pp. 222–240. doi: 10.1177/1528083711414960.

Goy, R. C., Britto, D. de and Assis, O. B. G. (2009) 'A review of the antimicrobial activity of chitosan', *Polímeros*, 19(3), pp. 241–247. doi: 10.1093/jac/dkg286.

Guidelli, R. *et al.* (2014) 'Defining the transfer coefficient in electrochemistry: An assessment (IUPAC Technical Report)', *Pure and Applied Chemistry*, 86(2), pp. 245–258. doi: 10.1515/pac-2014-5026.

Gunalan, S., Sivaraj, R. and Rajendran, V. (2012) 'Green synthesized ZnO nanoparticles against bacterial and fungal pathogens', *Progress in Natural Science: Materials International*. Elsevier, 22(6), pp. 693–700. doi: 10.1016/j.pnsc.2012.11.015.

Guo, S. and Dipietro, L. A. (2010) 'Factors Affecting Wound Healing', *Obstetrics & Gynecology*, (Mc 859), pp. 219–229. doi: 10.1177/0022034509359125.

Haghighat, S. and Dawlaty, J. M. (2016) 'pH Dependence of the Electron-Transfer Coefficient: Comparing a Model to Experiment for Hydrogen Evolution Reaction', *Journal of Physical Chemistry C*, 120(50), pp. 28489–28496. doi: 10.1021/acs.jpcc.6b10602.

Hajipour, M. J. *et al.* (2012) 'Coated Cotton Gauze with Ag/ZnO/chitosan Nanocomposite as

a Modern Wound Dressing', *Journal of Industrial Textiles*. Elsevier Ltd, 9(6), pp. 143–154. doi: 10.1155/2015/246012.

Hajipour, M. J., Fromm, K. M. and Ashkarran, A. (2012) 'Antibacterial properties of nanoparticles', *Trends in Biotechnology*. Elsevier Ltd, 30(10), pp. 499–511. doi: 10.1016/j.tibtech.2012.06.004.

Huh, A. J. and Kwon, Y. J. (2011) '"Nanoantibiotics": A new paradigm for treating infectious diseases using nanomaterials in the antibiotics resistant era', *Journal of Controlled Release*. Elsevier B.V., 156(2), pp. 128–145. doi: 10.1016/j.jconrel.2011.07.002.

I. Markova-Deneva (2010) 'Infrared Spectroscopy Investigation of Metallic Nanoparticles Based on Copper, Cobalt, and Nickel Synthesized Through Borohydride Reduction Method', *Journal of the University of Chemical Technology and Metallurgy*, 45(4), pp. 351–378.

Ijaz, F. *et al.* (2017) 'Green synthesis of copper oxide nanoparticles using abutilon indicum leaf extract: Antimicrobial, antioxidant and photocatalytic dye degradation activities', *Tropical Journal of Pharmaceutical Research*, 16(4), pp. 743–753. doi: 10.4314/tjpr.v16i4.2.

ISO (2007) 'ISO 21348 Definitions of Solar Irradiance Spectral Categories', *Environment*, (section 5), pp. 6–7.

Jain, K. K. (2007) 'Applications of nanobiotechnology in clinical diagnostics', *Clinical Chemistry*, 53(11), pp. 2002–2009. doi: 10.1373/clinchem.2007.090795.

Jemimah, V. H. and Arulpandi, I. (2014) 'Evaluation of Antimicrobial Property of Biosynthesized Zinc Oxide Nanoparticles (ZnO NPs) and its Application on Baby Diapers', 6(2), pp. 113–119.

Jin, T. *et al.* (2009) 'Antimicrobial efficacy of zinc oxide quantum dots against Listeria monocytogenes, Salmonella Enteritidis, and Escherichia coli O157:H7', *Journal of Food Science*, 74(1). doi: 10.1111/j.1750-3841.2008.01013.x.

John Kotz, Paul Treichel, J. T. (2009) *Chemistry and chemical reactivity .* 2nd edn, *Chemistry and chemical reactivity .* 2nd edn. Edited by Lisa Lockwood. Belmont: Brooks/Cole.

Joseph Wang (2006) *Analytical Electrochemistry*. 3rd edn. New Jersey: John Wiley and Sons.

Jyoti, K., Baunthiyal, M. and Singh, A. (2016) 'Characterization of silver nanoparticles synthesized using Urtica dioica Linn. leaves and their synergistic effects with antibiotics',

Journal of Radiation Research and Applied Sciences. Elsevier Ltd, 9(3), pp. 217–227. doi: 10.1016/j.jrras.2015.10.002.

Kalimuthu, K. *et al.* (2008) 'Biosynthesis of silver nanocrystals by Bacillus licheniformis', *Colloids and Surfaces B: Biointerfaces*, 65(1), pp. 150–153. doi: https://doi.org/10.1016/j.colsurfb.2008.02.018.

Kang, X. *et al.* (2009) 'Glucose Oxidase-graphene-chitosan modified electrode for direct electrochemistry and glucose sensing', *Biosensors and Bioelectronics*, 25(4), pp. 901–905. doi: 10.1016/j.bios.2009.09.004.

Karim-Nezhad, G. *et al.* (2009) *Kinetic Study of Electrocatalytic Oxidation of Carbohydrates on Cobalt Hydroxide Modified Glassy Carbon Electrode*, *J. Braz. Chem. Soc.* doi: 10.1590/S0103-50532009000100022.

Kayani, Z. N. *et al.* (2012) 'Synthesis and characterization of CuO nanowires by a simple wet chemical method', *International Letters of Chemistry, Physics and Astronomy*. Springer Open Ltd, 14(1), pp. 26–36. doi: 10.1186/1556-276X-7-70.

Kayani, Z. N. *et al.* (2015) 'Characterization of Copper Oxide Nanoparticles Fabricated by the Sol???Gel Method', *Journal of Electronic Materials*, 44(10), pp. 3704–3709. doi: 10.1007/s11664-015-3867-5.

Khatoon, N. *et al.* (2015) 'Biosynthesis, Characterization, and Antifungal Activity of the Silver Nanoparticles Against Pathogenic Candida species', *BioNanoScience*, 5(2), pp. 65–74. doi: 10.1007/s12668-015-0163-z.

Khorsand Zak, A. *et al.* (2011) 'Synthesis and characterization of a narrow size distribution of zinc oxide nanoparticles', *International Journal of Nanomedicine*, 6(1), pp. 1399–1403. doi: 10.2147/IJN.S19693.

Kong, M. *et al.* (2010) 'Antimicrobial properties of chitosan and mode of action: A state of the art review', *International Journal of Food Microbiology*. Elsevier B.V., 144(1), pp. 51–63. doi: 10.1016/j.ijfoodmicro.2010.09.012.

Krishna Veni (2016) 'Anti-Bacterial Coating of Chrysanthemum Extract on Bamboo Fabric for Healthcare Applications', *Journal of Textile Science & Engineering*, 6(4), pp. 6–8. doi: 10.4172/2165-8064.1000267.

Krishnamoorthy, K. and Kim, S. J. (2013) 'Growth, characterization and electrochemical

properties of hierarchical CuO nanostructures for supercapacitor applications', *Materials Research Bulletin*. Elsevier Ltd, 48(9), pp. 3136–3139. doi: 10.1016/j.materresbull.2013.04.082.

Kumar, H. and Rani, R. (2013) 'Structural Characterization of Silver Nanoparticles Synthesized by Micro emulsion Route', *International Journal of Engineering and Innovative Technology*, 3(3), pp. 344–348.

Kurien, S. (2005) 'Chapter 4: ANALYSIS OF FTIR SPECTRA OF NANOPARTICLES of MgAl2O4, SrAl2O4, and NiAl2O4', 1595, pp. 64–78. Available at: http://mgutheses.in/page/?q=T 1354&search=siby+kurien&page=1&rad=sc.

Laurent, D. and Schlenoff, J. B. (1997) 'Multilayer Assemblies of Redox Polyelectrolytes', *Langmuir*, 13(6), pp. 1552–1557. doi: 10.1021/la960959t.

Laviron, E. (1979) 'General expression of the linear potential sweep voltammogram in the case of diffusionless electrochemical systems', *Journal of Electroanalytical Chemistry and Interfacial Electrochemistry*, 101(1), pp. 19–28. doi: https://doi.org/10.1016/S0022-0728(79)80075-3.

Laviron, E. (1979) 'General expression of the linear potential sweep voltammogram in the case of diffusionless electrochemical systems', *Journal of Electroanalytical Chemistry*, 101(1), pp. 19–28. doi: 10.1016/S0022-0728(79)80075-3.

Laviron, E. (1995) 'The use of polarography and cyclic voltammetry for the study of redox systems with adsorption of the reactants. Heterogeneous vs. surface path', *Journal of Electroanalytical Chemistry*, 382(1–2), pp. 111–127. doi: 10.1016/0022-0728(94)03684-U.

Lionelli, G. T. and Lawrence, W. T. (2003) 'Wound dressings', *Surgical Clinics of North America*, pp. 617–638.

Liu, B. *et al.* (2013) 'Adsorption of heavy metal ions, dyes and proteins by chitosan composites and derivatives --- A review', *Journal of Ocean University of China*, 12(3), pp. 500–508. doi: 10.1007/s11802-013-2113-0.

Logothetidis, S. (2012) *Nanotechnology : Principles and Applications*. doi: 10.1007/978-3-642-22227-6.

Long, J. *et al.* (2016) 'A new class of nanocomposites of Zn–Al–Bi layered double oxides: large reversible capacity and better cycle performance for alkaline secondary batteries', *RSC*

Adv. Royal Society of Chemistry, 6(95), pp. 92896–92904. doi: 10.1039/C6RA18164C.

Lović, J. (2017) 'Glucose Sensing Using Glucose Oxidase-Glutaraldehyde- Cysteine Modified Gold Electrode', *International Journal of Electrochemical Science*, (July), pp. 5806–5817. doi: 10.20964/2017.07.65.

Luna, I. Z. *et al.* (2015) 'Preparation and Characterization of Copper Oxide Nanoparticles Synthesized via Chemical Precipitation Method', *OALib*, 2(3), pp. 1–8. doi: 10.4236/oalib.1101409.

Ma, A. *et al.* (2011) 'Evaluation of antibacterial activity of silver nanoparticles against MSSA and MRSA on isolates from skin infections', *Research Article Biology and Medicine*, 3(2), pp. 141–146.

Malinowska-Pańczyk, E. *et al.* (2009) 'The combined effect of moderate pressure and chitosan on Escherichia coli and Staphylococcus aureus cells suspended in a buffer and on natural microflora of apple juice and minced pork', *Food Technology and Biotechnology*, 47(2), pp. 202–209.

Maneerung, T., Tokura, S. and Rujiravanit, R. (2008) 'Impregnation of silver nanoparticles into bacterial cellulose for antimicrobial wound dressing', *Carbohydrate Polymers*, 72(1), pp. 43–51. doi: 10.1016/j.carbpol.2007.07.025.

Mansoori, G. A. (2005) 'Principles of Nanotechnology: Molecular Based Study of Condensed Matter in Small Systems'. doi: 10.1142/5749.

Mazloum-ardakani, M. *et al.* (2010) 'Voltammetric Determination of Dopamine at the Surface of TiO 2 Nanoparticles Modified Carbon Paste Electrode', 5, pp. 147–157.

Meftahi, A. *et al.* (2010) *The effects of cotton gauze coating with microbial cellulose*, *Cellulose*. doi: 10.1007/s10570-009-9377-y.

Mehta, B. K., Chhajlani, M. and Shrivastava, D. (2017) 'Green synthesis of silver nanoparticles and their characterization by XRD', *Frontiers of Physics and Plasma Science IOP Publishing IOP Conf. Series: Journal of Physics: Conf. Series*, 836. doi: 10.1088/1742-6596/836/1/012050.

Mohammad, F., A. Al-Lohedan, H. and N. Al-Haque, H. (2016) 'Chitosan-mediated fabrication of metal nanocomposites for enhanced biomedical applicationsf', *Advanced Materials Letters*, 8(2), pp. 89–100. doi: 10.5185/amlett.2017.6925.

Mohan, A. C. and Renjanadevi, B. (2016) ‘Preparation of Zinc Oxide Nanoparticles and its Characterization Using Scanning Electron Microscopy (SEM) and X-Ray Diffraction(XRD)’, *Procedia Technology*. Elsevier B.V., 24, pp. 761–766. doi: 10.1016/j.protcy.2016.05.078.

Muthukrishnan, A. M. (2015) ‘Green Synthesis of Copper-Chitosan Nanoparticles and Study of its Antibacterial Activity’, *Journal of Nanomedicine & Nanotechnology*, 6(1), pp. 1–6. doi: 10.4172/2157-7439.1000251.

Muzzarelli, R. (1973) *Natural chelating polymers; alginic acid, chitin, and chitosan*. 1st edn. Oxford: Pergamon press.

Muzzarelli, R. A. and Sipos, L. (1971) ‘Chitosan for the collection from seawater of naturally occurring zinc, cadmium, lead and copper’, *Talanta*, 18(9), p. 853—858. doi: 10.1016/0039-9140(71)80141-8.

Nam, H. C. and Schaak, R. E. (2007) ‘Shape-controlled conversion of ??-Sn nanocrystals into intermetallic M-Sn (M = Fe, Co, Ni, Pd) nanocrystals’, *Journal of the American Chemical Society*, 129(23), pp. 7339–7345. doi: 10.1021/ja069032y.

Norfazila, S. M. and Mohd, J. R. (2014) ‘Synthesis and Ultroviolet Visible Spectroscopy Studies of Chitosan Capped Gold Nanoparticles and Theri Reactions with Analytes’, *The Scientific World Journal*, 2014, p. 7. doi: http://dx.doi.org/10.1155/2014/184604.

Okumu, F. and Matoetoe, M. (2016) ‘Electrochemical Characterization of Silver-Platinum Various Ratio Bimetallic Nanoparticles Modified Electrodes’, *Journal of Nano Research*, 44, pp. 114–125. doi: 10.4028/www.scientific.net/JNanoR.44.114.

Olaniyan, O. J. *et al.* (2016) ‘Synthesis and Characterization of Chitosan-Silver Nanocomposite Film’, *Nano Hybrids and Composites*, 11, pp. 22–29. doi: 10.4028/www.scientific.net/NHC.11.22.

Ono, S. *et al.* (2015) ‘Increased wound pH as an indicator of local wound infection in second degree burns’, *Burns*. Elsevier Ltd and International Society of Burns Injuries, 41(4), pp. 820–824. doi: 10.1016/j.burns.2014.10.023.

Padil, V. and Cernik, M. (2013) *Green synthesis of copper oxide nanoparticles using gum karaya as a biotemplate and their antibacterial application*, *International journal of nanomedicine*. doi: 10.2147/IJN.S40599.

Paladini, F. *et al.* (2016) ‘In vitro assessment of the antibacterial potential of silver nano-

coatings on cotton gauzes for prevention of wound infections', *Materials*, 9(6), pp. 1–14. doi: 10.3390/ma9060411.

Panchakarla, L. S., Govindaraj, A. and Rao, C. N. R. (2007) 'Formation of ZnO nanoparticles by the reaction of zinc metal with aliphatic alcohols', *Journal of Cluster Science*, 18(3), pp. 660–670. doi: 10.1007/s10876-007-0129-6.

Pankratov, D. V. *et al.* (2014) 'Impact of surface modification with gold nanoparticles on the bioelectrocatalytic parameters of immobilized bilirubin oxidase', *Acta Naturae*, 6(20), pp. 102–106.

Patrulea, V. *et al.* (2015) 'Chitosan as a starting material for wound healing applications', *European Journal of Pharmaceutics and Biopharmaceutics*. Elsevier B.V., 97, pp. 417–426. doi: 10.1016/j.ejpb.2015.08.004.

Paul, H. J. and Leddy, J. (1995) 'Direct Determination of the Transfer Coefficient from Cyclic Voltammetry: Isopoints as Diagnostics', *Analytical Chemistry*, 67(10), pp. 1661–1668. doi: 10.1021/ac00106a003.

de Paz, L. E. C. *et al.* (2011) 'Antimicrobial effect of chitosan nanoparticles on Streptococcus mutans biofilms', *Applied and Environmental Microbiology*, 77(11), pp. 3892–3895. doi: 10.1128/AEM.02941-10.

Pinho, E. *et al.* (2011) 'Antimicrobial activity assessment of textiles: Standard methods comparison', *Annals of Microbiology*, 61(3), pp. 493–498. doi: 10.1007/s13213-010-0163-8.

Prodomis, M. I. *et al.* (2000) 'The Importance of Surface Coverage in the Electrochemical Study of Chemically Modified Electrodes', *Electroanalysis*, 12(18), pp. 1498–1501.

Puchalski, M. *et al.* (2007) 'The study of silver nanoparticles by scanning electron microscopy, energy dispersive X-ray analysis and scanning tunnelling microscopy', *Materials Science-Poland*, 25(2), pp. 473–478.

Raafat, D. and Sahl, H. G. (2009) 'Chitosan and its antimicrobial potential - A critical literature survey', *Microbial Biotechnology*, 2(2 SPEC. ISS.), pp. 186–201. doi: 10.1111/j.1751-7915.2008.00080.x.

Radecka, M. *et al.* (2008) 'Importance of the band gap energy and flat band potential for application of modified TiO2 photoanodes in water photolysis', *Journal of Power Sources*, 181(1), pp. 46–55. doi: https://doi.org/10.1016/j.jpowsour.2007.10.082.

Raghupathi, K. R., Koodali, R. T. and Manna, A. C. (2011) 'Size-dependent bacterial growth inhibition and mechanism of antibacterial activity of zinc oxide nanoparticles.', *Langmuir : the ACS journal of surfaces and colloids*, 27(7), pp. 4020–4028. doi: 10.1021/la104825u.

Rahman, A. *et al.* (2009) 'SYNTHESIS OF COPPER OXIDE NANO PARTICLES BY USING Phormidium cyanobacterium', *Indonesian Journal of Chemistry*, 9(3), pp. 355–360.

Rai, M., Yadav, A. and Gade, A. (2009) 'Silver nanoparticles as a new generation of antimicrobials', *Biotechnology Advances*. Elsevier Inc., 27(1), pp. 76–83. doi: 10.1016/j.biotechadv.2008.09.002.

Ravichandran, S. *et al.* (2015) 'A novel approach for the biosynthesis of silver oxide nanoparticles using aqueous leaf extract of Callistemon lanceolatus (Myrtaceae) and their therapeutic potential', *Journal of Experimental Nanoscience*. Taylor & Francis, 8080(August), pp. 1–14. doi: 10.1080/17458080.2015.1077534.

Rhazi, M. *et al.* (2002) 'Influence of the nature of the metal ions on the complexation with chitosan.: Application to the treatment of liquid waste', *European Polymer Journal*, 38, pp. 1523–1530.

Rhoades, J. and Roller, S. (2000) 'Antimicrobial actions of degraded and native chitosan against spoilage organisms in laboratory media and foods', *Applied and Environmental Microbiology*, 66(1), pp. 80–86. doi: 10.1128/AEM.66.1.80-86.2000.

Richards, R. and Bonnemann, H. (2005) 'Synthetic Approaches to Metallic Nanomaterials', *Nanofabrication Towards Biomedical Applications: Techniques, Tools, Applications, and Impact*, pp. 1–32. doi: 10.1002/3527603476.ch1.

Salehi, R. *et al.* (2010) 'Novel biocompatible composite (Chitosan-zinc oxide nanoparticle): Preparation, characterization and dye adsorption properties', *Colloids and Surfaces B: Biointerfaces*. Elsevier B.V., 80(1), pp. 86–93. doi: 10.1016/j.colsurfb.2010.05.039.

Sanpui, P. *et al.* (2008) 'The antibacterial properties of a novel chitosan-Ag-nanoparticle composite', *International Journal of Food Microbiology*, 124(2), pp. 142–146. doi: 10.1016/j.ijfoodmicro.2008.03.004.

Santos, C. L. *et al.* (2013) 'Nanomaterials with Antimicrobial Properties : Applications in Health Sciences', *Microbial pathogens and strategies for combating them: science, technology and education*, 1, pp. 143–154.

Sanyal, M. K., Datta, A. and Hazra, S. (2002) 'Morphology of nanostructured materials', *Pure and Applied Chemistry*, 74(9), pp. 1553–1570. doi: 10.1351/pac200274091553.

Schlenoff, J. B., Ly, H. and Li, M. (1998) 'Charge and Mass Balance in Polyelectrolyte Multilayers - Journal of the American Chemical Society (ACS Publications)', *Journal of the American Chemical …*, 7863(13), pp. 7626–7634. doi: 10.1021/ja980350.

Sehat, A. A. *et al.* (2015) 'Fast immobilization of glucose oxidase on graphene oxide for highly sensitive glucose biosensor fabrication', *International Journal of Electrochemical Science*, 10(1), pp. 272–286.

Seil, J. T. and Webster, T. J. (2012) 'Antimicrobial applications of nanotechnology: Methods and literature', *International Journal of Nanomedicine*, 7, pp. 2767–2781. doi: 10.2147/IJN.S24805.

Sezer, A. D. and Cevher, E. (1992) 'Biopolymers as Wound Healing Materials: Challenges and New Strategies', *Biomaterials Applications for Nanomedicine*, pp. 383–414. doi: 10.5772/25177.

Shen, X. S. *et al.* (2009) 'Nanospheres of silver nanoparticles: agglomeration, surface morphology control and application as SERS substrates', *Physical Chemistry Chemical Physics*. The Royal Society of Chemistry, 11(34), pp. 7450–7454. doi: 10.1039/B904712C.

Shrivastava, S. *et al.* (2010) 'Characterization of enhanced antibacterial effects of novel silver nanoparticles', *Nanotechnology*, 18(22), pp. 1–9. doi: 10.1088/0957-4484/18/22/225103.

Sirkka, T., Skiba, J. B. and Apell, S. P. (2016) 'Wound pH depends on actual wound size', p. 13.

Srivastava, S., Agrawal, A. and Kumar, S. (2013) 'Synthesis and Characterisation of Copper Oxide nanoparticles', *Journal of Applied Physics*, 5(4), pp. 61–65.

Street, E. and Lake, C. (2014) 'Aatcc t', pp. 2012–2015.

Sudheesh Kumar, P. T. *et al.* (2012) 'Flexible and microporous chitosan hydrogel/nano ZnO composite bandages for wound dressing: In vitro and in vivo evaluation', *ACS Applied Materials and Interfaces*, 4(5), pp. 2618–2629. doi: 10.1021/am300292v.

Sudheesh Kumar, P. T. *et al.* (2013) 'Evaluation of wound healing potential of β-chitin hydrogel/nano zinc oxide composite bandage', *Pharmaceutical Research*, 30(2), pp. 523–537. doi: 10.1007/s11095-012-0898-y.

Sun, K. and Li, Z. H. (2011) ‘Preparations, properties and applications of chitosan based nanofibers fabricated by electrospinning’, *Express Polymer Letters*, 5(4), pp. 342–361. doi: 10.3144/expresspolymlett.2011.34.

Sutherland, L. F. and D. (2012) *Nanotechnologies: Principles, Applications, Implications and Hands-on Activities*. doi: :10.2777/76945.

Talam, S., Karumuri, S. R. and Gunnam, N. (2012) ‘Synthesis, Characterization, and Spectroscopic Properties of ZnO Nanoparticles’, *ISRN Nanotechnology*, 2012, pp. 1–6. doi: 10.5402/2012/372505.

Tamayo, L. *et al.* (2016) ‘Copper-polymer nanocomposites: An excellent and cost-effective biocide for use on antibacterial surfaces’, *Materials Science and Engineering C*. Elsevier B.V., 69, pp. 1391–1409. doi: 10.1016/j.msec.2016.08.041.

Teterycz, H. *et al.* (2014) ‘Deposition of Zinc Oxide on the Materials Used in Medicine. Preliminary Results’, *FIBRES & TEXTILES in Eastern Europe*, 22(105), pp. 3–126.

Tikhonov, V. E. *et al.* (2006) ‘Bactericidal and antifungal activities of a low molecular weight chitosan and its N-/2(3)-(dodec-2-enyl)succinoyl/-derivatives’, *Carbohydrate Polymers*, 64(1), pp. 66–72. doi: 10.1016/j.carbpol.2005.10.021.

Tran, D. L. *et al.* (2011) ‘Some biomedical applications of chitosan-based hybrid nanomaterials’, *Advance in Natural Science: Nanoscience Nanotechnology*, 2, pp. 1–6. doi: 10.1088/2043-6262/2/4/045004.

Tran, T. H. and Nguyen, V. T. (2014) ‘Copper Oxide Nanomaterials Prepared by Solution Methods, Some Properties, and Potential Applications: A Brief Review’, *International Scholarly Research Notices*. Hindawi Publishing Corporation, 2014, pp. 1–14. doi: 10.1155/2014/856592.

Umesh, Kathad; Gajera, H. . (2014) ‘Synthesis of copper nanoparticles by two different methods and size comparison’, *Int J Pharm Bio Sci*, 5(1), pp. 978–982.

Usman, M. S. *et al.* (2012) ‘Copper nanoparticles mediated by chitosan: Synthesis and characterization via chemical methods’, *Molecules*, 17(12), pp. 14928–14936. doi: 10.3390/molecules171214928.

Valov, I. and Lu, W. D. (2016) ‘Nanoscale electrochemistry using dielectric thin films as solid electrolytes’, *Nanoscale*. The Royal Society of Chemistry, 8(29), pp. 13828–13837. doi:

10.1039/C6NR01383J.

Vaseeharan, B., Sivakamavalli, J. and Thaya, R. (2015) ‘Synthesis and characterization of chitosan-ZnO composite and its antibiofilm activity against aquatic bacteria’, *Journal of Composite Materials*, 49(2), pp. 177–184. doi: 10.1177/0021998313515289.

Velasco, J. G. (1997) ‘Determination of standard rate constants for electrochemical irreversible processes from linear sweep voltammograms’, *Electroanalysis*, 9(11), pp. 880–882. doi: 10.1002/elan.1140091116.

Wang, X. *et al.* (2005) ‘Chitosan- metal complexes as antimicrobial agent: Synthesis, characterization and Structure-activity study’, *Polymer Bulletin*, 55(1–2), pp. 105–113. doi: 10.1007/s00289-005-0414-1.

Wang, Z. L. (2004) ‘Zinc oxide nanostructures: growth, properties and applications’, *Journal of Physics: Condensed Matter*, 16(25), pp. R829–R858. doi: 10.1088/0953-8984/16/25/R01.

Wei, D. *et al.* (2009) ‘The synthesis of chitosan-based silver nanoparticles and their antibacterial activity’, *Carbohydrate Research*. Elsevier Ltd, 344(17), pp. 2375–2382. doi: 10.1016/j.carres.2009.09.001.

Wicramarachchi, P. and Hettiarachchi, M. (2011) ‘Synthesis of chitosan stabilised silver nanoparticles using gamma ray radiation and characterisation’, *Jousrnal of Scinece*, 6, pp. 65–75.

Xiliang, Q. *et al.* (2014) ‘Large-Scale Synthesis of Silver Nanoparticles by Aqueous Reduction for Low-Temperature Sintering Bonding’, 2014.

Xiong, G. *et al.* (2006) ‘Photoluminescence and FTIR study of ZnO nanoparticles: The impurity and defect perspective’, *Physica Status Solidi (C) Current Topics in Solid State Physics*, 3(10), pp. 3577–3581. doi: 10.1002/pssc.200672164.

Yukna, J. (Souther. I. U. at C. . (2014) ‘International Journal of Nano Dimension Synthesis and characterization of Copper and Copper Oxide nanoparticles by thermal decomposition method’, *Thesis paper*, 5(4), pp. 321–327.

Zhang, L., Zeng, Y. and Cheng, Z. (2016) ‘Removal of heavy metal ions using chitosan and modified chitosan: A review’, *Journal of Molecular Liquids*. Elsevier B.V., 214, pp. 175–191. doi: 10.1016/j.molliq.2015.12.013.

Zhou, E., Hashimoto, K. and Tajima, K. (2013) ‘Low band gap polymers for photovoltaic

device with photocurrent response wavelengths over 1000 nm', *Polymer (United Kingdom)*. Elsevier Ltd, 54(24), pp. 6501–6509. doi: 10.1016/j.polymer.2013.09.058.

CHAPTER FOUR
PREPARATION AND CHARACTERISATION OF CHITOSAN-NANOPARTICLE COMPOSITES.

4.1. Introduction

This chapter focuses on the synthesis and characterisation of chitosan-nanoparticle (CH-NPs) composites. It explores the formation dynamics and also goes into the changes in behaviour of the nanoparticles (NPs) after they are chelated by the chitosan polymer.

Chitosan which carries an electron rich amine group has high chelating capabilities making it a suitable polymer for the attachment of metallic nanoparticles on to electronically inert material such as cotton wound gauzes (Kong *et al.*, 2010). The chelating properties of chitosan via the amine group are highly sensitive to the pH of the medium. At pH below 7 the negatively charged amine groups are protonated and create electrostatic repulsion with the incoming cationic metals (Zhang, Zeng and Cheng, 2016). The large mass of H_3O^+ and H^+ that is present in lower pH media also compete with the NPs for the negatively charged amine site. Hence the chelating has to be done in a neutral to slightly basic medium of pH 7-8.5, to ensure that the uptake of the metallic ions is favoured. Since chitosan is soluble in acidic media, there is a need to correct the pH before addition of the NPs to form the CH-NPs composite so as to facilitate chelation. Correction of the pH is usually done adding a base with monitoring of the media using a pH meter.

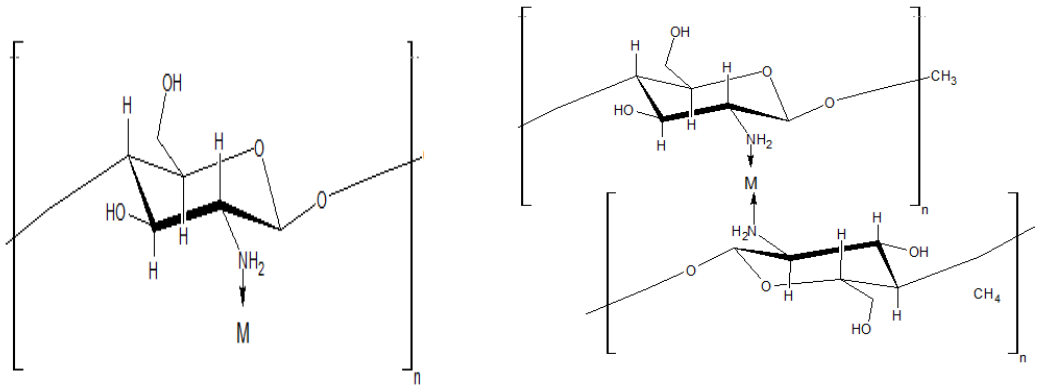

Figure 4. 1. Chelating behaviour of chitosan at a) at pH < 6 and b) at pH > 6

Several methods exist for the synthesis of CH-NPs and the ones that maintain NPs functionality and chitosan integrity are mostly used. The most common methods used are the sol-cast method and the simple chelation method. The synthesis of chitosan-ZnO composites

via the sol-cast formation has been reported (Vaseeharan, Sivakamavalli and Thaya, 2015). The sol-cast is an *in situ* synthesis method whereby the ZnO NPs are synthesised in the presence of the chitosan polymer and are cast on the amine groups. The process is resourceful; however, the process leaves no room to control the shape, and morphology of the ZnO NPs since caution has to be taken to protect the integrity of the chitosan polymer. The simple chelation method has been described during the synthesis of a chitosan-silver composite (Durga Praveena and Vijaya Kumar, 2013). The simple chelation method involves the synthesis of the metallic NPs separately then mixing them in together with chitosan to facilitate chelation. The method allows the size and shape of the metallic NPs to be controlled since they are synthesized *ex situ.* The simple chelation method is influenced by adsorption types which control the type of bond that forms between the chitosan and the NPs (Benavente, 2008). The adsorption types, electrostatic sorption, chemisorption, and physisorption are dependent on the metallic NPs species. Overall all the simple chelation method is favoured and is applicable in media with less controlled conditions such as heavy metal remediation of waste water (Liu *et al.*, 2013).

Optical activity of the CH-NPs composites was investigated using FTIR and UV-Visible spectroscopy. FTIR analysis of the composites helps in determining the vibrational transitions of functional groups that coordinated to the NPs in the composite. If used in complement with other techniques such as UV-Visible, it can be able to sufficiently aide in the description of the bonding between the NPs and the chitosan. A comparison of overlain pure NPs and CH-NPs composite spectra gives information that can help in the description of the inter bonding. Shifts in wavelength between the pure chitosan and the NPs in UV-Visible spectrometry signifies the existence of bonding between the chitosan and the NPs. Chitosan being dominantly hydrocarbon in nature, absorbs in the far UV(180-280) region and metallic NPs in the near UV(315-500) to visible range (Abiraman *et al.*, 2016). Therefore, it is easily distinguishable from the spectra of its composites and the NPs. UV-Visible spectroscopy is also paramount in the determination of the optical band gap of the composite. As elaborated in the previous chapter, the band gap of a substance gives information on the reactivity and conductivity of the substance. The band gap is calculated using the following equation (Babu, 2010):

$$E_{bg}=\frac{1240}{\lambda}(eV) \ldots\ldots\ldots\ldots\ldots\ldots\ldots\ldots\ldots\ldots\ldots\ldots\ldots Equation\ 4.1$$

Where E_{bg} is the band gap energy in eV and λ is the wavelength in nanometres.

A comparison of the band gaps of the pure nanoparticles with the CH-NPs composites will give information on the effect of chitosan on the band gap energies of the NPs thereby giving an insight into the change of reactivity. X-ray diffraction (XRD) studies can be employed to ascertain the immobilization of the NPs on the chitosan. XRD also gives information on the crystalline nature of the NPs that are immobilized on the chitosan.

The CH-NPs composites were prepared and the optical activity and band gap energies of the composites were studied using UV-visible spectroscopy. The nature of interaction between the NPs and the chitosan were investigated using FTIR spectroscopy. XRD was used to confirm the immobilization of the NPs on the chitosan.

4.2. Experimental

4.2.1. Reagents and materials

Chitosan (Aldrich, 98%), Acetic acid; CH_3COOH (Aldrich, 99%), Ammonium hydroxide; NH_4OH (Aldrich, 98%), Cotton wound gauze ;20 thread count/12Ply (Clicks,100%), Silver nanoparticles; Ag, Copper oxide nanoparticles; CuO, Zinc Oxide nanoparticles; ZnO were used. Water for aqueous solution preparation was purified by a Milli-QTM system (Millipore).

4.2.2. Preparation of CH-NPs composites

0.5% chitosan solution was prepared by dissolving 2.5 g of chitosan in 500ml of 1% acetic acid and stirring at room temperature for 20 hrs. The chitosan solution was neutralized to pH 6.5 by adding ammonium hydroxide drop wise and stirring using a pH meter to measure the pH. An aliquot of 250 µL of the Ag NPs, CuO NPs, ZnO NPs, and a combination of the three were added each to separate beakers containing 50ml of the dissolved chitosan thereby forming concentration of 0.5 mM for the whole range. The beakers were stirred at 500 rpm for 2 hours. The beakers containing the composites were covered with parafilm and stored in a dark cabinet at room temperature.

4.2.3. Characterisation of CH-NPs composites.

4.2.3.1. X-ray diffraction (XRD) studies

About 80mg of each CH-NPs sample was dried and ground into fine powder using a pestle and mortar. All the samples were then analysed using a Bruker-Axs D8 XRD with measurement recorded with Cu Kα radiation run at 40kV and 60mA in the range of 20° to 70°.

4.2.3.2. UV-Visible characterisation of CH-NPs

UV Vis studies of the four composites were carried out using a Cary IE Varian dual-beam spectrometer in the wavelength range of 200-600nm.1% acetic acid was use as the blank before the four composites were investigated using a 1cm quartz cuvette. The UVVis spectrum for each composite was overlain with the spectrum of chitosan and the pure NPs in order to study the difference in optical response.

4.2.3.3. FTIR characterisation of CH-NPs composites

FTIR characterisation was done using a PerkinElmer Spectrum Two ATR apparatus in the wavenumber range of 370 to 3000 cm^{-1}. 1% acetic acid was used as background and the CH-NPs composite fluid was dropped using a pipette dropper and analysed. The CH-NPs spectrum for was overlain with the spectrum of the pure NPs so as to study and compare the differences in the functional groups between the two.

4.2.3.4. Electrochemical studies of CH-NPs composites.

The electrochemical activity of the chitosan composites was undertaken by characterising Glassy Carbon Electrode (GCE) modified by the composites using Autolab PGSTAT 101 (Metrohm, South Africa). The drop coating was left to dry in the fume hood for 5 hours to ensure maximum adsorption of the composite matter on the electrode. Interval cleaning and polishing of the GCE was done in between different modifications of the GCE and analysis. After every run the GCE was gently rubbed on a filter paper to remove the composite film and then placed in a 50-50% ethanol water solution and ultra-sonicated for 10mins at 25 degrees Celsius and low sonication power. After this the GCE would be rinsed with distilled water and polished with 1, 0.3 and 0.05 µm alumina slurry for 15 minutes per polishing station. The slurry was rinsed off with distilled water then the GCE was ultra-sonicated with ethanol-water solution for 20 minutes. Reference electrode Ag/AgCl (3 M NaCl) and counter electrode, platinum wire was rinsed thoroughly with distilled water for 3 minutes after every run.

4.3. Results and discussion

4.3.1. UV-Vis spectroscopy studies

4.3.1.1. Characterization of CH-NPs composites

From the NPs – CH-NPs comparison spectra in Figure 4.2 it can be observed that there was a shift in λ_{max} and absorbance for the CH-NPs spectrum for each composite. The λ_{max} shift for all the CH-NPs composites was towards the shorter wavelength and the absorbance increased from the one of pure NPs. This phenomenon, known as the blue-shift, was

observed in all the spectra but the greatest effect was observed in the CH-Ag composite. Chitosan being an organic compound without an unsaturated bond or chromophore, usually absorbs by n to σ* transitions that give a band in the region of 200 to 290nm. Pure CuO, ZnO and Ag NPs being from the transition elements absorb in the longer wavelength region due to d-d electronic transitions having bands that are within the visible region. The blue shifts exhibited by all CH-NPs composites signify that there is significant interaction between the NPs and the chitosan. If no interaction was present two separate peaks in the ranges of 200 to 290 and 300 to 800 would be expected for both the chitosan and NPs respectively. Blue-shift absorption bands for chitosan-NPs composites have been reported in other studies (Vaseeharan, Sivakamavalli and Thaya, 2015)(Norfazila and Mohd, 2014).

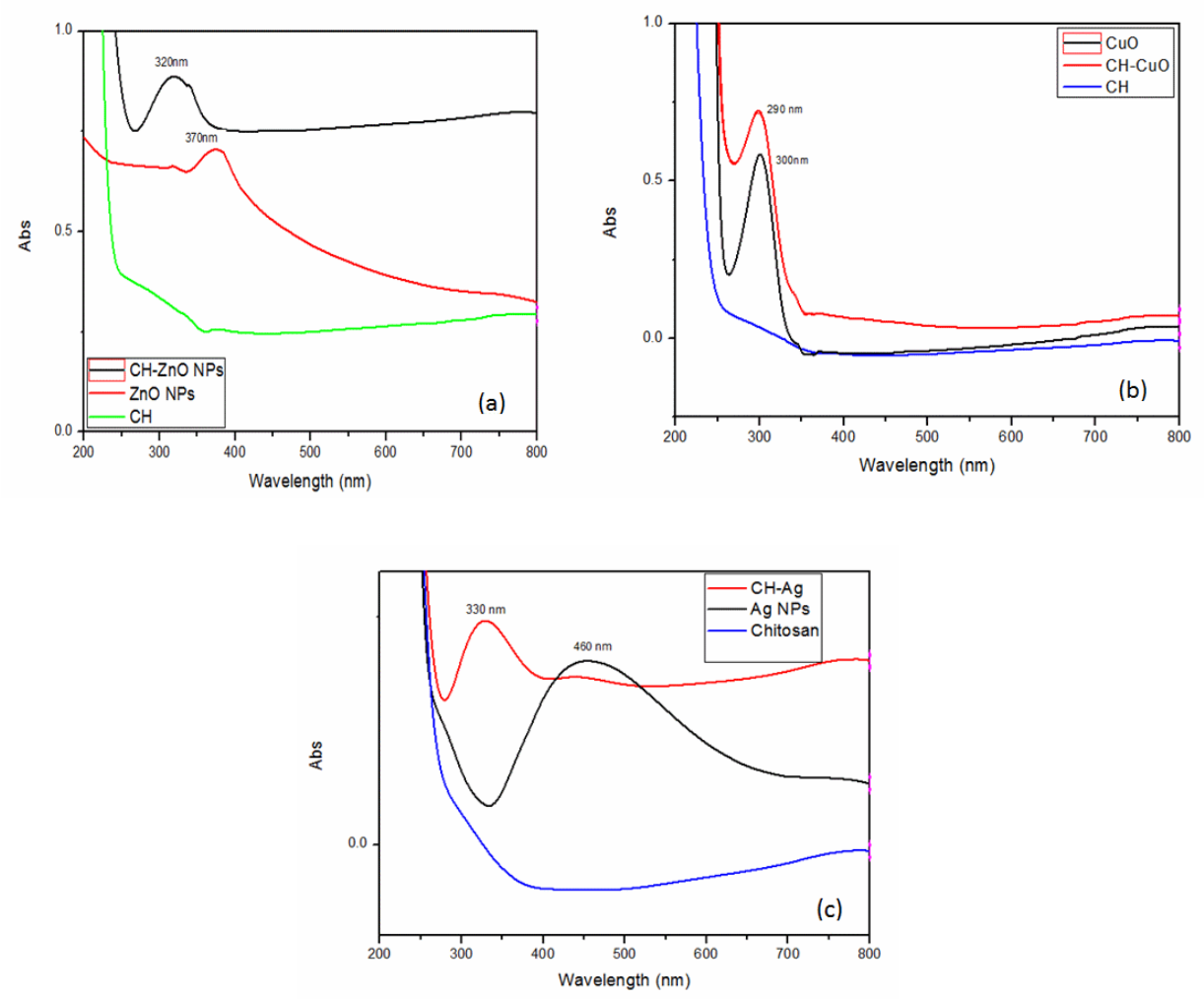

Figure 4. 2. Absorbance spectra of chitosan, NPs, and CH-NPs composites a) ZnO b) CuO and c) Ag

The blue-shift with respect to the NPs can be explained using the charge-transfer absorption effect. This is a phenomenon that exists between a metal and an organic ligand whereby during excitation, an electron is excited and leaves the donor going into an empty orbital of

the recipient metal (Douglas Skoog, James Holler, 2007). This phenomenon gives information on the type of bonding that is most likely to be present between the chitosan and the NPs to be coordinate or dative bonding. This type of bonding is paramount because it ensures that the purpose of the composite is still maintained since the coordinate bond can be formed and broken depending on the environment surrounding the composite. The information from this characterization gives evidence of interaction between the various NPs and the chitosan.

Table 4. 1. Relative λ_{max} and band gap energies of pure NPs and their chitosan composites.

	ZnO NPs	**CH-ZnO**	**CuO NPs**	**CH-CuO**	**Ag NPs**	**CH-Ag**
λ_{max}(nm)	370	320	300	290	460	330
E_{bg} (eV)	3.35	3.88	4.13	4.27	2.70	3.75

The blue-shift with respect to the NPs caused the energy band gaps for the three NPs to increase as shown in Table 4.1. The band gaps were calculated using equation 4.1 and a decrement in the wavelength caused an increase in the band gap energy. From the table it can be noticed again that CH-ZnO and CH-CuO had marginal increment in band energy due to their slight shift in wavelength compared to CH-Ag composite. The CH-Ag composite and the pure Ag NPs had a relatively bigger band gap value difference and this may be attributed to the difference in bond strength between the CH-Ag composites and the CH-CuO, CH-ZnO composites. Ag NPs have extra empty orbitals which increase the shielding of the valence electrons from the nucleus. Due to the novel nature of the study of CH- NPs composites much is not yet known with regards to their band gap energies. Generally an increment in band energy of a substance translates to low reactivity of the substance (John Kotz, Paul Treichel, 2009). The widening of the gap between the valence band and the conduction band in a metal or composite renders the metal or composite a semi-conductor or insulator in electrical terms. In chemical terms it means that the reactivity fervency of the composite has declined unless the initial band gap is restored. Table 4.1 shows that the band gaps of the three NPs declined after interacting with the chitosan polymer meaning that the NPs have

low reactivity when chelated to the polymer. This can to some extent indicate an expected low efficacy in terms of bactericidal efficacy. However, the NPs are expected to be released from the chitosan when the composite comes into contact with the wound cavity, due to the pH sensitive chelating properties of the chitosan, thereby liberating the NPs and restoring their original band gap energy enabling them to undertake their bactericidal activity. Lowering of the band gap energy ensures that the wound gauze modified by the CH-NPs composite can be stored in state without the risk of the nanoparticles causing gradual degradation of the wound gauze material.

4.3.1.2. Characterization of the prototype CH-Ag-ZnO-CuO

The prototype composite, CH-Ag-ZnO-CuO, which was mainly under study in this research, was found to have red shifts compared to the ones that were exhibited by the individual chitosan-NPs (Figure 4.3). The spectrum for the prototype had a lower absorbance than that of the combination of the NPs in the absence of chitosan chelating. The lower absorbance is attributed to the increase in electron density between the bond of the NPs and the amine group (Wicramarachchi and Hettiarachchi, 2011). Silver and zinc showed weak red-shifted plasmon bands at 480 and 390 nm respectively within the prototype composite. These wavelengths are longer than they had in their individual combination with chitosan whereas copper exhibited similar wavelengths as it had in its individual composite with chitosan.

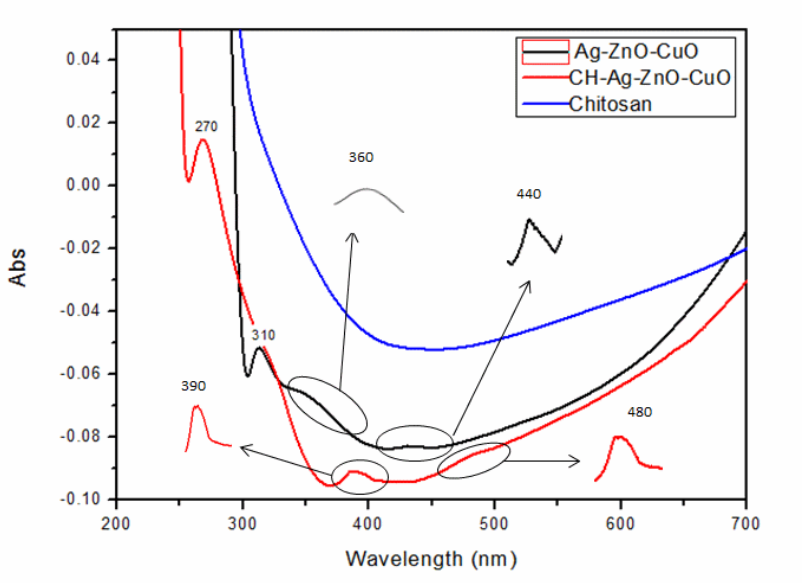

Figure 4. 3. Absorption spectra of the prototype composite, CH-Ag-ZnO-CuO.

This phenomenon indicates that the energy band gaps of the individual chitosan-NPs composites and the prototype differ and hence the reactivity or action against bacterium will

also differ. Due to the novel nature of the composite, there is no much information that can sufficiently elaborate why the ZnO and CuO NPs are blue-shifted in their individual composites with chitosan but however red-shifted in their combination composite with chitosan.

Table 4.2: Comparison of λ_{max} and optical band gap energy (E_{bg}) of different components within the CH-Ag-ZnO-CuO composite.

	NPs Components			**CH-NPs Components**		
	ZnO NPs	Ag NPs	CuO NPs	CH-Cu	CH-ZnO	CH-Ag
λ_{max}(nm)	360	440	310	270	390	480
E_{bg} (eV)	3.44	2.82	4.00	4.59	3.20	2.58

In the CH-Ag-ZnO-CuO composite, the band gap energies of all the nanoparticles are elevated save for copper (Table 4.2). The band gap of copper actually widens with respect to energy within the prototype composite. Though not conclusive until other parameters are determined and studied, the increase in the band gap energies can signify an overall increment in the overall reactivity. It can be assumed that the composite will yield better bactericidal results than the other composites.

4.3.2. FTIR studies

FTIR spectroscopy was carried out in the wavenumber region of 400 to 4000cm^{-1} for all the three CH-NPs composites and also the prototype composite. It can be seen in Figure 4.4 that there was a difference in band appearance from pure chitosan (Figure 4.4d) to the CH-NPs composites. The CH-NPs composites showed major characteristic peaks though the bands are slightly shifted due to electron density changes within the various composites. Interactions with the amine or hydroxyl groups on chitosan and other electron donor or acceptor species has been seen to cause shifts in the appearance of the characteristic bands of chitosan in FTIR studies (Brugnerotto *et al.*, 2001). Normal C-H vibrations and stretches are seen in the pure chitosan and also in the composites due to the fact that they do not participate in any interaction with the incoming NPs so the electron densities around them are not significantly altered.

From the spectra in Figure 4.4 and band assignments in Table 4.2 it can be seen that asymmetrical stretch band for the amine group(N-H_2) is only present in the pure chitosan

spectra but is absent in the CH-NPs composites. The is due to the fact that when a metallic NPs attaches to the amine group, it reduces the vibration intensity of the N-H bond due to the greater weight of the NPs thereby reducing the vibrational intensity of the band (Wei *et al.*, 2009). This indicates that there is an interaction between the NPs and the chitosan. The interaction maybe caused by the reduction of electron density due to chelation of the amine group.

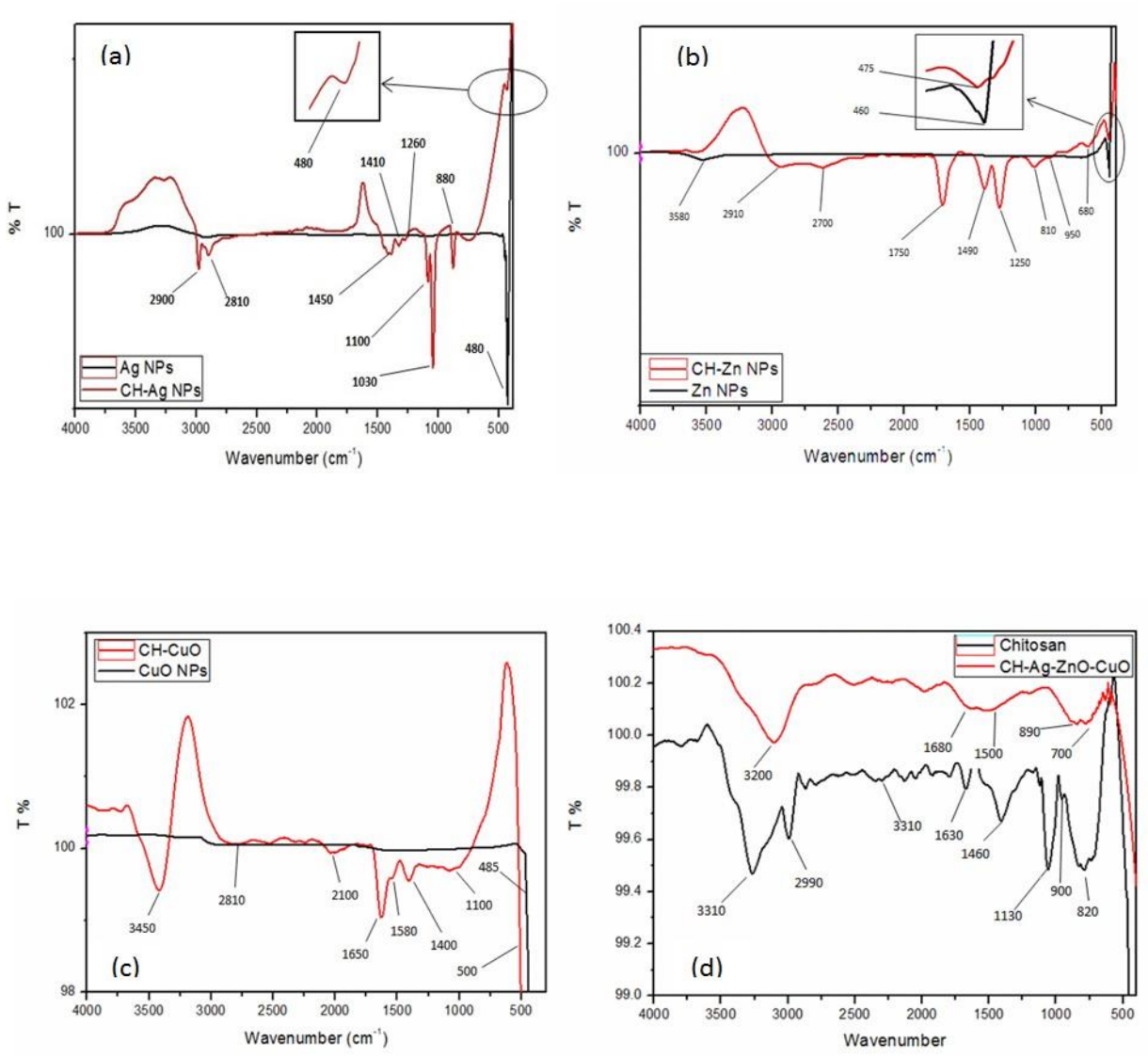

Figure 4. 4. FTIR spectra of composites a) CH-Ag b) CH-ZnO c) CH-CuO and d) CH-Ag-ZnO-CuO

The bonding of the NPs to the amine group alters the electron density of the amine region thereby causing the IR band for the amine asymmetrical stretch to shift to a lower wavelength usually giving a broader and stronger peak (Wicramarachchi and Hettiarachchi, 2011). The rise to that peak is attributed to the strong interaction between the chitosan's amine group and the NPs according to similar results (AbdElhady, 2012). The bands at

1630cm^{-1} exhibited by pure chitosan corresponds to the stretching vibration of the -NH_2 and -OH groups. In the composites the bands only appear in the CH-CuO composite at a shifted lower wavenumber and in the CH-Ag-ZnO-CuO composite. This indicates that the –OH group is involved in the chelating of the chitosan and the NPs (Vaseeharan, Sivakamavalli and Thaya, 2015)(Figure 4.5).

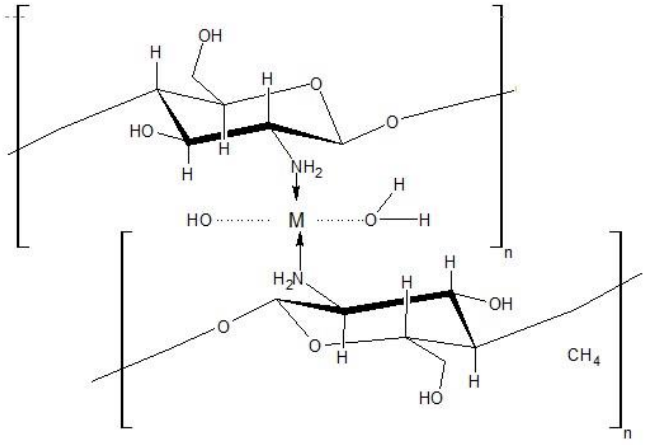

Figure 4. 5. Stabilization of CH-NPs composites by -OH groups.

Therefore, besides being complexed to the amine group of the chitosan, the NPs complexation is stabilised by the presence of the electron rich oxygen atom on the OH groups from both the chitosan and solvent. An attempt to illustrate the phenomenon is shown in Figure 4.5. The same suggestion was made by (Rhazi *et al.*, 2002),who suggested that at lower pH(<6), the CH-NPs complex is stabilised by the –OH groups of other neighbouring chitosan molecules and also from H_2O. This phenomenon then alters the electron densities around the amine and hydroxyl groups hence the change in the absorption bands and lowering of the wavenumbers of the characteristic peak appearances. The bands observed between 400 and 500cm^{-1} signify the formation of a new composite different from pure chitosan and the NPs (Vaseeharan, Sivakamavalli and Thaya, 2015). All in all, these FTIR studies indicate that there is formation of a composite by the interaction of the chitosan and the NPs (Muzzarelli and Sipos, 1971; Muzzarelli, 1973; Alagumuthu and Kumar, 2013).

Table 4. 2. FTIR band assignments for chitosan and NPs composites.

Peak Positions (cm^{-1})					
Assignment	Pure Chitosan	CH-Ag	CH-ZnO	CH-CuO	CH-Ag-ZnO-CuO
NH wag primary amine	900	880	950	none	890
C-O-C vibrations	1130	1100	none	1100	none
CH wag	1210	1260	1250	none	none
OH and CH deformation ring	1460	1450	1490	1400	1500
NH_2 deformation	1630	none	none	1580	1680
C-H asymmetrical stretch	2800	2810	2700	2810	2700
C-H symmetrical stretch	2900	2900	2910	none	none
N-H_2 asymmetrical stretch	3310	none	none	none	none

4.3.3. X-ray (XRD) studies

The presence and immobilisation of the NPs in the chitosan was confirmed using XRD. Figure 4.1 shows the x-ray diffraction patterns of the CH-Ag, CH-CuO, CH-ZnO and CH-Ag-CuO-ZnO composites. The diffraction patterns for all the composites exhibited sharp narrow peaks, weak broad peaks and also numerous indistinguishable peaks. The numerous indistinguishable weak peaks appearing in all the diffraction patterns are due to the amorphous nature of the polymer chitosan.

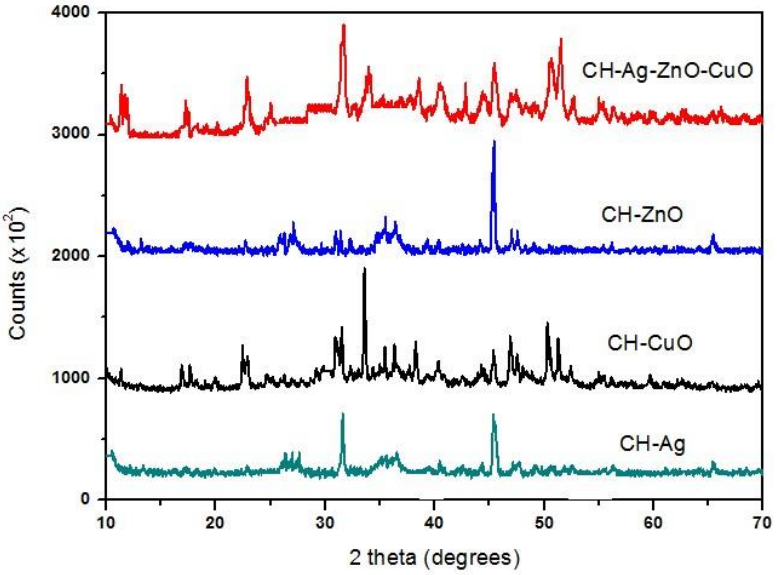

Figure 4. 6 X-ray diffractogram of CH-NPs composites

The diffraction pattern of the CH-Ag exhibited some weak broad peaks and some narrow sharp peaks as depicted by Figure 4.1. The two sharp narrow peaks at 2θ at 46° and 32° correspond to the crystal lattice of silver (hkl) designation (200) and (111) respectively (Olaniyan *et al.*, 2016). The other weak peaks at 67°and 40° correspond to the (hkl) values of (220) and (111) values. The peaks and their (hkl) value assignments indicate the presence of crystalline face-centred cubic structured Ag NPs within the composite. The weak broad peak at 10.1° can be attributed to the characteristic peak of pure chitosan (Ali, Rajendran and Joshi, 2011) .

The CH-CuO diffraction pattern showed the presence of numerous peaks. Characteristic peaks of Cu_2O were exhibited at 31° and 42° and these are (202) and (113) assignments respectively. CuO had characteristic peaks at 36° and 39° which are due to reflection planes

of (111) and (-111) respectively within the crystalline structure. Other identified characteristic peaks within the diffraction pattern were at 49°,66°,43° which are due to the (202), (220) and (200) planes respectively. The results indicate the presence of CuO NPs of base-centred crystalline structure within the CH-CuO composite. Similar results have been reported elsewhere (Usman *et al.*, 2012; Muthukrishnan, 2015).

CH-ZnO composite had one distinct narrow sharp peak at 47° and other relatively weak broad peaks. The strong narrow peak at 47° is of the (hkl) assignment (102) and it is characteristic of the presence of ZnO NPs (Salehi *et al.*, 2010). Other characteristic peaks were exhibited at 34°, 31 °,36°,68°, and 67° which are assigned to the (hkl) values of (002), (100), (101), (201) and (112) respectively. The results indicate the presence of immobilized hexagonal ZnO NPs on the chitosan (Salehi *et al.*, 2010; Dehaghi *et al.*, 2014).

The prototype composite, CH-Ag-ZnO-CuO, showed major characteristic peaks for all the NPs indicating that the NPs are immobilized within the chitosan and there is no significant interaction or change in structure within the immobilized NPs.

4.3.4. Electrochemical studies

4.3.4.1. Characterisation CH-NPs composites

Peaks obtained during the cyclic voltammetry of the CH-NPs composites were sharp in appearance with the greater response being of the CH-CuO composite. It could also be seen that the sharp peaks were observed during the anodic sweep, which may indicate fast electron transfer rate, while the cathodic sweep did not exhibit any significant sharp peaks (Figure 4.6). Peaks observed during the anodic sweep of the composites are due to the Cu/Cu^{+}, Cu^{+}/Cu^{2+},Zn/Zn^{+} and Ag/Ag^{+} redox couples as depicted by the equations within the voltammogram. The cathodic sweep yielded two weak peaks attributed to the Ag/Ag^{+} and Cu^{+}/Cu redox couples. The fast electron transfers maybe explained by the fact that when the chitosan chelates with the NPs, the lone pair of electrons from the amine group increase the electron density in the NPs d-orbitals and this makes it easy for an electron in the d-orbital of the NPs to jump out since after the departure of the electron the atom is electron stability due to the lone pair.

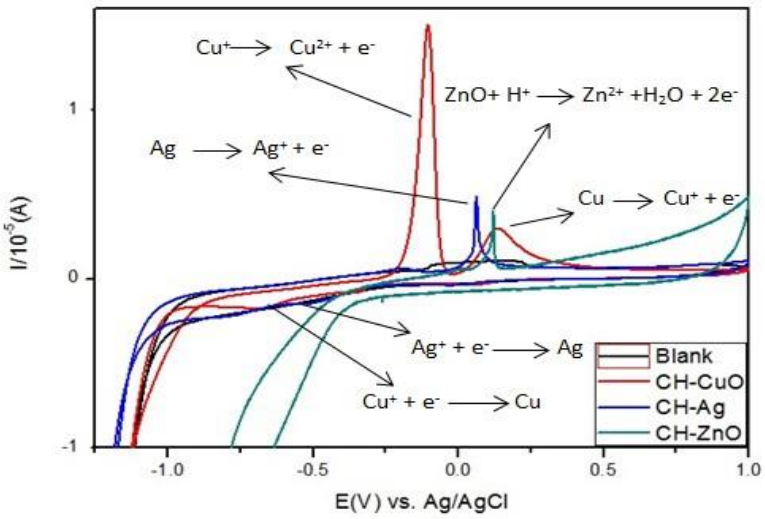

Figure 4. 7 Overlain cyclic voltammograms of a) CH-Ag b) CH-ZnO c) CH-CuO modified GCE in 0.1 M PBS pH 7.0. Scan rate: 80 mVs^{-1}.

It was observed in the voltammograms of the composites that there is a shift in the redox potentials of the various NPs within the composites towards the more negative potentials (Figure 4.6). A comparison between the redox potentials of the pure NPs (from Chapter 3) and their chitosan composites show that there is a significant shift in the oxidation potential for all CH-NPs composites (Table 4.3). This can be explained by considering that chitosan being a polymer has the ability to behave as a membrane thereby causing the Donnan effect potential (Calvo and Wolosiuk, 2002). The Donnan potential in cyclic voltammetry is a phenomenon that occurs when there is a distribution of ions in two different solutions that are separated by a semipermeable membrane (Fievet, 2015). The difference in concentrations in the two membrane separated solutions cause uneven potential differences across the boundary which eventually cause a net change in the potential difference of the reading and that translates in the shift of an oxidation or reduction potential.

Table 4. 3 Redox potential comparison of pure NPs and their chitosan composites.

	Pure Ag NPs	**CH-Ag composite**	**Pure ZnO NPs**	**CH-ZnO composite**	**Pure CuO;Cu_2O**	**CH-CuO; CH-Cu_2O composite**
E_{Ox} (mV)	+250	+100	-810	-1100	+90;-310	-125;-130
E_{Red} (mV)	-500	-500	-1400	No peak	-750	No peak;-700

In the cyclic voltammetry studies of the CH-NPs composites, chitosan in the composite behaved as a membrane between the working electrode and the reference electrode thereby creating two regions which are the one between the composite and the electrode and one in which the reference electrode is subjected to (Laurent and Schlenoff, 1997). This consequently causes a net change in the potentials for the pure NPs. The current responses at $80mVs^{-1}$ (Fig 4.6) indicate that the oxidation reaction of the NPs in the composites occurs at a faster rate. During the cathodic sweep Zn NPs was oxidised to ZnO, Cu^{+} was oxidised to Cu^{2+}, Cu to Cu^{+} and Ag to Ag^{+} as shown by the equations within the voltammogram. The various oxidation potentials for the different ionic species are given in table 4.3. During the anodic sweep weak peaks for the reduction of Cu^{+} to Cu and Ag^{+} to Ag can be observed. This can be explained by the fact that the chitosan to NPs chelation is anchored on the ability of the NPs to receive a lone pair of electrons from the amine group of the chitosan. So the acceptance of NPs of a pair of electrons lowers its chances of reduction. This phenomenon is however dependent on the pH of the media and pH that is below 6 can liberate the NPs from the amine group as the amine group favours protonating in lower pH.

4.3.4.2. Electron-transfer kinetics studies

To study the electron, transfer kinetics taking place at the electrodes during the analysis of the CH-NPs composites, sweeps were ran at different scan rates in 0.1M PBS (pH 6.8) in the range of 20 to 100mV. It was observed that the current peaks for both the cathodic and anodic sweep were proportional to the increase in scan rate (Figure 4.7). The shift of the redox potentials towards the positive with increasing scan rate which was observed in the CH-CuO composite suggesting possibility of kinetic limitation at the surface of the electrodes (Mazloum-ardakani *et al.*, 2010). In these studies the kinetic limitation is expected to have been caused by the presence of uneven or non-equivalent sites within the composite film on the electrode and also chemical interactions between the composite modification film and the electrolyte ions (Lović, 2017). The chitosan in the composite behaves as a self-assembly monolayer thereby acting as a membrane and also the presence of unevenness distribution of NPs within the film brings about non-equivalence during electron transfer (Schlenoff, Ly and Li, 1998). For CH-ZnO and CH-Ag voltammograms it can be observed that there was no shift in potential with increasing scan rate suggesting that there is minimal kinetic limitation on the modifier film drop coated on the electrode (Karim-Nezhad *et al.*, 2009).

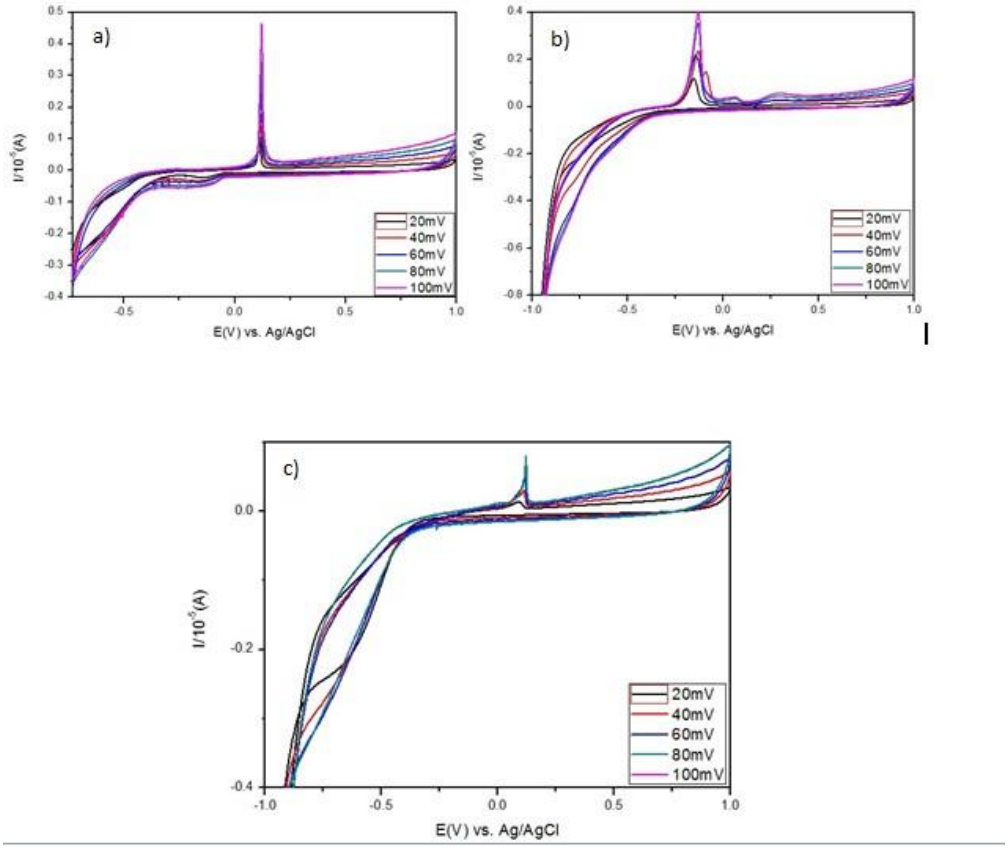

Figure 4. 8. Voltammograms of a) CH-Ag b) CH-CuO c) CH-ZnO composites in 0.1M PBS ,pH 6.8 at various scan rates

To understand the type of surface reaction taking place on the modified GCEs, plots of Ip vs. V and Ip vs. $V^{1/2}$ can be plotted and the correlation between the current the scan rates can be used for determination. In theoretical terms, as discussed in chapter 3, a linear plot of Ip vs. $V^{½}$ with strong correlation means that the process is diffusion controlled and a linear plot of Ip vs. V with a strong correlation means that the process is adsorption controlled (Bard *et al.*, 1944). The studies on the surface reaction processes during the study of the CH-NPs composites show that both the diffusion controlled and the adsorption processes are taking place (Figure 4.8) since both linear plots exhibit linear relationship of the Ip and the scan rate. It can however be observed that the linear plot of Ip vs. scan rate V exhibits the best linear plots as shown by the correlation values. So it means in the dominant surface reactions taking place at the composite modified GCE surface are adsorption controlled and it resonates with the type of surface process that also take place for the pure NPs. In comparison with the pure NPs from chapter 3, it can be concluded that the interaction of the chitosan and pure NPs does not have a significant influence on the type of electron transfer process that occurs on the electrode surface.

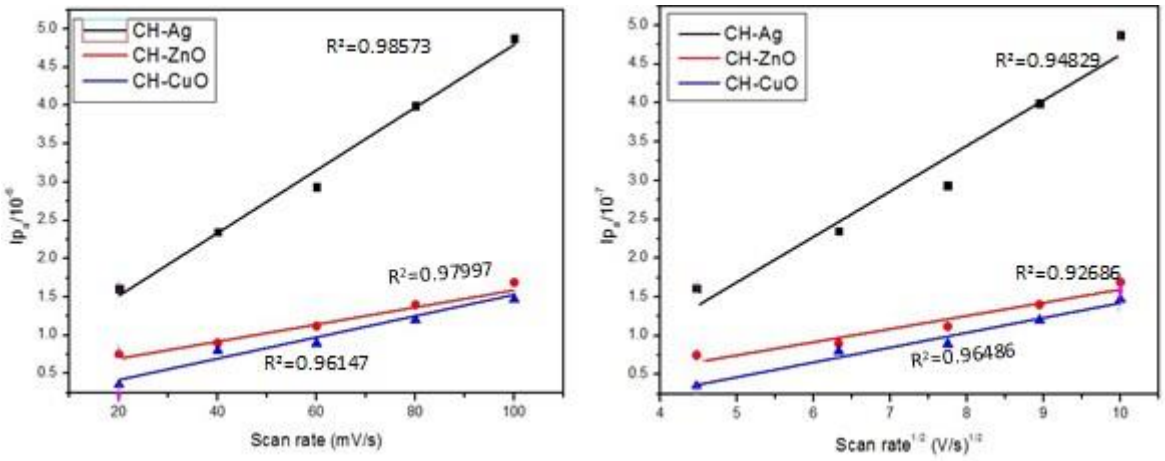

Figure 4. 9. Ipa of voltammograms vs. a) scan rates b) square root of scan rate in the range of 20-100mV

The Laviron's equation can be used to calculate the electrochemical parameters to understand the relationship between the redox potentials and the scan rates. The following Laviron's equations are applied (E. Laviron, 1979):

$$E_{pa}=E^0+\frac{2.3RT}{(1-\alpha)nF}\log v \quad \text{4.1a}$$

$$E_{pc}=E^0-\frac{2.3RT}{(1-\alpha)nF}\log v \quad \text{4.1b}$$

$$\text{Log } k_s=\alpha \log(1-\alpha)+(1-\alpha)\log\alpha-\log\left(\frac{RT}{nF}\right)-(1-\alpha)\alpha nF\frac{\Delta Ep}{2.3RT} \quad \text{4.1c}$$

Equation 4. 1 Laviron's equations

Where E_{pc} and E_{pa} are the cathodic and anodic peak potentials, respectively, α is the electron transfer coefficient, k_s is standard rate constant for surface reaction, v is the scan rate, R is the universal gas constant (8.314 J mol^{-1} K^{-1}), T is absolute temperature (273.15 K), F the Faraday constant (96 485 C/mol), E^0 is the formal potential and n is the electron transfer number. Using the above equation, if the E^0 is known, Ep is in linear with ln v then the αn value can be calculated from the slope and k_s from the intercept. The E^0 value can be deduced from the intercept of Ep vs. v plot on the ordinate by extrapolating the line to v = 0, when v was approached to zero, then Ep was approached to E^0.

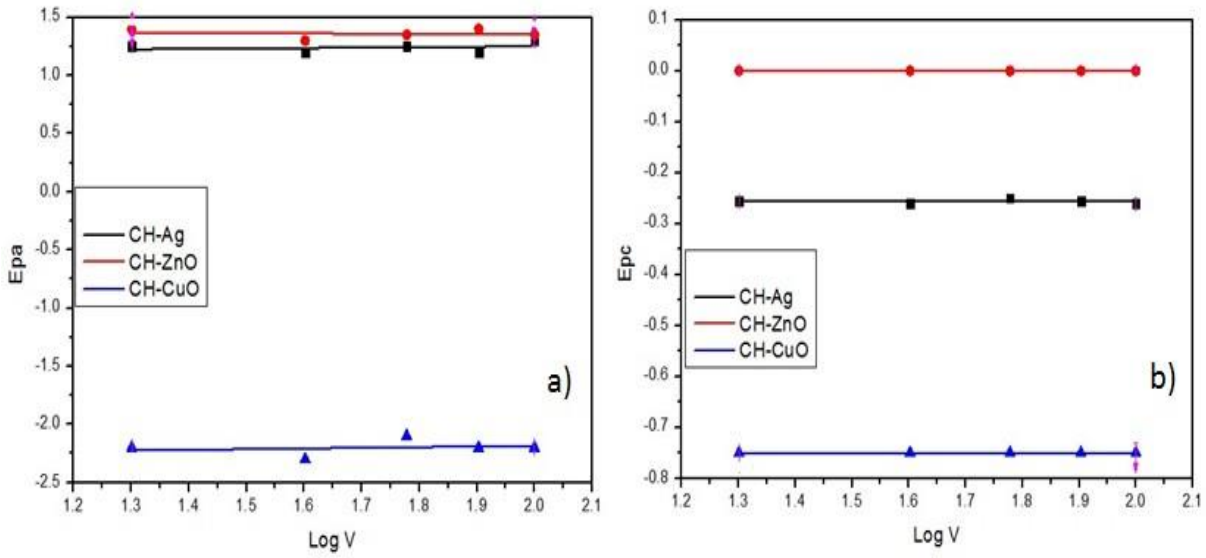

Figure 4. 10 Variation of (a) Epa versus logarithm of scan rate and (b) Epc versus logarithm of scan rate(log V) for the CH-NPs composites in PBS, pH 6.8.

The plots of Epa and Epc vs. Log V showed a strong linear correlation indicating that increase in the scan rate does not affect the potential difference of either the anodic or cathodic reaction (Figure 4.9). The values of α in Table 4.4 confirm the irreversibility of the electrochemical activity of the CH-NPs composites. The α value usually gives information on the reversibility of a reaction and it is stated that when α=0.5±0.2 the reaction is deemed reversible (Brown, 2015). It has been suggested that when the value is closer to 1 it means that the redox reaction needs more energy to overcome over potential and the value also means that the Gibbs energy of the reaction varies with potential (Brown and Gray, 2010; Haghighat and Dawlaty, 2016). In general terms it means that the redox reactions of the CH-Ag and CH-ZnO composites are not reversible therefore they are asymmetrical. This can be explained chemically by the electron stability the amine group of the chitosan offers to the NPs species. The NPs on the composite is willing to readily lose an electron hence the sharp peaks observed on the anodic sweep. However, the NP is not willing to take up any electrons to be reduced due to the high electron density in its environment. This causes the forward oxidation sweep to take place with ease whereas the reverse reduction reaction is not so due to a high activation energy barrier. The CH-CuO composite exhibited a α value of 0.4 which is in proximity with the unity of reaction value 0.5. This is evidence that the reaction of the redox couple Cu/Cu^{+} is quasi-reversible and it also evident on the voltammogram of the CH-CuO composite where a strong anodic peak is observed and also a weak cathodic peak is observed. This can be attributed to the ability of copper to lose two electrons via the steady state reaction route. Similar results with α>1 due adornment of metals has been reported elsewhere (Paul and Leddy, 1995).

Table 4. 4 The electrochemical parameters of CH-Ag, CH-ZnO and CH-CuO composites using Laviron's equation (Equation 4.1a-c)

NPs	ΔE^0_p(mV)	Slope	α
CH-Ag	370	0.0347	1.6
CH-ZnO	0	0.0578	1.4
CH-CuO	980	0.0189	0.4

The standard rate constant, K_s, values were all zero and this indicates that there is no equilibrium in existence between the forward and the reverse reaction (Bard *et al.*, 1944). This confirms what other parameters have confirmed and also the voltammograms where there is no cathodic peak for the CH-NPs composites. A redox reaction with a standard rate constant value of between 0.1 and 10 cms^{-1} tends to achieve an equilibrium faster whereas a reaction with a value lower than 0.1 is torpid and has no certain equilibrium(Velasco, 1997). The values obtained for all the composites indicate that the equilibrium is reached via a torpid route or there is no equilibrium at all.

4.4. Conclusion

CH-NPs composites were successfully synthesized and characterized by UV-Visible, FTIR and Cyclic Voltammetry with results being contrasted with those of pure NPs.

The UV-Visible spectra of the various composites all showed a shift towards lower wavelengths with increased frequency compared to the absorption spectra of the pure NPs thereby supplementing that there is an interaction and some form of bonding that existing between the chitosan and the NPs. The band gap energy of the CH-NPs composites was found to be in the semi-conductor range of 3.70eV to 4.50eV, which is narrower compared to that of the pure NPs from Chapter 3. The difference in optical band gaps between the pure NPs and the CH-NPs also supports that there is interaction between the NPs and the chitosan. The relatively narrow range of the band gaps for the composites also suggests that the reactivity of the composites is expected to differ significantly from that of the pure NPs. FTIR studies showed the absence of chitosan bands and the presence of new absorption bands within the CH-NPs composites. This was due to the interaction between the chitosan and the NPs which altered the electron density within the composites giving rise to the new bands.

Electrochemical studies confirmed the presence of the NPs within the CH-NPs composites and the oxidation peaks exhibited the Donnan effect signifying the effect of the chitosan on the electrochemical activity of the NPs. The surface reaction process occurring on the composite modified GCEs was observed to be the adsorption process. The electrochemical studies confirm that there is change in the electro activity of the NPs after they are adorned with chitosan. The α and k_s values of the composites indicated that there is no equilibrium between the anodic sweep and cathodic sweep reactions. Overall the work of this chapter proved that the interaction of chitosan and the NPs produces a composite with optical, electrochemical, and chemical characteristics that do exist in neither chitosan nor the pure NPs. The composite, CH-Ag-ZnO-CuO, was successfully formed and showed by characterisation that is presents more diverse reactivity potential than individual CH-NPs composites. The XRD investigations indicated that there is no significant change of the crystalline structures within the NPs of the composites.

From these results, it can be concluded that the CH-NPs composites were successfully synthesized. The consolidated results also indicate that the CH-NPs composites exhibit optical, electrochemical, and structural attributes that are not found in the pure chitosan or pure NPs.

4.5. References

Abbasipour, M. *et al.* (2014) 'Coated Cotton Gauze with Ag/ZnO/chitosan Nanocomposite as a Modern Wound Dressing', *Journal of Engineered Fibers and Fabrics*, 9(1), pp. 124–130.

AbdElhady, M. M. (2012) 'Preparation and Characterization of Chitosan/Zinc Oxide Nanoparticles for Imparting Antimicrobial and UV Protection to Cotton Fabric', *International Journal of Carbohydrate Chemistry*, 2012, pp. 1–6. doi: 10.1155/2012/840591.

Abiraman, T. *et al.* (2016) 'Antifouling behavior of chitosan adorned zinc oxide nanorods', *RSC Adv.* Royal Society of Chemistry, 6(73), pp. 69206–69217. doi: 10.1039/C6RA13321E.

Ahmed, S. and Ikram, S. (2016) 'Chitosan Based Scaffolds and Their Applications in Wound Healing', *Achievements in the Life Sciences*. Far Eastern Federal University, 10(1), pp. 27–37. doi: 10.1016/j.als.2016.04.001.

Alagumuthu, G. and Kumar, T. A. (2013) 'Synthesis and Characterization of Chitosan / TiO 2 Nanocomposites Using Liquid Phase Deposition Technique', 4(1), pp. 105–111.

Algawi, S. D. A. L. (no date) ‘Copper Oxide Nanostructures ; Syntheses and Characterization’, 71, pp. 0–4.

Ali, S. W., Rajendran, S. and Joshi, M. (2011) ‘Synthesis and characterization of chitosan and silver loaded chitosan nanoparticles for bioactive polyester’, *Carbohydrate Polymers*. Elsevier Ltd., 83(2), pp. 438–446. doi: 10.1016/j.carbpol.2010.08.004.

Alvarez, P. J. J. and Lowry, G. (2009) ‘Nanomaterials with Antimicrobial Properties : Mechanisms , Implications and Applications pp l i’.

Applerot, G. *et al.* (2012) ‘Understanding the antibacterial mechanism of CuO nanoparticles: Revealing the route of induced oxidative stress’, *Small*, 8(21), pp. 3326–3337. doi: 10.1002/smll.201200772.

Arefi, M. R. and Rezaei-Zarchi, S. (2012) ‘Synthesis of zinc oxide nanoparticles and their effect on the compressive strength and setting time of self-compacted concrete paste as cementitious composites’, *International Journal of Molecular Sciences*, 13(4), pp. 4340–4350. doi: 10.3390/ijms13044340.

Atiyeh, B. S. *et al.* (2007) ‘Effect of silver on burn wound infection control and healing: Review of the literature’, *Burns*, 33(2), pp. 139–148. doi: 10.1016/j.burns.2006.06.010.

Azuma, K. *et al.* (2015) *Chitin, Chitosan, and Its Derivatives for Wound Healing: Old and New Materials*, *Journal of Functional Biomaterials*. doi: 10.3390/jfb6010104.

Babu, V. S. (2010) *Solid State Devices and Technology*. 3rd edn, *Solid states devices and technology.* 3rd edn. Mumbai: Pearson.

Bagabas, A. *et al.* (2013) ‘Room-temperature synthesis of zinc oxide nanoparticles in different media and their application in cyanide photodegradation’, *Nanoscale Research Letters*, 8(1), p. 516. doi: 10.1186/1556-276X-8-516.

Balamurugan, B. and Mehta, B. R. (2001) ‘Optical and structural properties of nanocrystalline copper oxide thin films prepared by activated reactive evaporation’, *Thin Solid Films*, 396(1–2), pp. 90–96. doi: 10.1016/S0040-6090(01)01216-0.

Balu, S. S. and Bhakat, C. (2012) ‘SYNTHESIS OF SILVER NANOPARTICLES BY CHEMICAL REDUCTION AND THEIR ANTIMICROBIAL ACTIVITY Materials and Methods ’:, 1(6), pp. 1–5.

Bard, A. J. *et al.* (1944) *ELECTROCHEMICAL METHODS Fundamentals and Applications*,

Electrochemistry. I. Faulkner, Larry R. doi: 10.1016/B978-0-12-381373-2.00056-9.

Benavente, M. (2008) *Adsorption of metallic ions onto chitosan: equilibrium and kinetic studies*. doi: 976–988.

Beyth, N. *et al.* (2015) 'Alternative Antimicrobial Approach: Nano-Antimicrobial Materials', *Evidence-Based Complementary and Alternative Medicine*, 2015, pp. 1–16. doi: 10.1155/2015/246012.

Biovation, L. (2010) *Testing for Antimicrobial Activity in Textiles.* Boothbay.

Bonnemann, H. and Richards, R. M. (2001) 'Nanoscopic metal particles - synthetic methods and potential applications', *Eur. J. Inorg. Chem.*, pp. 2455–2480. doi: 10.1002/1099-0682(200109)2001:10<2455::AID-EJIC2455>3.0.CO;2-Z.

Brintha, S. R. and Ajitha, M. (2015) 'Synthesis and characterization of ZnO nanoparticles via aqueous solution, sol-gel and hydrothermal methods', *IOSR Journal of Applied Chemistry*, 8(11), pp. 66–72. doi: 10.9790/5736-081116672.

Brown, J. H. (2015) 'Development and Use of a Cyclic Voltammetry Simulator To Introduce Undergraduate Students to Electrochemical Simulations', *Journal of Chemical Education*. American Chemical Society, 92(9), pp. 1490–1496. doi: 10.1021/acs.jchemed.5b00225.

Brown, K. and Gray, S. B. (2010) 'Cyclic Voltammetric Studies of Electropolymerized Films Based on Ruthenium (II/III) Bis (1, 10phenanthroline)(4-methyl-4'vinyl-2, 2'-bipyridine).', *International Journal of Chemistry*, 2(2), pp. 3–9. Available at: http://search.ebscohost.com/login.aspx?direct=true&profile=ehost&scope=site&authtype=crawler&jrnl=19169698&AN=52739860&h=s7r8gpPlt9tlQXU1DwQKvth6GpoG/uSIl9+y7buDKd4ozaZ6T7n2jMZlVbnZRzIKzPwKahBTG9vQKJVjeYgNcA==&crl=c.

Brownson, D. A. C. and Banks, C. E. (2014) *The Handbook of Graphene Electrochemistry*, *The Handbook of Graphene Electrochemistry*. doi: 10.1007/978-1-4471-6428-9.

Brugnerotto, J. *et al.* (2001) 'An infrared investigation in relation with chitin and chitosan characterization', *Polymer*, 42(8), pp. 3569–3580. doi: 10.1016/S0032-3861(00)00713-8.

Budhiraja, N. *et al.* (2013) 'Synthesis and Optical Characteristics of Silver Nanoparticles on Different Substrates', *International Letters of Chemistry, Physics and Astronomy*, 19, pp. 80–88. doi: 10.18052/www.scipress.com/ILCPA.19.80.

Calvo, E. J. and Wolosiuk, A. (2002) 'Donnan permselectivity in layer-by-layer self-

assembled redox polyelectrolye thin films', *Journal of the American Chemical Society*, 124(28), pp. 8490–8497. doi: 10.1021/ja020107h.

Cavassin, E. D. *et al.* (2015) 'Comparison of methods to detect the in vitro activity of silver nanoparticles (AgNP) against multidrug resistant bacteria', *Journal of Nanobiotechnology*. BioMed Central, 13(1). doi: 10.1186/s12951-015-0120-6.

Dai, T. *et al.* (2011) *NIH Public Access*, *Expert Rev Anti Infect Ther*. doi: 10.1586/eri.11.59.Chitosan.

Dash, M. *et al.* (2011) 'Chitosan - A versatile semi-synthetic polymer in biomedical applications', *Progress in Polymer Science (Oxford)*. Elsevier Ltd, 36(8), pp. 981–1014. doi: 10.1016/j.progpolymsci.2011.02.001.

Davis, J. and McLister, A. (2016) 'Chapter Four - Passive and Interactive Dressing Materials', in Davis, J. et al. (eds) *Smart Bandage Technologies*. Academic Press, pp. 93–144. doi: https://doi.org/10.1016/B978-0-12-803762-1.00004-7.

Debanath, M. K. and Karmakar, S. (2013) 'Study of blueshift of optical band gap in zinc oxide (ZnO) nanoparticles prepared by low-temperature wet chemical method', *Materials Letters*. Elsevier, 111, pp. 116–119. doi: 10.1016/j.matlet.2013.08.069.

Dehaghi, S. M. *et al.* (2014) 'Removal of permethrin pesticide from water by chitosan–zinc oxide nanoparticles composite as an adsorbent', *Journal of Saudi Chemical Society*, 18(4), pp. 348–355. doi: https://doi.org/10.1016/j.jscs.2014.01.004.

Devi, H. S. and Singh, T. D. (2014) 'Synthesis of Copper Oxide Nanoparticles by a Novel Method and its Application in the Degradation of Methyl Orange', *Advance in Electronic and Electric Engineering*, 4(1), pp. 83–88.

Douglas Skoog, James Holler, S. C. (2007) 'Principles of instrumental analysis.', in Harris, D. (ed.) *Principles of instrumental analysis.* 6th edn. Belmont: Brooks/Cole, p. 371.

Durga Praveena, V. and Vijaya Kumar, K. (2013) 'Synthesis and Characterization of Chitosan based Silver Nano Composite System for Antibacterial Applications', *Proceedings of the International Conference on Advanced Nanomaterials & Emerging Engineering Technologies*, pp. 76–79.

Faiz, U. *et al.* (2011) 'Efficacy of zinc as an antibacterial agent against enteric bacterial pathogens.', *Journal of Ayub Medical College*, 23(2), pp. 18–21.

Feng, Q. L. *et al.* (2000) ‘A mechanistic study of the antibacterial effect of silver ions on <I>Escherichia coli</I> and <I>Staphylococcus aureus</I>’, *Journal of Biomedical Materials Research*, pp. 662–668. doi: 10.1002/1097-4636(20001215)52:4<662::aid-jbm10>3.0.co;2-3.

Fielicke, A., Rabin, I. and Meijer, G. (2006) ‘Far-infrared spectroscopy of small neutral silver clusters’, *Journal of Physical Chemistry A*, 110(26), pp. 8060–8063. doi: 10.1021/jp062095i.

Fievet, P. (2015) ‘Donnan Potential BT - Encyclopedia of Membranes’, in Drioli, E. and Giorno, L. (eds). Berlin, Heidelberg: Springer Berlin Heidelberg, pp. 1–3. doi: 10.1007/978-3-642-40872-4_1716-1.

Franci, G. *et al.* (2015) ‘Silver nanoparticles as potential antibacterial agents’, *Molecules*, 20(5), pp. 8856–8874. doi: 10.3390/molecules20058856.

Gliga, A. R. *et al.* (2014) ‘Size-dependent cytotoxicity of silver nanoparticles in human lung cells: the role of cellular uptake, agglomeration and Ag release’, *Particle and Fibre Toxicology*, 11(1), p. 11. doi: 10.1186/1743-8977-11-11.

Gogoi, S. K. *et al.* (2006) ‘Green fluorescent protein-expressing Escherichia coli as a model system for investigating the antimicrobial activities of silver nanoparticles’, *Langmuir*, 22(22), pp. 9322–9328. doi: 10.1021/la060661v.

Gouda, M. (2012) ‘Nano-zirconium oxide and nano-silver oxide/cotton gauze fabrics for antimicrobial and wound healing acceleration’, *Journal of Industrial Textiles*, 41(3), pp. 222–240. doi: 10.1177/1528083711414960.

Goy, R. C., Britto, D. de and Assis, O. B. G. (2009) ‘A review of the antimicrobial activity of chitosan’, *Polímeros*, 19(3), pp. 241–247. doi: 10.1093/jac/dkg286.

Guidelli, R. *et al.* (2014) ‘Defining the transfer coefficient in electrochemistry: An assessment (IUPAC Technical Report)’, *Pure and Applied Chemistry*, 86(2), pp. 245–258. doi: 10.1515/pac-2014-5026.

Gunalan, S., Sivaraj, R. and Rajendran, V. (2012) ‘Green synthesized ZnO nanoparticles against bacterial and fungal pathogens’, *Progress in Natural Science: Materials International*. Elsevier, 22(6), pp. 693–700. doi: 10.1016/j.pnsc.2012.11.015.

Guo, S. and Dipietro, L. A. (2010) ‘Factors Affecting Wound Healing’, *Obstetrics & Gynecology*, (Mc 859), pp. 219–229. doi: 10.1177/0022034509359125.

Haghighat, S. and Dawlaty, J. M. (2016) ‘pH Dependence of the Electron-Transfer

Coefficient: Comparing a Model to Experiment for Hydrogen Evolution Reaction', *Journal of Physical Chemistry C*, 120(50), pp. 28489–28496. doi: 10.1021/acs.jpcc.6b10602.

Hajipour, M. J. *et al.* (2012) 'Coated Cotton Gauze with Ag/ZnO/chitosan Nanocomposite as a Modern Wound Dressing', *Journal of Industrial Textiles*. Elsevier Ltd, 9(6), pp. 143–154. doi: 10.1155/2015/246012.

Hajipour, M. J., Fromm, K. M. and Ashkarran, A. (2012) 'Antibacterial properties of nanoparticles', *Trends in Biotechnology*. Elsevier Ltd, 30(10), pp. 499–511. doi: 10.1016/j.tibtech.2012.06.004.

Huh, A. J. and Kwon, Y. J. (2011) '"Nanoantibiotics": A new paradigm for treating infectious diseases using nanomaterials in the antibiotics resistant era', *Journal of Controlled Release*. Elsevier B.V., 156(2), pp. 128–145. doi: 10.1016/j.jconrel.2011.07.002.

I. Markova-Deneva (2010) 'Infrared Spectroscopy Investigation of Metallic Nanoparticles Based on Copper, Cobalt, and Nickel Synthesized Through Borohydride Reduction Method', *Journal of the University of Chemical Technology and Metallurgy*, 45(4), pp. 351–378.

Ijaz, F. *et al.* (2017) 'Green synthesis of copper oxide nanoparticles using abutilon indicum leaf extract: Antimicrobial, antioxidant and photocatalytic dye degradation activities', *Tropical Journal of Pharmaceutical Research*, 16(4), pp. 743–753. doi: 10.4314/tjpr.v16i4.2.

ISO (2007) 'ISO 21348 Definitions of Solar Irradiance Spectral Categories', *Environment*, (section 5), pp. 6–7.

Jain, K. K. (2007) 'Applications of nanobiotechnology in clinical diagnostics', *Clinical Chemistry*, 53(11), pp. 2002–2009. doi: 10.1373/clinchem.2007.090795.

Jemimah, V. H. and Arulpandi, I. (2014) 'Evaluation of Antimicrobial Property of Biosynthesized Zinc Oxide Nanoparticles (ZnO NPs) and its Application on Baby Diapers', 6(2), pp. 113–119.

Jin, T. *et al.* (2009) 'Antimicrobial efficacy of zinc oxide quantum dots against Listeria monocytogenes, Salmonella Enteritidis, and Escherichia coli O157:H7', *Journal of Food Science*, 74(1). doi: 10.1111/j.1750-3841.2008.01013.x.

John Kotz, Paul Treichel, J. T. (2009) *Chemistry and chemical reactivity .* 2nd edn, *Chemistry and chemical reactivity .* 2nd edn. Edited by Lisa Lockwood. Belmont: Brooks/Cole.

Joseph Wang (2006) *Analytical Electrochemistry*. 3rd edn. New Jersey: John Wiley and

Sons.

Jyoti, K., Baunthiyal, M. and Singh, A. (2016) ‘Characterization of silver nanoparticles synthesized using Urtica dioica Linn. leaves and their synergistic effects with antibiotics’, *Journal of Radiation Research and Applied Sciences*. Elsevier Ltd, 9(3), pp. 217–227. doi: 10.1016/j.jrras.2015.10.002.

Kalimuthu, K. *et al.* (2008) ‘Biosynthesis of silver nanocrystals by Bacillus licheniformis’, *Colloids and Surfaces B: Biointerfaces*, 65(1), pp. 150–153. doi: https://doi.org/10.1016/j.colsurfb.2008.02.018.

Kang, X. *et al.* (2009) ‘Glucose Oxidase-graphene-chitosan modified electrode for direct electrochemistry and glucose sensing’, *Biosensors and Bioelectronics*, 25(4), pp. 901–905. doi: 10.1016/j.bios.2009.09.004.

Karim-Nezhad, G. *et al.* (2009) *Kinetic Study of Electrocatalytic Oxidation of Carbohydrates on Cobalt Hydroxide Modified Glassy Carbon Electrode*, *J. Braz. Chem. Soc.* doi: 10.1590/S0103-50532009000100022.

Kayani, Z. N. *et al.* (2012) ‘Synthesis and characterization of CuO nanowires by a simple wet chemical method’, *International Letters of Chemistry, Physics and Astronomy*. Springer Open Ltd, 14(1), pp. 26–36. doi: 10.1186/1556-276X-7-70.

Kayani, Z. N. *et al.* (2015) ‘Characterization of Copper Oxide Nanoparticles Fabricated by the Sol???Gel Method’, *Journal of Electronic Materials*, 44(10), pp. 3704–3709. doi: 10.1007/s11664-015-3867-5.

Khatoon, N. *et al.* (2015) ‘Biosynthesis, Characterization, and Antifungal Activity of the Silver Nanoparticles Against Pathogenic Candida species’, *BioNanoScience*, 5(2), pp. 65–74. doi: 10.1007/s12668-015-0163-z.

Khorsand Zak, A. *et al.* (2011) ‘Synthesis and characterization of a narrow size distribution of zinc oxide nanoparticles’, *International Journal of Nanomedicine*, 6(1), pp. 1399–1403. doi: 10.2147/IJN.S19693.

Kong, M. *et al.* (2010) ‘Antimicrobial properties of chitosan and mode of action: A state of the art review’, *International Journal of Food Microbiology*. Elsevier B.V., 144(1), pp. 51–63. doi: 10.1016/j.ijfoodmicro.2010.09.012.

Krishna Veni (2016) ‘Anti-Bacterial Coating of Chrysanthemum Extract on Bamboo Fabric for

Healthcare Applications', *Journal of Textile Science & Engineering*, 6(4), pp. 6–8. doi: 10.4172/2165-8064.1000267.

Krishnamoorthy, K. and Kim, S. J. (2013) 'Growth, characterization and electrochemical properties of hierarchical CuO nanostructures for supercapacitor applications', *Materials Research Bulletin*. Elsevier Ltd, 48(9), pp. 3136–3139. doi: 10.1016/j.materresbull.2013.04.082.

Kumar, H. and Rani, R. (2013) 'Structural Characterization of Silver Nanoparticles Synthesized by Micro emulsion Route', *International Journal of Engineering and Innovative Technology*, 3(3), pp. 344–348.

Kurien, S. (2005) 'Chapter 4: ANALYSIS OF FTIR SPECTRA OF NANOPARTICLES of MgAl2O4, SrAl2O4, and NiAl2O4', 1595, pp. 64–78. Available at: http://mgutheses.in/page/?q=T 1354&search=siby+kurien&page=1&rad=sc.

Laurent, D. and Schlenoff, J. B. (1997) 'Multilayer Assemblies of Redox Polyelectrolytes', *Langmuir*, 13(6), pp. 1552–1557. doi: 10.1021/la960959t.

Laviron, E. (1979) 'General expression of the linear potential sweep voltammogram in the case of diffusionless electrochemical systems', *Journal of Electroanalytical Chemistry and Interfacial Electrochemistry*, 101(1), pp. 19–28. doi: https://doi.org/10.1016/S0022-0728(79)80075-3.

Laviron, E. (1979) 'General expression of the linear potential sweep voltammogram in the case of diffusionless electrochemical systems', *Journal of Electroanalytical Chemistry*, 101(1), pp. 19–28. doi: 10.1016/S0022-0728(79)80075-3.

Laviron, E. (1995) 'The use of polarography and cyclic voltammetry for the study of redox systems with adsorption of the reactants. Heterogeneous vs. surface path', *Journal of Electroanalytical Chemistry*, 382(1–2), pp. 111–127. doi: 10.1016/0022-0728(94)03684-U.

Lionelli, G. T. and Lawrence, W. T. (2003) 'Wound dressings', *Surgical Clinics of North America*, pp. 617–638.

Liu, B. *et al.* (2013) 'Adsorption of heavy metal ions, dyes and proteins by chitosan composites and derivatives --- A review', *Journal of Ocean University of China*, 12(3), pp. 500–508. doi: 10.1007/s11802-013-2113-0.

Logothetidis, S. (2012) *Nanotechnology : Principles and Applications*. doi: 10.1007/978-3-

642-22227-6.

Long, J. *et al.* (2016) ‘A new class of nanocomposites of Zn–Al–Bi layered double oxides: large reversible capacity and better cycle performance for alkaline secondary batteries’, *RSC Adv.* Royal Society of Chemistry, 6(95), pp. 92896–92904. doi: 10.1039/C6RA18164C.

Lović, J. (2017) ‘Glucose Sensing Using Glucose Oxidase-Glutaraldehyde- Cysteine Modified Gold Electrode’, *International Journal of Electrochemical Science*, (July), pp. 5806–5817. doi: 10.20964/2017.07.65.

Luna, I. Z. *et al.* (2015) ‘Preparation and Characterization of Copper Oxide Nanoparticles Synthesized via Chemical Precipitation Method’, *OALib*, 2(3), pp. 1–8. doi: 10.4236/oalib.1101409.

Ma, A. *et al.* (2011) ‘Evaluation of antibacterial activity of silver nanoparticles against MSSA and MRSA on isolates from skin infections’, *Research Article Biology and Medicine*, 3(2), pp. 141–146.

Malinowska-Pańczyk, E. *et al.* (2009) ‘The combined effect of moderate pressure and chitosan on Escherichia coli and Staphylococcus aureus cells suspended in a buffer and on natural microflora of apple juice and minced pork’, *Food Technology and Biotechnology*, 47(2), pp. 202–209.

Maneerung, T., Tokura, S. and Rujiravanit, R. (2008) ‘Impregnation of silver nanoparticles into bacterial cellulose for antimicrobial wound dressing’, *Carbohydrate Polymers*, 72(1), pp. 43–51. doi: 10.1016/j.carbpol.2007.07.025.

Mansoori, G. A. (2005) ‘Principles of Nanotechnology: Molecular Based Study of Condensed Matter in Small Systems’. doi: 10.1142/5749.

Mazloum-ardakani, M. *et al.* (2010) ‘Voltammetric Determination of Dopamine at the Surface of TiO 2 Nanoparticles Modified Carbon Paste Electrode’, 5, pp. 147–157.

Meftahi, A. *et al.* (2010) *The effects of cotton gauze coating with microbial cellulose*, *Cellulose*. doi: 10.1007/s10570-009-9377-y.

Mehta, B. K., Chhajlani, M. and Shrivastava, D. (2017) ‘Green synthesis of silver nanoparticles and their characterization by XRD’, *Frontiers of Physics and Plasma Science IOP Publishing IOP Conf. Series: Journal of Physics: Conf. Series*, 836. doi: 10.1088/1742-6596/836/1/012050.

Mohammad, F., A. Al-Lohedan, H. and N. Al-Haque, H. (2016) ‘Chitosan-mediated fabrication of metal nanocomposites for enhanced biomedical applicationsf’, *Advanced Materials Letters*, 8(2), pp. 89–100. doi: 10.5185/amlett.2017.6925.

Mohan, A. C. and Renjanadevi, B. (2016) ‘Preparation of Zinc Oxide Nanoparticles and its Characterization Using Scanning Electron Microscopy (SEM) and X-Ray Diffraction(XRD)’, *Procedia Technology*. Elsevier B.V., 24, pp. 761–766. doi: 10.1016/j.protcy.2016.05.078.

Muthukrishnan, A. M. (2015) ‘Green Synthesis of Copper-Chitosan Nanoparticles and Study of its Antibacterial Activity’, *Journal of Nanomedicine & Nanotechnology*, 6(1), pp. 1–6. doi: 10.4172/2157-7439.1000251.

Muzzarelli, R. (1973) *Natural chelating polymers; alginic acid, chitin, and chitosan*. 1st edn. Oxford: Pergamon press.

Muzzarelli, R. A. and Sipos, L. (1971) ‘Chitosan for the collection from seawater of naturally occurring zinc, cadmium, lead and copper’, *Talanta*, 18(9), p. 853—858. doi: 10.1016/0039-9140(71)80141-8.

Nam, H. C. and Schaak, R. E. (2007) ‘Shape-controlled conversion of ??-Sn nanocrystals into intermetallic M-Sn (M = Fe, Co, Ni, Pd) nanocrystals’, *Journal of the American Chemical Society*, 129(23), pp. 7339–7345. doi: 10.1021/ja069032y.

Norfazila, S. M. and Mohd, J. R. (2014) ‘Synthesis and Ultroviolet Visible Spectroscopy Studies of Chitosan Capped Gold Nanoparticles and Theri Reactions with Analytes’, *The Scientific World Journal*, 2014, p. 7. doi: http://dx.doi.org/10.1155/2014/184604.

Okumu, F. and Matoetoe, M. (2016) ‘Electrochemical Characterization of Silver-Platinum Various Ratio Bimetallic Nanoparticles Modified Electrodes’, *Journal of Nano Research*, 44, pp. 114–125. doi: 10.4028/www.scientific.net/JNanoR.44.114.

Olaniyan, O. J. *et al.* (2016) ‘Synthesis and Characterization of Chitosan-Silver Nanocomposite Film’, *Nano Hybrids and Composites*, 11, pp. 22–29. doi: 10.4028/www.scientific.net/NHC.11.22.

Ono, S. *et al.* (2015) ‘Increased wound pH as an indicator of local wound infection in second degree burns’, *Burns*. Elsevier Ltd and International Society of Burns Injuries, 41(4), pp. 820–824. doi: 10.1016/j.burns.2014.10.023.

Padil, V. and Cernik, M. (2013) *Green synthesis of copper oxide nanoparticles using gum*

karaya as a biotemplate and their antibacterial application, *International journal of nanomedicine*. doi: 10.2147/IJN.S40599.

Paladini, F. *et al.* (2016) 'In vitro assessment of the antibacterial potential of silver nano-coatings on cotton gauzes for prevention of wound infections', *Materials*, 9(6), pp. 1–14. doi: 10.3390/ma9060411.

Panchakarla, L. S., Govindaraj, A. and Rao, C. N. R. (2007) 'Formation of ZnO nanoparticles by the reaction of zinc metal with aliphatic alcohols', *Journal of Cluster Science*, 18(3), pp. 660–670. doi: 10.1007/s10876-007-0129-6.

Pankratov, D. V. *et al.* (2014) 'Impact of surface modification with gold nanoparticles on the bioelectrocatalytic parameters of immobilized bilirubin oxidase', *Acta Naturae*, 6(20), pp. 102–106.

Patrulea, V. *et al.* (2015) 'Chitosan as a starting material for wound healing applications', *European Journal of Pharmaceutics and Biopharmaceutics*. Elsevier B.V., 97, pp. 417–426. doi: 10.1016/j.ejpb.2015.08.004.

Paul, H. J. and Leddy, J. (1995) 'Direct Determination of the Transfer Coefficient from Cyclic Voltammetry: Isopoints as Diagnostics', *Analytical Chemistry*, 67(10), pp. 1661–1668. doi: 10.1021/ac00106a003.

de Paz, L. E. C. *et al.* (2011) 'Antimicrobial effect of chitosan nanoparticles on Streptococcus mutans biofilms', *Applied and Environmental Microbiology*, 77(11), pp. 3892–3895. doi: 10.1128/AEM.02941-10.

Pinho, E. *et al.* (2011) 'Antimicrobial activity assessment of textiles: Standard methods comparison', *Annals of Microbiology*, 61(3), pp. 493–498. doi: 10.1007/s13213-010-0163-8.

Prodomis, M. I. *et al.* (2000) 'The Importance of Surface Coverage in the Electrochemical Study of Chemically Modified Electrodes', *Electroanalysis*, 12(18), pp. 1498–1501.

Puchalski, M. *et al.* (2007) 'The study of silver nanoparticles by scanning electron microscopy, energy dispersive X-ray analysis and scanning tunnelling microscopy', *Materials Science-Poland*, 25(2), pp. 473–478.

Raafat, D. and Sahl, H. G. (2009) 'Chitosan and its antimicrobial potential - A critical literature survey', *Microbial Biotechnology*, 2(2 SPEC. ISS.), pp. 186–201. doi: 10.1111/j.1751-7915.2008.00080.x.

Radecka, M. *et al.* (2008) ‘Importance of the band gap energy and flat band potential for application of modified TiO2 photoanodes in water photolysis’, *Journal of Power Sources*, 181(1), pp. 46–55. doi: https://doi.org/10.1016/j.jpowsour.2007.10.082.

Raghupathi, K. R., Koodali, R. T. and Manna, A. C. (2011) ‘Size-dependent bacterial growth inhibition and mechanism of antibacterial activity of zinc oxide nanoparticles.’, *Langmuir : the ACS journal of surfaces and colloids*, 27(7), pp. 4020–4028. doi: 10.1021/la104825u.

Rahman, A. *et al.* (2009) ‘SYNTHESIS OF COPPER OXIDE NANO PARTICLES BY USING Phormidium cyanobacterium’, *Indonesian Journal of Chemistry*, 9(3), pp. 355–360.

Rai, M., Yadav, A. and Gade, A. (2009) ‘Silver nanoparticles as a new generation of antimicrobials’, *Biotechnology Advances*. Elsevier Inc., 27(1), pp. 76–83. doi: 10.1016/j.biotechadv.2008.09.002.

Ravichandran, S. *et al.* (2015) ‘A novel approach for the biosynthesis of silver oxide nanoparticles using aqueous leaf extract of Callistemon lanceolatus (Myrtaceae) and their therapeutic potential’, *Journal of Experimental Nanoscience*. Taylor & Francis, 8080(August), pp. 1–14. doi: 10.1080/17458080.2015.1077534.

Rhazi, M. *et al.* (2002) ‘Influence of the nature of the metal ions on the complexation with chitosan.: Application to the treatment of liquid waste’, *European Polymer Journal*, 38, pp. 1523–1530.

Rhoades, J. and Roller, S. (2000) ‘Antimicrobial actions of degraded and native chitosan against spoilage organisms in laboratory media and foods’, *Applied and Environmental Microbiology*, 66(1), pp. 80–86. doi: 10.1128/AEM.66.1.80-86.2000.

Richards, R. and Bonnemann, H. (2005) ‘Synthetic Approaches to Metallic Nanomaterials’, *Nanofabrication Towards Biomedical Applications: Techniques, Tools, Applications, and Impact*, pp. 1–32. doi: 10.1002/3527603476.ch1.

Salehi, R. *et al.* (2010) ‘Novel biocompatible composite (Chitosan-zinc oxide nanoparticle): Preparation, characterization and dye adsorption properties’, *Colloids and Surfaces B: Biointerfaces*. Elsevier B.V., 80(1), pp. 86–93. doi: 10.1016/j.colsurfb.2010.05.039.

Sanpui, P. *et al.* (2008) ‘The antibacterial properties of a novel chitosan-Ag-nanoparticle composite’, *International Journal of Food Microbiology*, 124(2), pp. 142–146. doi: 10.1016/j.ijfoodmicro.2008.03.004.

Santos, C. L. *et al.* (2013) 'Nanomaterials with Antimicrobial Properties : Applications in Health Sciences', *Microbial pathogens and strategies for combating them: science, technology and education*, 1, pp. 143–154.

Sanyal, M. K., Datta, A. and Hazra, S. (2002) 'Morphology of nanostructured materials', *Pure and Applied Chemistry*, 74(9), pp. 1553–1570. doi: 10.1351/pac200274091553.

Schlenoff, J. B., Ly, H. and Li, M. (1998) 'Charge and Mass Balance in Polyelectrolyte Multilayers - Journal of the American Chemical Society (ACS Publications)', *Journal of the American Chemical …*, 7863(13), pp. 7626–7634. doi: 10.1021/ja980350.

Sehat, A. A. *et al.* (2015) 'Fast immobilization of glucose oxidase on graphene oxide for highly sensitive glucose biosensor fabrication', *International Journal of Electrochemical Science*, 10(1), pp. 272–286.

Seil, J. T. and Webster, T. J. (2012) 'Antimicrobial applications of nanotechnology: Methods and literature', *International Journal of Nanomedicine*, 7, pp. 2767–2781. doi: 10.2147/IJN.S24805.

Sezer, A. D. and Cevher, E. (1992) 'Biopolymers as Wound Healing Materials: Challenges and New Strategies', *Biomaterials Applications for Nanomedicine*, pp. 383–414. doi: 10.5772/25177.

Shen, X. S. *et al.* (2009) 'Nanospheres of silver nanoparticles: agglomeration, surface morphology control and application as SERS substrates', *Physical Chemistry Chemical Physics*. The Royal Society of Chemistry, 11(34), pp. 7450–7454. doi: 10.1039/B904712C.

Shrivastava, S. *et al.* (2010) 'Characterization of enhanced antibacterial effects of novel silver nanoparticles', *Nanotechnology*, 18(22), pp. 1–9. doi: 10.1088/0957-4484/18/22/225103.

Sirkka, T., Skiba, J. B. and Apell, S. P. (2016) 'Wound pH depends on actual wound size', p. 13.

Srivastava, S., Agrawal, A. and Kumar, S. (2013) 'Synthesis and Characterisation of Copper Oxide nanoparticles', *Journal of Applied Physics*, 5(4), pp. 61–65.

Street, E. and Lake, C. (2014) 'Aatcc t', pp. 2012–2015.

Sudheesh Kumar, P. T. *et al.* (2012) 'Flexible and microporous chitosan hydrogel/nano ZnO composite bandages for wound dressing: In vitro and in vivo evaluation', *ACS Applied Materials and Interfaces*, 4(5), pp. 2618–2629. doi: 10.1021/am300292v.

Sudheesh Kumar, P. T. *et al.* (2013) 'Evaluation of wound healing potential of β-chitin hydrogel/nano zinc oxide composite bandage', *Pharmaceutical Research*, 30(2), pp. 523–537. doi: 10.1007/s11095-012-0898-y.

Sun, K. and Li, Z. H. (2011) 'Preparations, properties and applications of chitosan based nanofibers fabricated by electrospinning', *Express Polymer Letters*, 5(4), pp. 342–361. doi: 10.3144/expresspolymlett.2011.34.

Sutherland, L. F. and D. (2012) *Nanotechnologies: Principles, Applications, Implications and Hands-on Activities*. doi: :10.2777/76945.

Talam, S., Karumuri, S. R. and Gunnam, N. (2012) 'Synthesis, Characterization, and Spectroscopic Properties of ZnO Nanoparticles', *ISRN Nanotechnology*, 2012, pp. 1–6. doi: 10.5402/2012/372505.

Tamayo, L. *et al.* (2016) 'Copper-polymer nanocomposites: An excellent and cost-effective biocide for use on antibacterial surfaces', *Materials Science and Engineering C*. Elsevier B.V., 69, pp. 1391–1409. doi: 10.1016/j.msec.2016.08.041.

Teterycz, H. *et al.* (2014) 'Deposition of Zinc Oxide on the Materials Used in Medicine. Preliminary Results', *FIBRES & TEXTILES in Eastern Europe*, 22(105), pp. 3–126.

Tikhonov, V. E. *et al.* (2006) 'Bactericidal and antifungal activities of a low molecular weight chitosan and its N-/2(3)-(dodec-2-enyl)succinoyl/-derivatives', *Carbohydrate Polymers*, 64(1), pp. 66–72. doi: 10.1016/j.carbpol.2005.10.021.

Tran, D. L. *et al.* (2011) 'Some biomedical applications of chitosan-based hybrid nanomaterials', *Advance in Natural Science: Nanoscience Nanotechnology*, 2, pp. 1–6. doi: 10.1088/2043-6262/2/4/045004.

Tran, T. H. and Nguyen, V. T. (2014) 'Copper Oxide Nanomaterials Prepared by Solution Methods, Some Properties, and Potential Applications: A Brief Review', *International Scholarly Research Notices*. Hindawi Publishing Corporation, 2014, pp. 1–14. doi: 10.1155/2014/856592.

Umesh, Kathad; Gajera, H. . (2014) 'Synthesis of copper nanoparticles by two different methods and size comparison', *Int J Pharm Bio Sci*, 5(1), pp. 978–982.

Usman, M. S. *et al.* (2012) 'Copper nanoparticles mediated by chitosan: Synthesis and characterization via chemical methods', *Molecules*, 17(12), pp. 14928–14936. doi:

10.3390/molecules171214928.

Valov, I. and Lu, W. D. (2016) ‘Nanoscale electrochemistry using dielectric thin films as solid electrolytes’, *Nanoscale*. The Royal Society of Chemistry, 8(29), pp. 13828–13837. doi: 10.1039/C6NR01383J.

Vaseeharan, B., Sivakamavalli, J. and Thaya, R. (2015) ‘Synthesis and characterization of chitosan-ZnO composite and its antibiofilm activity against aquatic bacteria’, *Journal of Composite Materials*, 49(2), pp. 177–184. doi: 10.1177/0021998313515289.

Velasco, J. G. (1997) ‘Determination of standard rate constants for electrochemical irreversible processes from linear sweep voltammograms’, *Electroanalysis*, 9(11), pp. 880–882. doi: 10.1002/elan.1140091116.

Wang, X. *et al.* (2005) ‘Chitosan- metal complexes as antimicrobial agent: Synthesis, characterization and Structure-activity study’, *Polymer Bulletin*, 55(1–2), pp. 105–113. doi: 10.1007/s00289-005-0414-1.

Wang, Z. L. (2004) ‘Zinc oxide nanostructures: growth, properties and applications’, *Journal of Physics: Condensed Matter*, 16(25), pp. R829–R858. doi: 10.1088/0953-8984/16/25/R01.

Wei, D. *et al.* (2009) ‘The synthesis of chitosan-based silver nanoparticles and their antibacterial activity’, *Carbohydrate Research*. Elsevier Ltd, 344(17), pp. 2375–2382. doi: 10.1016/j.carres.2009.09.001.

Wicramarachchi, P. and Hettiarachchi, M. (2011) ‘Synthesis of chitosan stabilised silver nanoparticles using gamma ray radiation and characterisation’, *Jousrnal of Scinece*, 6, pp. 65–75.

Xiliang, Q. *et al.* (2014) ‘Large-Scale Synthesis of Silver Nanoparticles by Aqueous Reduction for Low-Temperature Sintering Bonding’, 2014.

Xiong, G. *et al.* (2006) ‘Photoluminescence and FTIR study of ZnO nanoparticles: The impurity and defect perspective’, *Physica Status Solidi (C) Current Topics in Solid State Physics*, 3(10), pp. 3577–3581. doi: 10.1002/pssc.200672164.

Yukna, J. (Souther. I. U. at C. . (2014) ‘International Journal of Nano Dimension Synthesis and characterization of Copper and Copper Oxide nanoparticles by thermal decomposition method’, *Thesis paper*, 5(4), pp. 321–327.

Zhang, L., Zeng, Y. and Cheng, Z. (2016) ‘Removal of heavy metal ions using chitosan and

modified chitosan: A review', *Journal of Molecular Liquids*. Elsevier B.V., 214, pp. 175–191. doi: 10.1016/j.molliq.2015.12.013.

Zhou, E., Hashimoto, K. and Tajima, K. (2013) 'Low band gap polymers for photovoltaic device with photocurrent response wavelengths over 1000 nm', *Polymer (United Kingdom)*. Elsevier Ltd, 54(24), pp. 6501–6509. doi: 10.1016/j.polymer.2013.09.058.

CHAPTER FIVE

MODIFICATION OF WOUND GAUZES AND BACTERICIDAL EFFICACY TESTS.

5.1 Introduction

This chapter looks into the modification of the cotton wound gauzes using the chitosan composites and their bactericidal activity on *Staphylococcus aureus* and *Escherichia coli* both qualitatively and quantitatively.

Metallic nanoparticles have been applied on cotton wound gauzes by methods such as immobilization, pad-dry-cure method, thermal, radiation, and chemical treatments. The use of biocompatible polymers such as chitosan has been recently favoured for the incorporation of nanoparticles on cotton and cotton-composite wound gauzes (Sezer and Cevher, 1992). Biocompatible polymers present a less toxic risk to the body which the modified wound dressings is being administered to. Besides being a biocompatible polymer, chitosan presents other advantages that enable it to be used for modifying wound gauzes by NPs incorporation. Chitosan has the ability to form hydrogen bonds with the cellulose on the cotton gauze using its hydroxyl groups and it also forms chelates with metals using the amine group. This gives the polymer the ability to be a useful agent of incorporating metallic nanoparticles in cotton based wound gauzes (Kong *et al.*, 2010). The chitosan chelates the NPs at a pH range which is higher than 6.5, but when it comes into contact with the wound cavity, which has a pH range of 5-7 during epidermalization (Ono *et al.*, 2015), the amine group is forced to release the NPs to take up the H^+/H_3O^+ thereby releasing the NPs into the wound cavity. The release of the NPs initiates the healing and antibacterial activity of the NPs. This phenomenon makes chitosan an excellent drug delivery agent for the NPs as antibacterial agents.

Several methods of cotton wound gauze modification using biopolymers and NPs exist as *in situ* and *ex situ* options. *In situ* is when the wound gauze is modified by synthesizing the CH-NPs in the presence of the gauze. This method is time conservative but however causes the inability to control the deposition happening on the gauze and presents uncertainty on the amount of CH-NPs deposited onto the wound gauze (Gouda, 2012). *Ex situ* involves the formation of CH-NPs composite in the absence of the wound gauze and later treating the wound gauze with a known amount of the CH-NPs. *Ex situ* method is favoured where the wound gauze will be applied where both qualitative and quantitative parameters are paramount. In this research the *ex situ* method of dip-dry and cure method was used to modify the cotton wound gauzes using the CH-NPs composites.

The dip-dry-cure method is the *ex situ* procedure that is usually applied in the modification of wound gauzes. The method involves a regular piece of wound gauze material of known weight and/or length being dipped in the NPs solution or CH-NPs composite of known strength, dried and cured at a prescribed temperature (Hajipour *et al.*, 2012). Drying is done gradually at a relatively lower temperature than curing to ensure thorough expulsion of moisture yet making sure that the wound gauze is not baked rendering the modification of non-effect. Curing is done at a fairly high temperature and it is done to set permanently the composite unto the wound gauze thereby increasing the stability of the modification on the wound gauze. Both drying and curing procedures should ensure that the composite is set on the cotton wound gauze at a level of stability that will still allow its functionality as an antimicrobial agent when it comes into contact with moisture. In this research the modification of the wound gauze was done using the dip-dry and cure method.

Water retention is paramount for a wound gauze to ensure that optimum moisture levels that facilitate wound healing are maintained. An ideal wound gauze should have 17 threads of cotton per square centimetre 10 threads of the same should be able to hold 23 g of water (Guo and Dipietro, 2010). Thread count per square centimetre is an indirect measure of the porosity and water retention ability of the gauze. During the modification process the chitosan fills the space that is in between the threads thereby altering the expected ability of water holding capacity of the gauze. This usually increases the water retention of the wound gauze. Therefore, it is imperative that the water retention ability of the wound gauze is investigated to ensure that it falls within requirements.

Diverse protocols exist for the assessment of bactericidal activity and efficacy of material against specific bacteria. The assessment of the bactericidal effect of an agent is usually assessed in two steps which are susceptibility then efficacy. Bactericidal susceptibility is a qualitative test that is used to determine the ability of a potential bactericidal agent against specific bacteria (Krishna Veni, 2016). The quantitative test makes it easier to select out the agents that are not bactericidal before the next step is carried out. The next step is to determine the bactericidal effect of the agents that have shown signs of being bactericidal. This is done by carrying quantitative tests which give out the information on the relative efficacies of the agents in quantitative form. A common method is the use of the percentage reduction test where the bactericidal agents are ranked in efficacy using information obtained from their ability to reduce and eliminate bacterial growth.

AATCC test methods are universally used to assess the bactericidal efficacy of textile based bactericidal agents. The AATCC (American Association of Textile Chemists and Colourists) is an independent organisation which provides method development and quality systems and

control for the textile industry globally. The AATCC has several methods that have been developed for the assessment of different parameters of textiles which are widely adopted (Biovation, 2010). The method used to assess the bactericidal susceptibility of a textile is called the AATCC 147 Method. The objective of the method is to detect the bacteriostatic activity of textile material samples by exposing growing bacteria to the textile agent thereby by assessing the effect of the textile sample on the growth of bacteria (Raghupathi, Koodali and Manna, 2011). This test method is also referred to as the zone of inhibition detection method. The procedure is undertaken by placing the textile sample intimately with a nutrient agar surface that has been recently inoculated or streaked with the test bacterium. The plates are incubated as per bacterium requirement, and then afterwards the plates are assessed for zones of inhibition. Zones of inhibition are clear areas around or alongside the textile sample showing interrupted growth as a result of the presence of the textile sample. The clear areas around the textile sample indicate that the textile sample had a bacteriostatic effect on the bacterium. The AATCC 100 protocol is very simple and reproducible with a high degree of sensitivity (Pinho *et al.*, 2011).

However, the AATCC 147 only gives information on the textiles samples that exhibit bactericidal effects but the protocol does not give sufficient information on how effective each of the bactericidal samples are. Therefore, there is a need to carry out a further assessment that can enable us to quantitatively determine which of the bactericidal active textile samples is more effective and the level of its effectiveness. The quantitative bactericidal effects of a textile are carried out using the protocol, AATCC 100. The AATCC 100 is a protocol developed to test quantitatively the ability of a textile to effectively inhibit and kill bacteria within an 24hour incubation exposure (Street and Lake, 2014). The protocol involves exerting the textile sample to bacteria and then placing it into an agar dish. The dish is then incubated incubating according to the bacterium requirements after which colonies will be counted against an untreated textile sample control.

5.2 Experimental

5.2.1 Materials and reagents

Nutrient Agar (ThermoFisher), Nutrient Broth (ThermoFisher), *E. coli* (ATCC 6538), and *S. aureus* (ATCC 4157) was prepared by the Biotechnology Lab of Cape Peninsula University. Modified wound gauzes; CH-Ag, CH-ZnO, CH-CuO, CH-Ag-ZnO-CuO, Water for aqueous solution preparation was purified by a milli-QTM system (Millipore).

4.5.1. Modification of the wound gauze

Cotton wound gauzes were washed using deionised water to remove unwanted dust and unwanted debris. They were then dried in air at room temperature in dust proof cabinet. The cotton wound gauzes were cut into square pieces measuring 20 mm x 20 mm of average weight 0.0300g. Six pieces each were dipped in each beaker containing the CH-NPs composites for 5 minutes with stirring at 400 rpm. The pieces were individually placed on ceramic tiles for drying and were placed in a preheated oven at 80 ºC for 15 minutes. After 15mins the temperature of the oven was increased to 120 ºC and the gauzes were cured for 5 minutes. After the 5 minutes the gauzes were removed and were cooled and stored in a desiccator.

4.5.2. Water retention studies

The studies were done using the test method provided by the T-PACC (research centre for on textile comfort and protection) (Hajipour *et al.*, 2012) (Meftahi *et al.*, 2010). Square pieces measuring 20 mm x 20 mm of both the untreated gauze and the prototype wound gauze were prepared and weighed. The pieces were then fully immersed in deionised water for 20 seconds after which they were weighed again. The reduction in their weight was measured at 5 minute intervals until their weight was the same as their initial weight before wetting. The procedure was carried out 5 times and means tabulated. A student t-test was performed to test if there is a significant difference between the means of the untreated and the modified wound gauze.

5.2.2 Bacterial susceptibility tests. (AATCC 147)

Bactericidal susceptibility of the modified wound gauzes was carried out using the parallel streak method (AATCC 147). The tests were done against gram negative bacterium (*Escherichia coli*) and gram positive bacterium (*Staphylococcus aureus*). The modified wound gauzes were autoclaved for 15 minutes at 120 ºC. Fresh bacterium was grown by placing bacterium species in 5 ml of nutrient broth and then incubating for 24 hours at 37 ºC. After 24 hours the grown bacterium was inoculated at 1µl in Agar petri dishes in triplicate for each bacterium and each composite test. The wound gauze was introduced into the media by gently pressing it down into the Agar after inoculation. The petri dishes were incubated at 37 ºC for 24 hours. After this the zones of inhibition were assessed visually.

5.2.3 Percentage Reduction tests (AATCC 100)

The AATCC 100 method was used to assess the percentage reduction of the wound gauze samples (Abbasipour *et al.*, 2014). Fresh cultures were prepared as before and serially

diluted into test tubes. The test-tube with a dilution factor of 1:10000 was used to dip the two modified gauzes and the modified gauzes were placed in agar plates. The plates were incubated for 24 hours and after that the colonies in each plate were counted and used to calculate the percentage reduction. The percentage reduction was calculated using equation 5.1.

$$R\,(\%) = (B - A)x\ \frac{100}{B} \quad \text{Equation 5.1}$$

Where B is the number of colonies from plate with no wound gauze, A is the number of colonies containing sample and R is the reduction percentage. The results were tabulated a t-test was done to test whether there was a significant difference between the results of the close value samples.

5.3 Results and discussion

5.3.1 Surface characteristics of modified wound gauzes.

It can be observed that the presence of chitosan and its NPs composites significantly changes the surface characteristics of the standard cotton gauze (Figure 5.1).

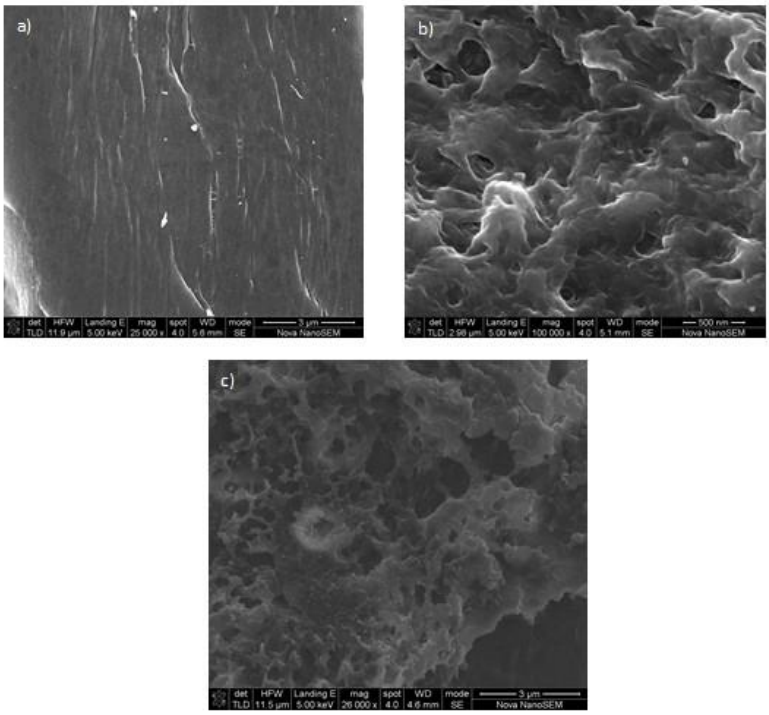

Figure 5 1. SEM images of a) untreated wound gauze b) chitosan treated wound gauze c) CH-Ag-ZnO-CuO treated wound gauze.

The SEM image of the chitosan treated wound gauze shows that the introduction of chitosan seals the narrow longitudinal crevices between the fibres of the gauze thereby increasing the surface area of gauze to wound contact. However, this decreases the porosity of the gauze thereby presenting an aeration challenge since the chitosan polymer seals the crevices in-between the woven fibres. An efficient wound dressing should be able to allow considerable aeration of the wound to facilitate the drying and sealing up of the wound (Sun and Li, 2011). The wound gauze treated with the chitosan-NPs composite, CH-Ag-ZnO-CuO, shows that there is increased surface area due to ruggedness of the wound gauze surface (Figure 5.1c). It can also be observed that there are interspatial cavities within the composite surface which can be assumed to have been caused by the nature of bonding and structure within the composite.

The nanoparticle powders disturb the normal structure of the chitosan polymer and this disturbance causing micro fractures within the composite when it is dried at high temperatures. The surface characteristic of the CH-Ag-ZnO-CuO treated wound gauze presents more benefits for its utilisation in wound healing. The surface nature of the modified wound gauze ensures increased surface area for gauze to wound contact and the interspatial cavities allow considerable aeration of the wound. Therefore, the modification of the wound gauze is able to maintain utility properties and also enhance its functionality.

5.3.2 Water retention tests

Table 5. 1 Mean drying times of gauze samples.

Sample	Average drying time (minutes)
Untreated wound gauze	37±3
Modified wound gauze	57±3
Percentage difference in drying time between untreated and modified.	65%

During the water retention tests it was observed that the modified wound gauze did not readily absorb water but it only started to soak in water after a while compared to the untreated wound gauze. This can be explained by the partial hydrophobic nature of the chitosan within the modifying composite. After the gauze was wet, its rate of water loss was lesser compared to the untreated wound gauze. This is due to the hydrogen bonding that

exists between the amine group of the chitosan and the water molecules. Five tests were conducted for each gauze and the means were reported. Overall, the modified wound gauze had 65% better water retention properties than the untreated wound gauze as displayed in Table 5.1.

A one-tailed student t-test at the 95% confidence interval was performed to test if drying time of the modified gauze is statistically greater than of the untreated gauze.

H_0:$\mu_{untreated} < \mu_{modified}$

H_1: $\mu_{untreated} = \mu_{modified}$

Reject H_0 if $p_{value} < 0.05$

The spreadsheet-calculated p_{value} was found to be 0.000758. Since $p_{value} < 0.05$ we therefore reject H_0 and conclude that drying mean drying time of the modified wound gauze is greater than the one for the untreated one. This means besides the bactericidal potential the modified gauze possesses, the modified wound gauze also presents an added advantage of better water retention. Moisture retention offered by wound gauze is paramount in the healing course of a wound (Meftahi *et al.*, 2010). This indicates that the modification of the wound gauze did not only maintain the utility properties of conventional wound gauze but rather enhanced its utility properties.

5.3.3 Bacterial susceptibility tests

5.3.3.1 Activity against *S. aureus*

The bacteria species showed varied response to the different type of modified wound gauzes. The first step of the bacterial susceptibility was to determine which modified gauzes were bactericidal active against the different species at the concentration of 0.5 mM of the NPs in the CH-NPs composites. The response of *S.aureus* to the composites was observed with most composites showing a certain level of response. The media with the untreated wound gauze showed no bactericidal activity at all (Figure 5.1c). Figure 5.2 shows that the order of bacterial inhibition strength was CH-Ag-ZnO-CuO > CH-Ag > CH-CuO = CH-ZnO in order of decreasing strength left to right. The response of the CH-CuO and CH-ZnO modified gauzes showed similar inhibition behaviour due to the fact that their effect covered the whole petri dish but eventually some bacteria grew in an area close to the wound gauze.

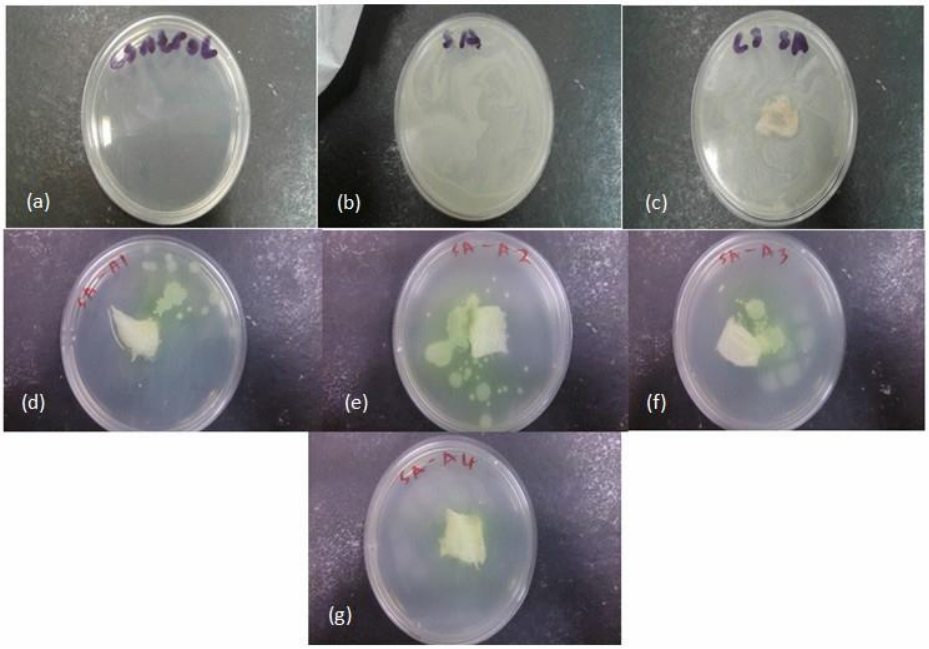

Figure 5. 1. Bacterial susceptibility response of S.aureus to modified wound gauzes a) control b) blank (no gauze) c) untreated wound gauze d) CH-Ag e) CH-ZnO f) CH-CuO and g) CH-Ag-ZnO-CuO

The inhibitory work of CH-ZnO is known to be affected by the pH of the media that it is operating in (Vaseeharan, Sivakamavalli and Thaya, 2015). The composite is also sensitive to the percentage of the amine groups ($-NH_2$) that are exposed on the chitosan surface (Malinowska-Pańczyk *et al.*, 2009). These make the CH-ZnO relatively less effective in bactericidal effects compared to the other modified gauze composites. Among the three individual composites of the NPs, the CH-Ag modified wound gauze was found to attain the highest inhibition coverage of 85%. Ag NPs generally have elevated bactericidal efficacies compared to other nanoparticles due to its immunity to multi-drug resistant bacteria mechanisms (Cavassin *et al.*, 2015). The mechanism of the bactericidal activity has not been fully elaborated though it is suggested that Ag NPs operates by targeting ribosomal DNA, cytoplasmic cavity and the peptidoglycan wall of the bacterium species(Ma *et al.*, 2011). This distinct target mechanism gives it an added advantage in comparison with the other NPs. It can also be noted that the CH-Ag composite had higher efficacies compared to CuO NPs and ZnO NPs against *S.aureus* owing to Ag NPs' ability disrupt the DNA replication pathway within the bacterium nucleus (Hajipour, Fromm and Ashkarran, 2012).

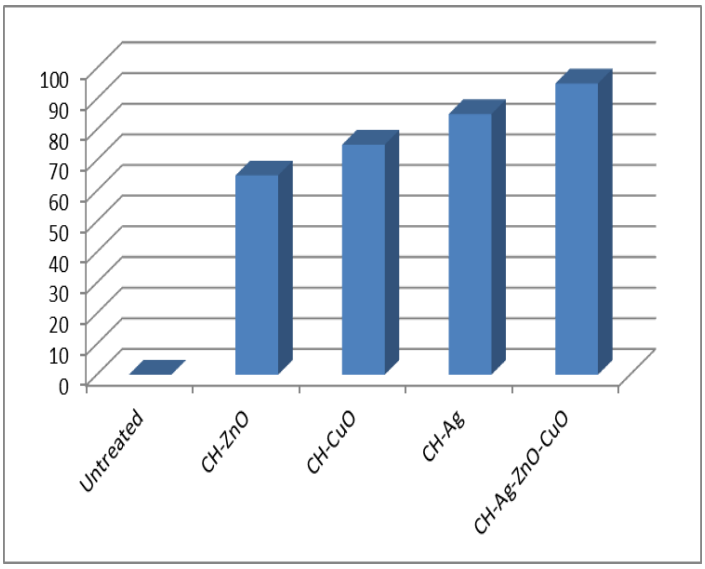

Figure 5. 2. Inhibition effect (%) of modified wound gauzes on *S.aureus*.

The prototype composite, CH-Ag-CuO-ZnO, modified wound gauze had an inhibition cover rate of about 95% against *S.aureus* as shown in Figure 5.2. The whole petri dish was clear except for under the gauze where there was slight colonisation of about 4 colony units. Due to the novelty of the composite there is not much literature to elaborate of the reason of high efficacy though it can be assumed that the high efficacy is attributed to the synergetic effects of the components within the composite. A similar study of the bactericidal efficacy of a CH-ZnO-Ag modified wound gauze displayed similar results against *S.aureus* and *E.coli* (Hajipour *et al.*, 2012).

5.3.3.2 Activity against *E.coli.*

All composites had inhibitory effects against the bacterium *E.coli* as seen in Figure 5.3 where visible clear regions of inhibition which are absent in the petri dish containing an untreated wound gauze can be seen. In comparison of the inhibition areas it can be noted that *S.aureus* exhibited a better response to the bactericidal activity of the composites than E.coli. For the individual composites, CH-ZnO was found to exhibit better inhibition activity than the other composites.

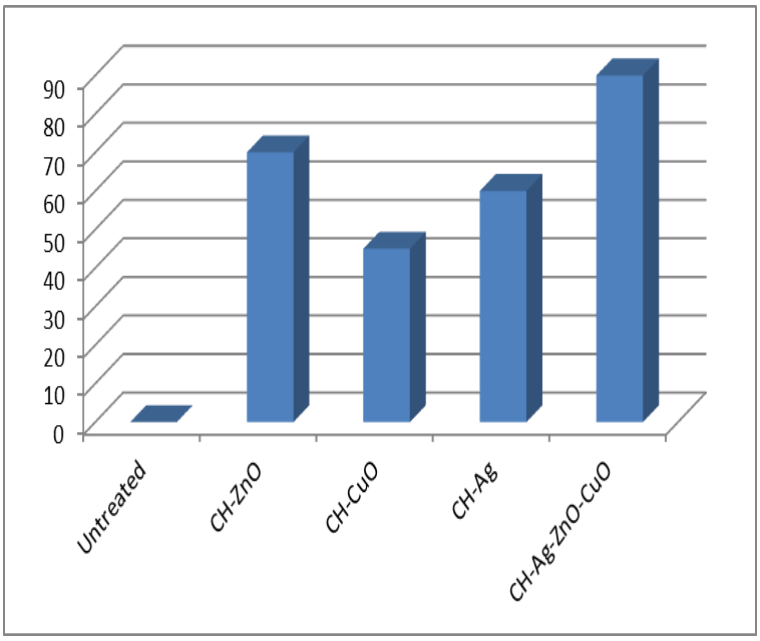

Figure 5. 3. Inhibition effect (%) of modified gauzes on *E.coli.*

CH-ZnO studies show that the composite has increased bactericidal effects on gram negative bacteria like *E.coli* when the amount of ZnO NPs in the composite is elevated (Wang, 2004; Vaseeharan, Sivakamavalli and Thaya, 2015). In this research the dosage of all the NPs in the indicvidual composites and in the prototype composite was 0.5mM and it falls within the concetration of opitmum CH-ZnO activity of 40-70-mgL^{-1}. The proptotype composite,CH-Ag-ZnO-CuO, exhibited 90% inhibition coverage throughout the plate with only the edges of the media having wall adjacent growing colonies of the bacterium. This again can be contributed to the synergetice effects of the various components within the prototype composite

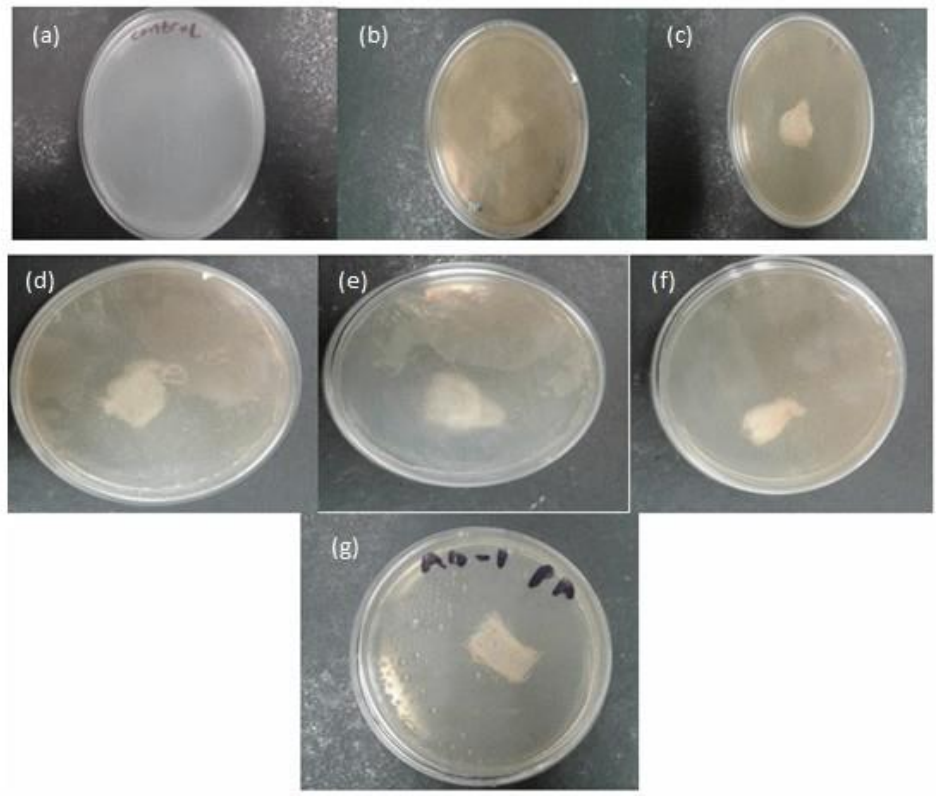

Figure 5. 4. Bacterial susceptibility response of E.coli to modified wound gauzes a) Control b) no gauze c) untreated wound gauze d) CH-Ag e) CH-ZnO f) CH-CuO g) CH-Ag-ZnO-CuO

5.3.4 Percentage reduction tests

The percentage reduction studies were undertaken using the prototype in comparison with the CH-Ag composite on both species of bacteria. Both bacterium species responded to the bactericidal activity of the composites with the response to the prototype being much greater (Figure 5.5). For the percentage reduction test the CH-Ag composite had a dosage of 54 mg L^{-1} and the prototype composite had dosages as follows: ZnO; 41 mg L^{-1}, CuO; 40 mg L^{-1} and Ag; 54 mg L^{-1}. During the percentage reduction investigations it can be seen that the CH-Ag modified gauze continued to exhibit greater bactericidal activity towards *S.aureus* than *E.coli* (Table 5.1).

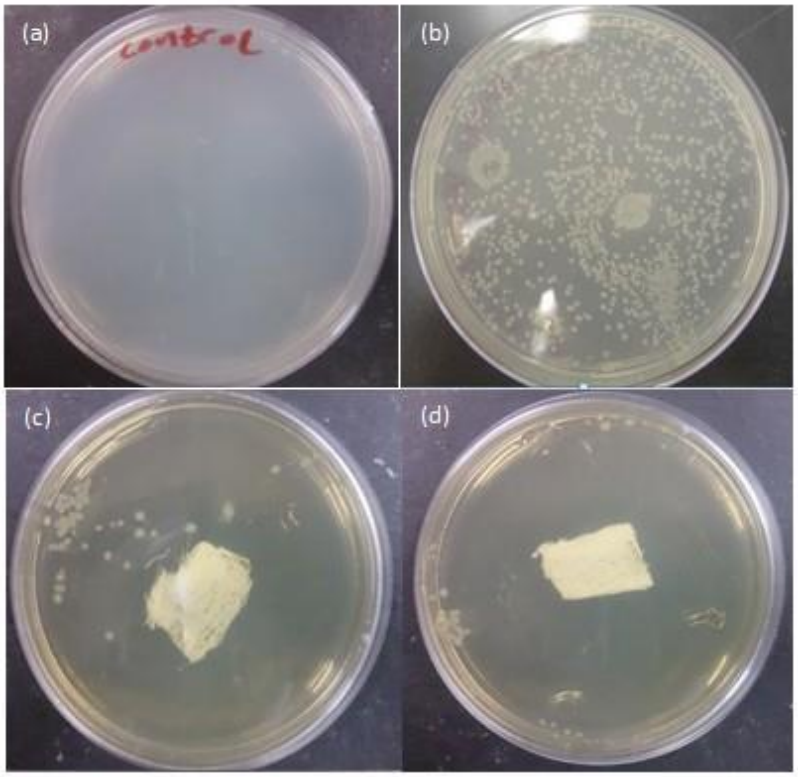

Figure 5. 5 Percentage reduction test for S.aureus a) Control b) E.coli only c) CH-Ag treated gauze d) CH-Ag-ZnO-CuO treated gauze.

CH-Ag composite is usually known to exhibit identical effect against both gram positive and gram negative bacteria under the same conditions (Cavassin *et al.*, 2015). However studies show that if biofilms, which are responsible for the drug resistance capabilities of the bacterium, form before the NPs are active, the bactericidal efficacy of the NPs is reduced (Hajipour, Fromm and Ashkarran, 2012). In this research it can be assumed that during the first inoculation it is possible that the bacterium had formed biofilms around them before they came into contact with the NPs. The exceptional efficacy of the CH-Ag composite can be attributed to the fact that during TEM characterisation of NPs in this research (Chapter 3) ,Ag NPs was found to have the smallest size and also an even size distribution that is coupled by a smaller size standard deviation. NPs of smaller size exhibit elevated of efficacy in their bactericidal activity due to their ability to evade regions of electrostatic repulsion and also the ability to penetrate through the bacterium walls (Gogoi *et al.*, 2006). The band gap energy of the Ag NPs component in both the CH-Ag and CH-Ag-ZnO-CuO composites was the highest therefore it confirming that the bactericidal activity of NPs is influenced by the band gap energy of the NPs.

Table 5. 2. Percentage reduction of bacteria by modified wound gauzes.

Gauze modification composite	No. of *S.aureus* Colonies	Reduction (%)	No. of *E.coli* colonies	Reduction (%)
Untreated	1000>	0	1000>	0
CH-Ag	66	93.4	143	86
CH-Ag-ZnO-CuO	31	96	13	99

The prototype composite which was the scope of this study proved to be effective against both gram positive and gram negative bacteria. The efficacy exhibited by the prototype composite is attributed to the co-operate action by all the nanoparticles present within the composites. All the CH-NPs composites exhibited inhibitory activity during the bactericidal susceptibility test indicating that the all the components were active in the CH-Ag-CuO-ZnO composite though at different efficacy levels. It is however important to note that the Ag NPs could have been a big contributor to the bactericidal activity since in the individual CH-NPs composites it exhibited higher efficacy levels that were only marginally lower than that of the prototype composite. It is therefore valid to suggest that the prototype composite can still remain effective against the specific test bacteria even if the concentration of the CuO and ZnO NPs were lowered to a certain optimum degree since the Ag NPs are the biggest player in the composite. A study of a wound gauze modified using CH-Ag-ZnO produced similar results against the same gram positive and gram negative bacteria (Hajipour, Fromm, Akbar Ashkarran, et al. 2012).

5.4 Conclusion

The cotton wound gauzes were successfully modified using the various composites and the composites adhered fully to the wound gauze. The wound gauze showed remarkable and significant increase in water retention abilities. The student t-test proved that the water retention property of the modified wound gauze was greater than the unmodified wound gauze.

The bactericidal susceptibility of the modified wound gauzes was successfully carried out against the gram positive and gram negative bacteria. All modified wound gauzes showed bactericidal behaviour against the bacterium species showing evident zones of inhibition. The range of inhibition efficacy for all composites was between 50 and 96%. Among the individual composites used to modify the wound gauzes, CH-Ag was found to be the most effective. The CH-Ag-ZnO-CuO modified gauze exhibited remarkable inhibition and percentage reduction efficacies. The gauze managed to reduce bacterial viability by 96% and 99% for *S.aureus* and *E.coli* respectively.

The wound gauze modified by the CH-Ag-ZnO-CuO showed elevated bactericidal efficacy against common wound bacteria *S.aureus* and *E.coli*.

5.5 References

Abbasipour, M. *et al.* (2014) 'Coated Cotton Gauze with Ag/ZnO/chitosan Nanocomposite as a Modern Wound Dressing', *Journal of Engineered Fibers and Fabrics*, 9(1), pp. 124–130.

AbdElhady, M. M. (2012) 'Preparation and Characterization of Chitosan/Zinc Oxide Nanoparticles for Imparting Antimicrobial and UV Protection to Cotton Fabric', *International Journal of Carbohydrate Chemistry*, 2012, pp. 1–6. doi: 10.1155/2012/840591.

Abiraman, T. *et al.* (2016) 'Antifouling behavior of chitosan adorned zinc oxide nanorods', *RSC Adv.* Royal Society of Chemistry, 6(73), pp. 69206–69217. doi: 10.1039/C6RA13321E.

Ahmed, S. and Ikram, S. (2016) 'Chitosan Based Scaffolds and Their Applications in Wound Healing', *Achievements in the Life Sciences*. Far Eastern Federal University, 10(1), pp. 27–37. doi: 10.1016/j.als.2016.04.001.

Alagumuthu, G. and Kumar, T. A. (2013) 'Synthesis and Characterization of Chitosan / TiO 2 Nanocomposites Using Liquid Phase Deposition Technique', 4(1), pp. 105–111.

Algawi, S. D. A. L. (no date) 'Copper Oxide Nanostructures ; Syntheses and Characterization', 71, pp. 0–4.

Ali, S. W., Rajendran, S. and Joshi, M. (2011) 'Synthesis and characterization of chitosan and silver loaded chitosan nanoparticles for bioactive polyester', *Carbohydrate Polymers*. Elsevier Ltd., 83(2), pp. 438–446. doi: 10.1016/j.carbpol.2010.08.004.

Alvarez, P. J. J. and Lowry, G. (2009) 'Nanomaterials with Antimicrobial Properties : Mechanisms , Implications and Applications pp I i'.

Applerot, G. *et al.* (2012) ‘Understanding the antibacterial mechanism of CuO nanoparticles: Revealing the route of induced oxidative stress’, *Small*, 8(21), pp. 3326–3337. doi: 10.1002/smll.201200772.

Arefi, M. R. and Rezaei-Zarchi, S. (2012) ‘Synthesis of zinc oxide nanoparticles and their effect on the compressive strength and setting time of self-compacted concrete paste as cementitious composites’, *International Journal of Molecular Sciences*, 13(4), pp. 4340–4350. doi: 10.3390/ijms13044340.

Atiyeh, B. S. *et al.* (2007) ‘Effect of silver on burn wound infection control and healing: Review of the literature’, *Burns*, 33(2), pp. 139–148. doi: 10.1016/j.burns.2006.06.010.

Azuma, K. *et al.* (2015) *Chitin, Chitosan, and Its Derivatives for Wound Healing: Old and New Materials*, *Journal of Functional Biomaterials*. doi: 10.3390/jfb6010104.

Babu, V. S. (2010) *Solid State Devices and Technology*. 3rd edn, *Solid states devices and technology.* 3rd edn. Mumbai: Pearson.

Bagabas, A. *et al.* (2013) ‘Room-temperature synthesis of zinc oxide nanoparticles in different media and their application in cyanide photodegradation’, *Nanoscale Research Letters*, 8(1), p. 516. doi: 10.1186/1556-276X-8-516.

Balamurugan, B. and Mehta, B. R. (2001) ‘Optical and structural properties of nanocrystalline copper oxide thin films prepared by activated reactive evaporation’, *Thin Solid Films*, 396(1–2), pp. 90–96. doi: 10.1016/S0040-6090(01)01216-0.

Balu, S. S. and Bhakat, C. (2012) ‘SYNTHESIS OF SILVER NANOPARTICLES BY CHEMICAL REDUCTION AND THEIR ANTIMICROBIAL ACTIVITY Materials and Methods ’:, 1(6), pp. 1–5.

Bard, A. J. *et al.* (1944) *ELECTROCHEMICAL METHODS Fundamentals and Applications*, *Electrochemistry. I. Faulkner, Larry R*. doi: 10.1016/B978-0-12-381373-2.00056-9.

Benavente, M. (2008) *Adsorption of metallic ions onto chitosan: equilibrium and kinetic studies*. doi: 976–988.

Beyth, N. *et al.* (2015) ‘Alternative Antimicrobial Approach: Nano-Antimicrobial Materials’, *Evidence-Based Complementary and Alternative Medicine*, 2015, pp. 1–16. doi: 10.1155/2015/246012.

Biovation, L. (2010) *Testing for Antimicrobial Activity in Textiles.* Boothbay.

Bonnemann, H. and Richards, R. M. (2001) 'Nanoscopic metal particles - synthetic methods and potential applications', *Eur. J. Inorg. Chem.*, pp. 2455–2480. doi: 10.1002/1099-0682(200109)2001:10<2455::AID-EJIC2455>3.0.CO;2-Z.

Brintha, S. R. and Ajitha, M. (2015) 'Synthesis and characterization of ZnO nanoparticles via aqueous solution, sol-gel and hydrothermal methods', *IOSR Journal of Applied Chemistry*, 8(11), pp. 66–72. doi: 10.9790/5736-081116672.

Brown, J. H. (2015) 'Development and Use of a Cyclic Voltammetry Simulator To Introduce Undergraduate Students to Electrochemical Simulations', *Journal of Chemical Education*. American Chemical Society, 92(9), pp. 1490–1496. doi: 10.1021/acs.jchemed.5b00225.

Brown, K. and Gray, S. B. (2010) 'Cyclic Voltammetric Studies of Electropolymerized Films Based on Ruthenium (II/III) Bis (1, 10phenanthroline)(4-methyl-4'vinyl-2, 2'-bipyridine).', *International Journal of Chemistry*, 2(2), pp. 3–9. Available at: http://search.ebscohost.com/login.aspx?direct=true&profile=ehost&scope=site&authtype=crawler&jrnl=19169698&AN=52739860&h=s7r8gpPlt9tlQXU1DwQKvth6GpoG/uSIl9+y7buDKd4ozaZ6T7n2jMZlVbnZRzIKzPwKahBTG9vQKJVjeYgNcA==&crl=c.

Brownson, D. A. C. and Banks, C. E. (2014) *The Handbook of Graphene Electrochemistry*, *The Handbook of Graphene Electrochemistry*. doi: 10.1007/978-1-4471-6428-9.

Brugnerotto, J. *et al.* (2001) 'An infrared investigation in relation with chitin and chitosan characterization', *Polymer*, 42(8), pp. 3569–3580. doi: 10.1016/S0032-3861(00)00713-8.

Budhiraja, N. *et al.* (2013) 'Synthesis and Optical Characteristics of Silver Nanoparticles on Different Substrates', *International Letters of Chemistry, Physics and Astronomy*, 19, pp. 80–88. doi: 10.18052/www.scipress.com/ILCPA.19.80.

Calvo, E. J. and Wolosiuk, A. (2002) 'Donnan permselectivity in layer-by-layer self-assembled redox polyelectrolye thin films', *Journal of the American Chemical Society*, 124(28), pp. 8490–8497. doi: 10.1021/ja020107h.

Cavassin, E. D. *et al.* (2015) 'Comparison of methods to detect the in vitro activity of silver nanoparticles (AgNP) against multidrug resistant bacteria', *Journal of Nanobiotechnology*. BioMed Central, 13(1). doi: 10.1186/s12951-015-0120-6.

Dai, T. *et al.* (2011) *NIH Public Access*, *Expert Rev Anti Infect Ther*. doi: 10.1586/eri.11.59.Chitosan.

Dash, M. *et al.* (2011) ‘Chitosan - A versatile semi-synthetic polymer in biomedical applications’, *Progress in Polymer Science (Oxford)*. Elsevier Ltd, 36(8), pp. 981–1014. doi: 10.1016/j.progpolymsci.2011.02.001.

Davis, J. and McLister, A. (2016) ‘Chapter Four - Passive and Interactive Dressing Materials’, in Davis, J. et al. (eds) *Smart Bandage Technologies*. Academic Press, pp. 93–144. doi: https://doi.org/10.1016/B978-0-12-803762-1.00004-7.

Debanath, M. K. and Karmakar, S. (2013) ‘Study of blueshift of optical band gap in zinc oxide (ZnO) nanoparticles prepared by low-temperature wet chemical method’, *Materials Letters*. Elsevier, 111, pp. 116–119. doi: 10.1016/j.matlet.2013.08.069.

Dehaghi, S. M. *et al.* (2014) ‘Removal of permethrin pesticide from water by chitosan–zinc oxide nanoparticles composite as an adsorbent’, *Journal of Saudi Chemical Society*, 18(4), pp. 348–355. doi: https://doi.org/10.1016/j.jscs.2014.01.004.

Devi, H. S. and Singh, T. D. (2014) ‘Synthesis of Copper Oxide Nanoparticles by a Novel Method and its Application in the Degradation of Methyl Orange’, *Advance in Electronic and Electric Engineering*, 4(1), pp. 83–88.

Douglas Skoog, James Holler, S. C. (2007) ‘Principles of instrumental analysis.’, in Harris, D. (ed.) *Principles of instrumental analysis.* 6th edn. Belmont: Brooks/Cole, p. 371.

Durga Praveena, V. and Vijaya Kumar, K. (2013) ‘Synthesis and Characterization of Chitosan based Silver Nano Composite System for Antibacterial Applications’, *Proceedings of the International Conference on Advanced Nanomaterials & Emerging Engineering Technologies*, pp. 76–79.

Faiz, U. *et al.* (2011) ‘Efficacy of zinc as an antibacterial agent against enteric bacterial pathogens.’, *Journal of Ayub Medical College*, 23(2), pp. 18–21.

Feng, Q. L. *et al.* (2000) ‘A mechanistic study of the antibacterial effect of silver ions on <I>Escherichia coli</I> and <I>Staphylococcus aureus</I>’, *Journal of Biomedical Materials Research*, pp. 662–668. doi: 10.1002/1097-4636(20001215)52:4<662::aid-jbm10>3.0.co;2-3.

Fielicke, A., Rabin, I. and Meijer, G. (2006) ‘Far-infrared spectroscopy of small neutral silver clusters’, *Journal of Physical Chemistry A*, 110(26), pp. 8060–8063. doi: 10.1021/jp062095i.

Fievet, P. (2015) ‘Donnan Potential BT - Encyclopedia of Membranes’, in Drioli, E. and Giorno, L. (eds). Berlin, Heidelberg: Springer Berlin Heidelberg, pp. 1–3. doi: 10.1007/978-3-

642-40872-4_1716-1.

Franci, G. *et al.* (2015) ‘Silver nanoparticles as potential antibacterial agents’, *Molecules*, 20(5), pp. 8856–8874. doi: 10.3390/molecules20058856.

Gliga, A. R. *et al.* (2014) ‘Size-dependent cytotoxicity of silver nanoparticles in human lung cells: the role of cellular uptake, agglomeration and Ag release’, *Particle and Fibre Toxicology*, 11(1), p. 11. doi: 10.1186/1743-8977-11-11.

Gogoi, S. K. *et al.* (2006) ‘Green fluorescent protein-expressing Escherichia coli as a model system for investigating the antimicrobial activities of silver nanoparticles’, *Langmuir*, 22(22), pp. 9322–9328. doi: 10.1021/la060661v.

Gouda, M. (2012) ‘Nano-zirconium oxide and nano-silver oxide/cotton gauze fabrics for antimicrobial and wound healing acceleration’, *Journal of Industrial Textiles*, 41(3), pp. 222–240. doi: 10.1177/1528083711414960.

Goy, R. C., Britto, D. de and Assis, O. B. G. (2009) ‘A review of the antimicrobial activity of chitosan’, *Polímeros*, 19(3), pp. 241–247. doi: 10.1093/jac/dkg286.

Guidelli, R. *et al.* (2014) ‘Defining the transfer coefficient in electrochemistry: An assessment (IUPAC Technical Report)’, *Pure and Applied Chemistry*, 86(2), pp. 245–258. doi: 10.1515/pac-2014-5026.

Gunalan, S., Sivaraj, R. and Rajendran, V. (2012) ‘Green synthesized ZnO nanoparticles against bacterial and fungal pathogens’, *Progress in Natural Science: Materials International*. Elsevier, 22(6), pp. 693–700. doi: 10.1016/j.pnsc.2012.11.015.

Guo, S. and Dipietro, L. A. (2010) ‘Factors Affecting Wound Healing’, *Obstetrics & Gynecology*, (Mc 859), pp. 219–229. doi: 10.1177/0022034509359125.

Haghighat, S. and Dawlaty, J. M. (2016) ‘pH Dependence of the Electron-Transfer Coefficient: Comparing a Model to Experiment for Hydrogen Evolution Reaction’, *Journal of Physical Chemistry C*, 120(50), pp. 28489–28496. doi: 10.1021/acs.jpcc.6b10602.

Hajipour, M. J. *et al.* (2012) ‘Coated Cotton Gauze with Ag/ZnO/chitosan Nanocomposite as a Modern Wound Dressing’, *Journal of Industrial Textiles*. Elsevier Ltd, 9(6), pp. 143–154. doi: 10.1155/2015/246012.

Hajipour, M. J., Fromm, K. M. and Ashkarran, A. (2012) ‘Antibacterial properties of nanoparticles’, *Trends in Biotechnology*. Elsevier Ltd, 30(10), pp. 499–511. doi:

10.1016/j.tibtech.2012.06.004.

Huh, A. J. and Kwon, Y. J. (2011) '"Nanoantibiotics": A new paradigm for treating infectious diseases using nanomaterials in the antibiotics resistant era', *Journal of Controlled Release*. Elsevier B.V., 156(2), pp. 128–145. doi: 10.1016/j.jconrel.2011.07.002.

I. Markova-Deneva (2010) 'Infrared Spectroscopy Investigation of Metallic Nanoparticles Based on Copper, Cobalt, and Nickel Synthesized Through Borohydride Reduction Method', *Journal of the University of Chemical Technology and Metallurgy*, 45(4), pp. 351–378.

Ijaz, F. *et al.* (2017) 'Green synthesis of copper oxide nanoparticles using abutilon indicum leaf extract: Antimicrobial, antioxidant and photocatalytic dye degradation activities', *Tropical Journal of Pharmaceutical Research*, 16(4), pp. 743–753. doi: 10.4314/tjpr.v16i4.2.

ISO (2007) 'ISO 21348 Definitions of Solar Irradiance Spectral Categories', *Environment*, (section 5), pp. 6–7.

Jain, K. K. (2007) 'Applications of nanobiotechnology in clinical diagnostics', *Clinical Chemistry*, 53(11), pp. 2002–2009. doi: 10.1373/clinchem.2007.090795.

Jemimah, V. H. and Arulpandi, I. (2014) 'Evaluation of Antimicrobial Property of Biosynthesized Zinc Oxide Nanoparticles (ZnO NPs) and its Application on Baby Diapers', 6(2), pp. 113–119.

Jin, T. *et al.* (2009) 'Antimicrobial efficacy of zinc oxide quantum dots against Listeria monocytogenes, Salmonella Enteritidis, and Escherichia coli O157:H7', *Journal of Food Science*, 74(1). doi: 10.1111/j.1750-3841.2008.01013.x.

John Kotz, Paul Treichel, J. T. (2009) *Chemistry and chemical reactivity .* 2nd edn, *Chemistry and chemical reactivity .* 2nd edn. Edited by Lisa Lockwood. Belmont: Brooks/Cole.

Joseph Wang (2006) *Analytical Electrochemistry*. 3rd edn. New Jersey: John Wiley and Sons.

Jyoti, K., Baunthiyal, M. and Singh, A. (2016) 'Characterization of silver nanoparticles synthesized using Urtica dioica Linn. leaves and their synergistic effects with antibiotics', *Journal of Radiation Research and Applied Sciences*. Elsevier Ltd, 9(3), pp. 217–227. doi: 10.1016/j.jrras.2015.10.002.

Kalimuthu, K. *et al.* (2008) 'Biosynthesis of silver nanocrystals by Bacillus licheniformis', *Colloids and Surfaces B: Biointerfaces*, 65(1), pp. 150–153. doi:

https://doi.org/10.1016/j.colsurfb.2008.02.018.

Kang, X. *et al.* (2009) 'Glucose Oxidase-graphene-chitosan modified electrode for direct electrochemistry and glucose sensing', *Biosensors and Bioelectronics*, 25(4), pp. 901–905. doi: 10.1016/j.bios.2009.09.004.

Karim-Nezhad, G. *et al.* (2009) *Kinetic Study of Electrocatalytic Oxidation of Carbohydrates on Cobalt Hydroxide Modified Glassy Carbon Electrode*, *J. Braz. Chem. Soc.* doi: 10.1590/S0103-50532009000100022.

Kayani, Z. N. *et al.* (2012) 'Synthesis and characterization of CuO nanowires by a simple wet chemical method', *International Letters of Chemistry, Physics and Astronomy*. Springer Open Ltd, 14(1), pp. 26–36. doi: 10.1186/1556-276X-7-70.

Kayani, Z. N. *et al.* (2015) 'Characterization of Copper Oxide Nanoparticles Fabricated by the Sol???Gel Method', *Journal of Electronic Materials*, 44(10), pp. 3704–3709. doi: 10.1007/s11664-015-3867-5.

Khatoon, N. *et al.* (2015) 'Biosynthesis, Characterization, and Antifungal Activity of the Silver Nanoparticles Against Pathogenic Candida species', *BioNanoScience*, 5(2), pp. 65–74. doi: 10.1007/s12668-015-0163-z.

Khorsand Zak, A. *et al.* (2011) 'Synthesis and characterization of a narrow size distribution of zinc oxide nanoparticles', *International Journal of Nanomedicine*, 6(1), pp. 1399–1403. doi: 10.2147/IJN.S19693.

Kong, M. *et al.* (2010) 'Antimicrobial properties of chitosan and mode of action: A state of the art review', *International Journal of Food Microbiology*. Elsevier B.V., 144(1), pp. 51–63. doi: 10.1016/j.ijfoodmicro.2010.09.012.

Krishna Veni (2016) 'Anti-Bacterial Coating of Chrysanthemum Extract on Bamboo Fabric for Healthcare Applications', *Journal of Textile Science & Engineering*, 6(4), pp. 6–8. doi: 10.4172/2165-8064.1000267.

Krishnamoorthy, K. and Kim, S. J. (2013) 'Growth, characterization and electrochemical properties of hierarchical CuO nanostructures for supercapacitor applications', *Materials Research Bulletin*. Elsevier Ltd, 48(9), pp. 3136–3139. doi: 10.1016/j.materresbull.2013.04.082.

Kumar, H. and Rani, R. (2013) 'Structural Characterization of Silver Nanoparticles

Synthesized by Micro emulsion Route', *International Journal of Engineering and Innovative Technology*, 3(3), pp. 344–348.

Kurien, S. (2005) 'Chapter 4: ANALYSIS OF FTIR SPECTRA OF NANOPARTICLES of MgAl2O4, SrAl2O4, and NiAl2O4', 1595, pp. 64–78. Available at: http://mgutheses.in/page/?q=T 1354&search=siby+kurien&page=1&rad=sc.

Laurent, D. and Schlenoff, J. B. (1997) 'Multilayer Assemblies of Redox Polyelectrolytes', *Langmuir*, 13(6), pp. 1552–1557. doi: 10.1021/la960959t.

Laviron, E. (1979) 'General expression of the linear potential sweep voltammogram in the case of diffusionless electrochemical systems', *Journal of Electroanalytical Chemistry and Interfacial Electrochemistry*, 101(1), pp. 19–28. doi: https://doi.org/10.1016/S0022-0728(79)80075-3.

Laviron, E. (1979) 'General expression of the linear potential sweep voltammogram in the case of diffusionless electrochemical systems', *Journal of Electroanalytical Chemistry*, 101(1), pp. 19–28. doi: 10.1016/S0022-0728(79)80075-3.

Laviron, E. (1995) 'The use of polarography and cyclic voltammetry for the study of redox systems with adsorption of the reactants. Heterogeneous vs. surface path', *Journal of Electroanalytical Chemistry*, 382(1–2), pp. 111–127. doi: 10.1016/0022-0728(94)03684-U.

Lionelli, G. T. and Lawrence, W. T. (2003) 'Wound dressings', *Surgical Clinics of North America*, pp. 617–638.

Liu, B. *et al.* (2013) 'Adsorption of heavy metal ions, dyes and proteins by chitosan composites and derivatives --- A review', *Journal of Ocean University of China*, 12(3), pp. 500–508. doi: 10.1007/s11802-013-2113-0.

Logothetidis, S. (2012) *Nanotechnology : Principles and Applications*. doi: 10.1007/978-3-642-22227-6.

Long, J. *et al.* (2016) 'A new class of nanocomposites of Zn–Al–Bi layered double oxides: large reversible capacity and better cycle performance for alkaline secondary batteries', *RSC Adv.* Royal Society of Chemistry, 6(95), pp. 92896–92904. doi: 10.1039/C6RA18164C.

Lović, J. (2017) 'Glucose Sensing Using Glucose Oxidase-Glutaraldehyde- Cysteine Modified Gold Electrode', *International Journal of Electrochemical Science*, (July), pp. 5806–5817. doi: 10.20964/2017.07.65.

Luna, I. Z. *et al.* (2015) ‘Preparation and Characterization of Copper Oxide Nanoparticles Synthesized via Chemical Precipitation Method’, *OALib*, 2(3), pp. 1–8. doi: 10.4236/oalib.1101409.

Ma, A. *et al.* (2011) ‘Evaluation of antibacterial activity of silver nanoparticles against MSSA and MRSA on isolates from skin infections’, *Research Article Biology and Medicine*, 3(2), pp. 141–146.

Malinowska-Pańczyk, E. *et al.* (2009) ‘The combined effect of moderate pressure and chitosan on Escherichia coli and Staphylococcus aureus cells suspended in a buffer and on natural microflora of apple juice and minced pork’, *Food Technology and Biotechnology*, 47(2), pp. 202–209.

Maneerung, T., Tokura, S. and Rujiravanit, R. (2008) ‘Impregnation of silver nanoparticles into bacterial cellulose for antimicrobial wound dressing’, *Carbohydrate Polymers*, 72(1), pp. 43–51. doi: 10.1016/j.carbpol.2007.07.025.

Mansoori, G. A. (2005) ‘Principles of Nanotechnology: Molecular Based Study of Condensed Matter in Small Systems’. doi: 10.1142/5749.

Mazloum-ardakani, M. *et al.* (2010) ‘Voltammetric Determination of Dopamine at the Surface of TiO 2 Nanoparticles Modified Carbon Paste Electrode’, 5, pp. 147–157.

Meftahi, A. *et al.* (2010) *The effects of cotton gauze coating with microbial cellulose*, *Cellulose*. doi: 10.1007/s10570-009-9377-y.

Mehta, B. K., Chhajlani, M. and Shrivastava, D. (2017) ‘Green synthesis of silver nanoparticles and their characterization by XRD’, *Frontiers of Physics and Plasma Science IOP Publishing IOP Conf. Series: Journal of Physics: Conf. Series*, 836. doi: 10.1088/1742-6596/836/1/012050.

Mohammad, F., A. Al-Lohedan, H. and N. Al-Haque, H. (2016) ‘Chitosan-mediated fabrication of metal nanocomposites for enhanced biomedical applicationsf’, *Advanced Materials Letters*, 8(2), pp. 89–100. doi: 10.5185/amlett.2017.6925.

Mohan, A. C. and Renjanadevi, B. (2016) ‘Preparation of Zinc Oxide Nanoparticles and its Characterization Using Scanning Electron Microscopy (SEM) and X-Ray Diffraction(XRD)’, *Procedia Technology*. Elsevier B.V., 24, pp. 761–766. doi: 10.1016/j.protcy.2016.05.078.

Muthukrishnan, A. M. (2015) ‘Green Synthesis of Copper-Chitosan Nanoparticles and Study

of its Antibacterial Activity', *Journal of Nanomedicine & Nanotechnology*, 6(1), pp. 1–6. doi: 10.4172/2157-7439.1000251.

Muzzarelli, R. (1973) *Natural chelating polymers; alginic acid, chitin, and chitosan*. 1st edn. Oxford: Pergamon press.

Muzzarelli, R. A. and Sipos, L. (1971) 'Chitosan for the collection from seawater of naturally occurring zinc, cadmium, lead and copper', *Talanta*, 18(9), p. 853—858. doi: 10.1016/0039-9140(71)80141-8.

Nam, H. C. and Schaak, R. E. (2007) 'Shape-controlled conversion of ??-Sn nanocrystals into intermetallic M-Sn (M = Fe, Co, Ni, Pd) nanocrystals', *Journal of the American Chemical Society*, 129(23), pp. 7339–7345. doi: 10.1021/ja069032y.

Norfazila, S. M. and Mohd, J. R. (2014) 'Synthesis and Ultroviolet Visible Spectroscopy Studies of Chitosan Capped Gold Nanoparticles and Theri Reactions with Analytes', *The Scientific World Journal*, 2014, p. 7. doi: http://dx.doi.org/10.1155/2014/184604.

Okumu, F. and Matoetoe, M. (2016) 'Electrochemical Characterization of Silver-Platinum Various Ratio Bimetallic Nanoparticles Modified Electrodes', *Journal of Nano Research*, 44, pp. 114–125. doi: 10.4028/www.scientific.net/JNanoR.44.114.

Olaniyan, O. J. *et al.* (2016) 'Synthesis and Characterization of Chitosan-Silver Nanocomposite Film', *Nano Hybrids and Composites*, 11, pp. 22–29. doi: 10.4028/www.scientific.net/NHC.11.22.

Ono, S. *et al.* (2015) 'Increased wound pH as an indicator of local wound infection in second degree burns', *Burns*. Elsevier Ltd and International Society of Burns Injuries, 41(4), pp. 820–824. doi: 10.1016/j.burns.2014.10.023.

Padil, V. and Cernik, M. (2013) *Green synthesis of copper oxide nanoparticles using gum karaya as a biotemplate and their antibacterial application*, *International journal of nanomedicine*. doi: 10.2147/IJN.S40599.

Paladini, F. *et al.* (2016) 'In vitro assessment of the antibacterial potential of silver nano-coatings on cotton gauzes for prevention of wound infections', *Materials*, 9(6), pp. 1–14. doi: 10.3390/ma9060411.

Panchakarla, L. S., Govindaraj, A. and Rao, C. N. R. (2007) 'Formation of ZnO nanoparticles by the reaction of zinc metal with aliphatic alcohols', *Journal of Cluster Science*, 18(3), pp.

660–670. doi: 10.1007/s10876-007-0129-6.

Pankratov, D. V. *et al.* (2014) 'Impact of surface modification with gold nanoparticles on the bioelectrocatalytic parameters of immobilized bilirubin oxidase', *Acta Naturae*, 6(20), pp. 102–106.

Patrulea, V. *et al.* (2015) 'Chitosan as a starting material for wound healing applications', *European Journal of Pharmaceutics and Biopharmaceutics*. Elsevier B.V., 97, pp. 417–426. doi: 10.1016/j.ejpb.2015.08.004.

Paul, H. J. and Leddy, J. (1995) 'Direct Determination of the Transfer Coefficient from Cyclic Voltammetry: Isopoints as Diagnostics', *Analytical Chemistry*, 67(10), pp. 1661–1668. doi: 10.1021/ac00106a003.

de Paz, L. E. C. *et al.* (2011) 'Antimicrobial effect of chitosan nanoparticles on Streptococcus mutans biofilms', *Applied and Environmental Microbiology*, 77(11), pp. 3892–3895. doi: 10.1128/AEM.02941-10.

Pinho, E. *et al.* (2011) 'Antimicrobial activity assessment of textiles: Standard methods comparison', *Annals of Microbiology*, 61(3), pp. 493–498. doi: 10.1007/s13213-010-0163-8.

Prodomis, M. I. *et al.* (2000) 'The Importance of Surface Coverage in the Electrochemical Study of Chemically Modified Electrodes', *Electroanalysis*, 12(18), pp. 1498–1501.

Puchalski, M. *et al.* (2007) 'The study of silver nanoparticles by scanning electron microscopy, energy dispersive X-ray analysis and scanning tunnelling microscopy', *Materials Science-Poland*, 25(2), pp. 473–478.

Raafat, D. and Sahl, H. G. (2009) 'Chitosan and its antimicrobial potential - A critical literature survey', *Microbial Biotechnology*, 2(2 SPEC. ISS.), pp. 186–201. doi: 10.1111/j.1751-7915.2008.00080.x.

Radecka, M. *et al.* (2008) 'Importance of the band gap energy and flat band potential for application of modified TiO2 photoanodes in water photolysis', *Journal of Power Sources*, 181(1), pp. 46–55. doi: https://doi.org/10.1016/j.jpowsour.2007.10.082.

Raghupathi, K. R., Koodali, R. T. and Manna, A. C. (2011) 'Size-dependent bacterial growth inhibition and mechanism of antibacterial activity of zinc oxide nanoparticles.', *Langmuir : the ACS journal of surfaces and colloids*, 27(7), pp. 4020–4028. doi: 10.1021/la104825u.

Rahman, A. *et al.* (2009) 'SYNTHESIS OF COPPER OXIDE NANO PARTICLES BY USING

Phormidium cyanobacterium', *Indonesian Journal of Chemistry*, 9(3), pp. 355–360.

Rai, M., Yadav, A. and Gade, A. (2009) 'Silver nanoparticles as a new generation of antimicrobials', *Biotechnology Advances*. Elsevier Inc., 27(1), pp. 76–83. doi: 10.1016/j.biotechadv.2008.09.002.

Ravichandran, S. *et al.* (2015) 'A novel approach for the biosynthesis of silver oxide nanoparticles using aqueous leaf extract of Callistemon lanceolatus (Myrtaceae) and their therapeutic potential', *Journal of Experimental Nanoscience*. Taylor & Francis, 8080(August), pp. 1–14. doi: 10.1080/17458080.2015.1077534.

Rhazi, M. *et al.* (2002) 'Influence of the nature of the metal ions on the complexation with chitosan.: Application to the treatment of liquid waste', *European Polymer Journal*, 38, pp. 1523–1530.

Rhoades, J. and Roller, S. (2000) 'Antimicrobial actions of degraded and native chitosan against spoilage organisms in laboratory media and foods', *Applied and Environmental Microbiology*, 66(1), pp. 80–86. doi: 10.1128/AEM.66.1.80-86.2000.

Richards, R. and Bonnemann, H. (2005) 'Synthetic Approaches to Metallic Nanomaterials', *Nanofabrication Towards Biomedical Applications: Techniques, Tools, Applications, and Impact*, pp. 1–32. doi: 10.1002/3527603476.ch1.

Salehi, R. *et al.* (2010) 'Novel biocompatible composite (Chitosan-zinc oxide nanoparticle): Preparation, characterization and dye adsorption properties', *Colloids and Surfaces B: Biointerfaces*. Elsevier B.V., 80(1), pp. 86–93. doi: 10.1016/j.colsurfb.2010.05.039.

Sanpui, P. *et al.* (2008) 'The antibacterial properties of a novel chitosan-Ag-nanoparticle composite', *International Journal of Food Microbiology*, 124(2), pp. 142–146. doi: 10.1016/j.ijfoodmicro.2008.03.004.

Santos, C. L. *et al.* (2013) 'Nanomaterials with Antimicrobial Properties : Applications in Health Sciences', *Microbial pathogens and strategies for combating them: science, technology and education*, 1, pp. 143–154.

Sanyal, M. K., Datta, A. and Hazra, S. (2002) 'Morphology of nanostructured materials', *Pure and Applied Chemistry*, 74(9), pp. 1553–1570. doi: 10.1351/pac200274091553.

Schlenoff, J. B., Ly, H. and Li, M. (1998) 'Charge and Mass Balance in Polyelectrolyte Multilayers - Journal of the American Chemical Society (ACS Publications)', *Journal of the*

American Chemical …, 7863(13), pp. 7626–7634. doi: 10.1021/ja980350.

Sehat, A. A. *et al.* (2015) 'Fast immobilization of glucose oxidase on graphene oxide for highly sensitive glucose biosensor fabrication', *International Journal of Electrochemical Science*, 10(1), pp. 272–286.

Seil, J. T. and Webster, T. J. (2012) 'Antimicrobial applications of nanotechnology: Methods and literature', *International Journal of Nanomedicine*, 7, pp. 2767–2781. doi: 10.2147/IJN.S24805.

Sezer, A. D. and Cevher, E. (1992) 'Biopolymers as Wound Healing Materials: Challenges and New Strategies', *Biomaterials Applications for Nanomedicine*, pp. 383–414. doi: 10.5772/25177.

Shen, X. S. *et al.* (2009) 'Nanospheres of silver nanoparticles: agglomeration, surface morphology control and application as SERS substrates', *Physical Chemistry Chemical Physics*. The Royal Society of Chemistry, 11(34), pp. 7450–7454. doi: 10.1039/B904712C.

Shrivastava, S. *et al.* (2010) 'Characterization of enhanced antibacterial effects of novel silver nanoparticles', *Nanotechnology*, 18(22), pp. 1–9. doi: 10.1088/0957-4484/18/22/225103.

Sirkka, T., Skiba, J. B. and Apell, S. P. (2016) 'Wound pH depends on actual wound size', p. 13.

Srivastava, S., Agrawal, A. and Kumar, S. (2013) 'Synthesis and Characterisation of Copper Oxide nanoparticles', *Journal of Applied Physics*, 5(4), pp. 61–65.

Street, E. and Lake, C. (2014) 'Aatcc t', pp. 2012–2015.

Sudheesh Kumar, P. T. *et al.* (2012) 'Flexible and microporous chitosan hydrogel/nano ZnO composite bandages for wound dressing: In vitro and in vivo evaluation', *ACS Applied Materials and Interfaces*, 4(5), pp. 2618–2629. doi: 10.1021/am300292v.

Sudheesh Kumar, P. T. *et al.* (2013) 'Evaluation of wound healing potential of β-chitin hydrogel/nano zinc oxide composite bandage', *Pharmaceutical Research*, 30(2), pp. 523–537. doi: 10.1007/s11095-012-0898-y.

Sun, K. and Li, Z. H. (2011) 'Preparations, properties and applications of chitosan based nanofibers fabricated by electrospinning', *Express Polymer Letters*, 5(4), pp. 342–361. doi: 10.3144/expresspolymlett.2011.34.

Sutherland, L. F. and D. (2012) *Nanotechnologies: Principles, Applications, Implications and Hands-on Activities*. doi: :10.2777/76945.

Talam, S., Karumuri, S. R. and Gunnam, N. (2012) 'Synthesis, Characterization, and Spectroscopic Properties of ZnO Nanoparticles', *ISRN Nanotechnology*, 2012, pp. 1–6. doi: 10.5402/2012/372505.

Tamayo, L. *et al.* (2016) 'Copper-polymer nanocomposites: An excellent and cost-effective biocide for use on antibacterial surfaces', *Materials Science and Engineering C*. Elsevier B.V., 69, pp. 1391–1409. doi: 10.1016/j.msec.2016.08.041.

Teterycz, H. *et al.* (2014) 'Deposition of Zinc Oxide on the Materials Used in Medicine. Preliminary Results', *FIBRES & TEXTILES in Eastern Europe*, 22(105), pp. 3–126.

Tikhonov, V. E. *et al.* (2006) 'Bactericidal and antifungal activities of a low molecular weight chitosan and its N-/2(3)-(dodec-2-enyl)succinoyl/-derivatives', *Carbohydrate Polymers*, 64(1), pp. 66–72. doi: 10.1016/j.carbpol.2005.10.021.

Tran, D. L. *et al.* (2011) 'Some biomedical applications of chitosan-based hybrid nanomaterials', *Advance in Natural Science: Nanoscience Nanotechnology*, 2, pp. 1–6. doi: 10.1088/2043-6262/2/4/045004.

Tran, T. H. and Nguyen, V. T. (2014) 'Copper Oxide Nanomaterials Prepared by Solution Methods, Some Properties, and Potential Applications: A Brief Review', *International Scholarly Research Notices*. Hindawi Publishing Corporation, 2014, pp. 1–14. doi: 10.1155/2014/856592.

Umesh, Kathad; Gajera, H. . (2014) 'Synthesis of copper nanoparticles by two different methods and size comparison', *Int J Pharm Bio Sci*, 5(1), pp. 978–982.

Usman, M. S. *et al.* (2012) 'Copper nanoparticles mediated by chitosan: Synthesis and characterization via chemical methods', *Molecules*, 17(12), pp. 14928–14936. doi: 10.3390/molecules171214928.

Valov, I. and Lu, W. D. (2016) 'Nanoscale electrochemistry using dielectric thin films as solid electrolytes', *Nanoscale*. The Royal Society of Chemistry, 8(29), pp. 13828–13837. doi: 10.1039/C6NR01383J.

Vaseeharan, B., Sivakamavalli, J. and Thaya, R. (2015) 'Synthesis and characterization of chitosan-ZnO composite and its antibiofilm activity against aquatic bacteria', *Journal of*

Composite Materials, 49(2), pp. 177–184. doi: 10.1177/0021998313515289.

Velasco, J. G. (1997) 'Determination of standard rate constants for electrochemical irreversible processes from linear sweep voltammograms', *Electroanalysis*, 9(11), pp. 880–882. doi: 10.1002/elan.1140091116.

Wang, X. *et al.* (2005) 'Chitosan- metal complexes as antimicrobial agent: Synthesis, characterization and Structure-activity study', *Polymer Bulletin*, 55(1–2), pp. 105–113. doi: 10.1007/s00289-005-0414-1.

Wang, Z. L. (2004) 'Zinc oxide nanostructures: growth, properties and applications', *Journal of Physics: Condensed Matter*, 16(25), pp. R829–R858. doi: 10.1088/0953-8984/16/25/R01.

Wei, D. *et al.* (2009) 'The synthesis of chitosan-based silver nanoparticles and their antibacterial activity', *Carbohydrate Research*. Elsevier Ltd, 344(17), pp. 2375–2382. doi: 10.1016/j.carres.2009.09.001.

Wicramarachchi, P. and Hettiarachchi, M. (2011) 'Synthesis of chitosan stabilised silver nanoparticles using gamma ray radiation and characterisation', *Jousrnal of Scinece*, 6, pp. 65–75.

Xiliang, Q. *et al.* (2014) 'Large-Scale Synthesis of Silver Nanoparticles by Aqueous Reduction for Low-Temperature Sintering Bonding', 2014.

Xiong, G. *et al.* (2006) 'Photoluminescence and FTIR study of ZnO nanoparticles: The impurity and defect perspective', *Physica Status Solidi (C) Current Topics in Solid State Physics*, 3(10), pp. 3577–3581. doi: 10.1002/pssc.200672164.

Yukna, J. (Souther. I. U. at C. . (2014) 'International Journal of Nano Dimension Synthesis and characterization of Copper and Copper Oxide nanoparticles by thermal decomposition method', *Thesis paper*, 5(4), pp. 321–327.

Zhang, L., Zeng, Y. and Cheng, Z. (2016) 'Removal of heavy metal ions using chitosan and modified chitosan: A review', *Journal of Molecular Liquids*. Elsevier B.V., 214, pp. 175–191. doi: 10.1016/j.molliq.2015.12.013.

Zhou, E., Hashimoto, K. and Tajima, K. (2013) 'Low band gap polymers for photovoltaic device with photocurrent response wavelengths over 1000 nm', *Polymer (United Kingdom)*. Elsevier Ltd, 54(24), pp. 6501–6509. doi: 10.1016/j.polymer.2013.09.058.

CHAPTER SIX

CONCLUSION AND RECOMMENDATION

6.1. Conclusion

This chapter particularly goes into the conclusions based on the results that were acquired during this research and also makes recommendations for further research.

Ag, ZnO, and CuO NPs and composites CH-ZnO, CH-CuO, CH-Ag and CH-Ag-CuO-ZnO, were successfully synthesised using the chemical reduction method and simple chelation method respectively.

The NPs materials synthesis were confirmed using UV-Visible spectroscopy that depicted characteristic absorption bands at 420nm, 305nm, 375nm for Ag, CuO, and ZnO NPs respectively. The chitosan-NPs composites (CH-NPs) absorption bands showed a blue-shift from those of pure NPs and were observed at 320nm, 290nm, and 330nm for CH-ZnO, CH-CuO, CH-Ag composites respectively. The optical and electronic band gap energies of the pure NPs ranged from 1 to 5eV whereas the ones for CH-NPs ranged from 3.80 to 4.30eV. These band gap energy ranges indicated that all pure NPS and their composites are semi-conductors in nature. The absorption bands for prototype composite, CH-Ag-ZnO-CuO, showed a blue-shift with respect to all the NPs present in the composite with a slightly wider band gaps of between 3.00 and 4.60eV were observed.

Bands of Fourier transform infrared spectroscopy (FTIR) for the three pure NPs were observed within the fingerprint region with the bands being between 490 and 620 cm^{-1} in all the NPs. While bands for the composites showed the distortion and non-appearance of the amine ($-NH_2$) and the hydroxyl (-OH) excitation bands. In addition, they were some new bands that were not present in chitosan polymer or pure NPs that were observed in the CH-NPs composites between 3500 to 3000 and 1500 to 1000. These spectra confirmed the presence of bonding between the NPs and the chitosan within the composite. The prototype composite, CH-Ag-ZnO-CuO, exhibited new excitation bands in its FTIR spectrum confirming interaction between the NPs and the chitosan.

Transmission electron microscopy (TEM) images exhibited a variety of shapes with the dominant shapes of the NPs being spherical, hexagonal, and rod-shaped for silver, copper oxide, zinc oxide respectively. The average sizes of the NPs from TEM were found to be 22nm, 38nm, 21nm for Ag, CuO, and ZnO NPs respectively with their orientation in media being dominantly polydispersed.

X-ray diffraction spectra indicated that the pure NPs had base-centred, face-centred, and hexagonal crystalline structures for CuO, Ag, and ZnO NPs respectively. The investigation of the CH-NPs composites confirmed the immobilization of the NPs on the chitosan and that the chitosan polymer caused no significant change in the structural backbone of all the pure NPs.

Electron-transfer kinetics of the NPs films on glassy carbon electrode (GCE), were investigate using cyclic voltammetry (CV) showed that both diffusion and the adsorption controlled processes were taking place at the surfaces of all the NPs. Electrochemical parameters evaluated using Laviron's equation showed that the standard electrochemical rate constant, ks, ranged from 0.02 to 2.5 cm/s indicating relatively fast electron transfer at the electrode surface whereas the charge transfer coefficient, α, range was 0.1 to 0.6 for the NPs. The CV voltammogram of the CH-NPs composites indicated the irreversibility of the electrochemical reactions taking place as well as the existence of the Donnan potential shift effect. These phenomenon was confirmed by the α and k_s values, which were found to range between 0.4 and 1.6 for α whereas the k_s values were found to be zero for all CH-NPs composites. Plots of Ipa vs. V indicated that the major electron transfer process taking place at the surface of the electrodes was adsorption controlled. From electrochemical studies presence of chitosan altered the electrochemical properties of the pure NPs.

The CH-NPs composites were used to modify cotton wound gauzes and the modified gauzes evaluated for bactericidal efficacy and water retention properties. SEM images of the modified wound gauze indicated an increase in surface area coupled with porous cavities within the polymer structure of chitosan on the wound gauze. Water retention of the modified wound gauze increased by 65%. The bactericidal susceptibility and bacterial viability of the wound gauzes was studied using the AATCC 147 and AATCC 100 tests respectively. The test bacteria, *Staphylococcus aureus* and *Escherichia coli*, both responded to the inhibitory action of all the composites. The best inhibition action was observed in the prototype wound gauze modified with the CH-Ag-ZnO-CuO composite followed by the CH-Ag composite. Reduction percentage tests showed the elevated bactericidal vigour exhibited by the prototype composite whose reduction percentage for *Staphylococcus aureus* and *Escherichia coli* was 96% and 99% respectively.

Over all the research showed the feasibility of cotton gauze modification using a biopolymer and metallic nanoparticles composite. These modified gauze produced has enhanced curative properties, as indicated by their efficiency to aide in controlling bacterial life in and around the wound. The composite CH-Ag-ZnO-CuO has the most enhanced bactericidal activity than individual NPs and their composites at the same concentration. This confirms

the synergetic effect that is brought about by the use of the three NPs together in bactericidal applications.

6.2 Recommendations

For further investigations the following areas can be considered;

- Determination of the minimum inhibitory concentration (MIC) and minimum bactericidal concentration (MBC) of the novel CH-Ag-CuO-ZnO composite modified wound.
- To conduct *in vivo* cyto-toxicity tests of the modified gauze so as to assess if the modified gauze is not toxic to human tissue.
- To investigate the surface topology and morphology of the modified wound gauze using atomic force microscope so as to comprehend the arrangement and alignment of the NPs on the cotton wound gauze.